

**Phenotypic heterogeneity and the biological
significance of a pyruvate sensing network in
*Escherichia coli***



Cláudia Sofia Jorge Vilhena

Dissertation der Fakultät für Biologie
der Ludwig-Maximilians-Universität München

München

2018

Erstgutachter: Prof. Dr. Kirsten Jung

Zweitgutachter: Prof. Dr. Marc Bramkamp

Datum der Abgabe: 13.03.2018

Datum der mündlichen Prüfung: 02.05.2018

Eidesstattliche Erklärung

Ich versichere hiermit an Eides statt, dass die vorgelegte Dissertation von mir selbstständig und ohne unerlaubte Hilfe angefertigt wurde. Des Weiteren erkläre ich, dass ich nicht anderweitig ohne Erfolg versucht habe, eine Dissertation einzureichen oder mich der Doktorprüfung zu unterziehen. Die folgende Dissertation liegt weder ganz, noch in wesentlichen Teilen einer anderen Prüfungskommission vor.

Munich,13.03.2018

Cláudia Sofia Jorge Vilhena

Statutory Declaration

I declare that I have authored this thesis independently, that I have not used other than the declared sources/resources. As well I declare that, I have not submitted a dissertation without success and not passed the oral exam. The present dissertation (neither the entire dissertation nor parts) has not been presented to another examination board.

Munich,13.03.2018

Cláudia Sofia Jorge Vilhena

Contents

Eidesstattliche Erklärung	iii
Statutory Declaration	iii
Abbreviations	vi
Publications and Manuscripts Originating from this Thesis	vii
Contributions to Publications and Manuscripts presented in this Thesis	viii
Summary	x
Zusammenfassung	xi
Chapter 1: Introduction	12
1.1- From populations to individuals- <i>Phenotypic Heterogeneity</i>	12
1.1-1. Metabolic specialization.....	13
1.2- Perceiving environmental cues: Two-component systems.....	14
1.2-1. LysS/LytTR-like two-component systems.....	16
1.3- The BtsS/BtsR two-component system of <i>Escherichia coli</i>	17
1.4- The YpdA/YpdB two-component system of <i>Escherichia coli</i>	18
1.5- Scope of this thesis.....	21
Chapter 2: A single-cell view of the BtsSR/YpdAB pyruvate sensing network in <i>Escherichia coli</i> and its biological relevance	22
Chapter 3: BtsT: a novel and specific pyruvate/H⁺ symporter in <i>Escherichia coli</i>	37
Chapter 4: Low <i>btsT</i> transcriptional activation: an add-on for <i>Escherichia coli</i> survival under antibiotic treatment	51
Chapter 5: Resuscitation from the Viable but Nonculturable State of <i>Escherichia coli</i>: the importance of a pyruvate sensing network	63
Chapter 6: Concluding discussion	83
6.1- Single-cell analysis of <i>btsT</i> (<i>yjiY</i>) and <i>yhjX</i> transcriptional activation.....	83
6.1-1. Heterogeneity of <i>btsT</i> and <i>yhjX</i> transcriptional activation.....	83
6.1-2. Modulators of the heterogeneous behavior.....	84
6.1-3. Cellular physiology at the post-exponential growth phase.....	86
6.2- Identification of the substrate transported by BtsT (YjiY).....	88
6.2-1. BtsT and other pyruvate transporters.....	88
6.2-2. The importance of pyruvate in prokaryotic cells.....	89
6.3- Investigation of the biological relevance of BtsS/BtsR and YpdA/YpdB systems.....	91

6.3-1. Heterogeneity of P_{btsR} activation relates to antibiotic persistence.....	91
6.3-2. The viable but nonculturable state of <i>E. coli</i>	91
6.3-3. BtsS/BtsR and YpdA/YpdB role in pathogenicity.....	92
6.4- Outlook.....	95
References (Chapter 1, 4, 5 and 6)	96
Supplemental Material (Chapter 2).....	103
Supplemental Material (Chapter 3).....	107
Supplemental Material (Chapter 4).....	119
Supplemental Material (Chapter 5).....	121
Acknowledgements	124
Curriculum Vitae	125

Abbreviations

APC - acid-polyamine-organocation

ATP - adenosine- 5'-triphosphate

cAMP - cyclic AMP

CRP- cAMP receptor protein

FRET- fluorescence resonance energy transfer

GAF- cGMP specific phosphodiesterases, adenylyl cyclases and FhlA

GFP- green fluorescent protein

HK- histidine kinase

IM- interaction map

RR- response regulator

MFS- Major Facilitator Superfamily

MPC- mitochondrial pyruvate carrier

OFA- Oxalate:Formate Antiporter

PDH- pyruvate dehydrogenase complex

ROS- reactive oxygen species

SBVS- structured-based virtual screening

SPR- surface plasmon resonance

TCA- tricarboxylic acid

TCS- two-component system

TM- transmembrane domain

VBNC- viable but nonculturable

Publications and Manuscripts Originating from this Thesis

Chapter 2:

Vilhena, C., Kaganovitch, E., Shin, J.Y., Grünberger, A., Behr, S., Kristoficova, I., Brameyer, S., Kohlheyer, D., Jung, K. (2018). A single-cell view of the BtsSR/YpdAB pyruvate sensing network in *Escherichia coli* and its biological relevance. *J Bacteriol*, 200:e00536-17.

Chapter 3:

Kristoficova, I., Vilhena, C., Behr, S., Jung, K. (2018). BtsT - a novel and specific pyruvate/H⁺ symporter in *Escherichia coli*. *J Bacteriol*, 200:e00599-17.

Chapter 4:

Kaganovitch, E., Vilhena, C., Grünberger, A, Kohlheyer, D., Jung, K. (2018). Low *btsT* transcriptional activation: an add-on for *Escherichia coli* survival under antibiotic treatment. (Manuscript)

Chapter 5:

Vilhena, C., Kaganovitch, E., Grünberger, A, Motz, M., Kohlheyer, D., Jung, K. (2018). Resuscitation from the viable but nonculturable state of *Escherichia coli*: the importance of a pyruvate sensing network. (Manuscript)

Contributions to Publications and Manuscripts presented in this Thesis

Chapter 2:

Cláudia Vilhena, Jae Yen Shin, Stefan Behr, and Kirsten Jung designed the experiments. Cláudia Vilhena performed all the experimental work presented in the publication. Cláudia Vilhena and Jae Yen Shin performed statistical analysis of the data. Ivica Kristoficova drew the model. Ivica Kristoficova and Cláudia Vilhena performed reporter assays for the elucidation of the crosstalk between the systems during the development of the manuscript. Eugen Kaganovitch, Alexander Grünberger and Dietrich Kohlheyer helped conceptualizing microfluidic experiments during the development of the manuscript. Sophie Brameyer performed plasmid-based experiments during the development of the manuscript. Cláudia Vilhena, Eugen Kaganovitch, Jae Yen Shin, Alexander Grünberger, Stefan Behr, Ivica Kristoficova, Sophie Brameyer, Dietrich Kohlheyer and Kirsten Jung wrote and corrected the manuscript.

Chapter 3:

Ivica Kristoficova, Cláudia Vilhena, Stefan Behr and Kirsten Jung designed the experiments. Stefan Behr performed comparative genomic studies. Ivica Kristoficova carried out the transport measurements with intact cells and proteoliposomes. Ivica Kristoficova and Cláudia Vilhena conceptually developed experimental conditions for transport assays. Ivica Kristoficova and Kirsten Jung wrote the manuscript.

Chapter 4:

Eugen Kaganovitch, Cláudia Vilhena, Alexander Grünberger, Dietrich Kohlheyer and Kirsten Jung designed the experiments. Cláudia Vilhena constructed bacterial strains. Eugen Kaganovitch and Alexander Grünberger performed the microfluidic experiments. Eugen Kaganovitch and Cláudia Vilhena performed data analysis. Cláudia Vilhena, Eugen Kaganovitch, Alexander Grünberger, Dietrich Kohlheyer and Kirsten Jung wrote the manuscript.

Chapter 5:

Cláudia Vilhena, Eugen Kaganovitch, Alexander Grünberger, Magdalena Motz, Dietrich Kohlheyer and Kirsten Jung designed the experiments. Cláudia Vilhena performed all the batch experiments. Cláudia Vilhena, Eugen Kaganovitch and Alexander Grünberger designed, performed and analysed the microfluidic experiments. Magdalena Motz prepared and analysed samples of mass spectrometry. Cláudia Vilhena, Eugen Kaganovitch, Alexander Grünberger, Dietrich Kohlheyer and Kirsten Jung wrote the manuscript.

We hereby confirm the above statements:

Cláudia Sofia Jorge Vilhena

Prof. Dr. Kirsten Jung

Summary

When facing nutrient limitation, bacterial populations are forced to optimize uptake systems for available substrates in order to adapt and survive. However, the physiological diversity of each individual in a population leads to differential activation of the uptake systems in response to the same environmental condition. Hence, heterogeneous phenotypes can be generated in a clonal population. A way for each bacterial individual to sense nutrient availability and transmit this information from the extra- to the intracellular spaces is via two-component systems (TCSs). *Escherichia coli* contains 30 TCSs, each composed of one histidine kinase (HK) and at least one response regulator (RR). The HK is responsible for perceiving the extracellular stimulus and the RR consequently mediates the output, generally a regulation of gene expression. BtsS/BtsR and YpdA/YpdB are examples of two TCSs in *E. coli*. BtsS/BtsR activation leads to the induction of *yjiY*, whereas YpdA/YpdB activates *yhjX* expression. *yjiY* and *yhjX* code for putative transporters. Both systems are functionally interconnected and are thought to form a large signalling network.

This thesis focuses on the analysis of the transcriptional activation of *yjiY* and *yhjX* at the single-cell level and on the biological significance of the two TCSs. The activation of the target promoters at the single-cell level was found to be heterogeneous and strongly influenced by the available nutrients. To exploit the biological relevance of the two TCSs, wild-type cells were compared to cells of a *btsSRypdAB* mutant under two metabolically modulated conditions: protein overproduction and persister formation. BtsS/BtsR and YpdA/YpdB network was shown to contribute to a balancing of the physiological state of all cells within a population.

YjiY, the putative transport protein resulting from BtsS/BtsR activation, was found to function as a high-affinity and specific pyruvate/H⁺ symporter. The protein was renamed for BtsT (Bts is an abbreviation of the German name for pyruvate, *Brenztraubensäure*, and T stands for Transporter). The correlation between the heterogeneous transcriptional activation of *btsT* and the number of persister cells was explored using microfluidic technology. It was shown that individuals with low *btsT* transcriptional activation were more prone to form persisters. A relevant biological application of a pyruvate transporter, the resuscitation from the viable but nonculturable (VBNC) state of *E. coli* was tested in bulk and single-cell assays and revealed that the concomitant presence of pyruvate and BtsS/BtsR and YpdA/YpdB network is required for proper resuscitation from this state.

For the first time, phenotypes associated to a mutant lacking the BtsS/BtsR and YpdA/YpdB systems were identified, which in general are related to metabolic challenges. This thesis contributes to a better understanding of the biological role of the two TCSs, BtsS/BtsR and YpdA/YpdB of *E. coli*.

Zusammenfassung

Eine Nährstofflimitation zwingt Bakterienpopulationen dazu, ihre Aufnahmesysteme für verfügbare Substrate zu optimieren, um Adaptation und Überleben zu gewährleisten. Die physiologische Diversität einer Population impliziert trotz gleicher Umweltbedingung eine je nach Individuum verschiedene Aktivierung der Aufnahmesysteme. Infolgedessen können sich in einer klonalen Population heterogene Phänotypen entwickeln. Zweikomponentensystem (TCSs) ermöglichen es jedem bakteriellen Individuum, die Nährstoffverfügbarkeit festzustellen und diese Information von dem extra- in den intrazellulären Raum zu übertragen. *Escherichia coli* besitzt 30 TCSs, jeweils bestehend aus einer Histidinkinase (HK) und mindestens einem Antwortregulator (RR). Die HK ist dafür verantwortlich, den extrazellulären Stimulus wahrzunehmen, während der RR anschließend den Ausgabewert vermittelt, üblicherweise in Form einer Regulation der Genexpression. BtsS/BtsR und YpdA/YpdB sind Beispiele für zwei TCSs in *E. coli*. Die Aktivierung von BtsS/BtsR führt zur Induktion von *yjiY*, während YpdA/YpdB die Expression von *yhjX* aktiviert. *YjiY* und *yhjX* kodieren mutmaßliche Transporter. Die beiden Systeme sind funktionell miteinander verbunden und bilden vermutlich ein großes Signalnetzwerk.

Diese Arbeit konzentriert sich auf die Einzelzellanalyse der transkriptionellen Aktivierung von *yjiY* und *yhjX*, sowie auf die biologische Signifikanz der beiden TCSs. Auf Einzelzellebene konnte eine heterogene Aktivierung der Ziel promotoren nachgewiesen werden, die stark von den verfügbaren Nährstoffen beeinflussbar ist. Um die biologische Relevanz der beiden TCSs zu untersuchen, wurden Wildtypzellen mit einer *btsSRypdAB* Mutante unter zwei metabolisch modifizierten Bedingungen verglichen: Proteinüberproduktion und Persistenz. Es konnte gezeigt werden, dass das Netzwerk aus BtsS/BtsR, sowie YpdA/YpdB zum Ausbalancieren des physiologischen Zustandes aller Zellen einer Population beitragen.

YjiY, das aus der BtsS/BtsR Aktivierung resultierende, mutmaßliche Transportprotein, funktioniert nachweislich als hochaffiner und spezifischer Pyruvat/H⁺ Symporter. Dementsprechend wurde das Protein umbenannt in BtsT (Bts: Abkürzung für Brenztraubensäure, T: Transporter). Die Korrelation zwischen heterogener transkriptioneller Aktivierung von *btsT* und der Anzahl an Persisterzellen wurde mittels Mikrofluidiktechnologie untersucht. Es konnte gezeigt werden, dass Individuen mit niedrigem *btsT* Expressionslevel tendenziell anfälliger für den Übergang in den Zustand der Persistenz sind. In Gesamt- und Einzelzelltests konnte belegt werden, dass die gleichzeitige Präsenz von Pyruvat und BtsS/BtsR, sowie YpdA/YpdB Netzwerk Voraussetzung ist für eine korrekte Umkehrung des VBNC Zustandes (viable but nonculturable) von *E. coli*.

Damit wurden zum ersten Mal Phänotypen, die gewöhnlich mit metabolisch herausfordernden Bedingungen in Zusammenhang stehen, bei einer Mutante identifiziert, der die BtsS/BtsR und YpdA/YpdB Systeme fehlen. Diese Arbeit trägt zu einem besseren Verständnis der biologischen Rolle der beiden *E. coli* TCSs BtsS/BtsR und YpdA/YpdB bei.

Chapter 1

Introduction

1.1- From populations to individuals – *Phenotypic Heterogeneity*

Escherichia coli and other bacteria, multiply by binary fission, resulting in two genetically identical daughter cells (1). Microbial research has traditionally considered bacterial populations *homogeneous* because they consist of clonal individuals derived from a common ancestor. Therefore, focus has been given only to bulk studies. Population-level measurements yield data representative of the population average of a certain studied parameter. However, differences among single individuals of a population can exist. Genetically identical populations which colonize homogeneous environments can display phenotypic differences among their individuals. This phenomenon is called *phenotypic heterogeneity* (2, 3). In a nutshell, phenotypic heterogeneity allows a population to maximize its metabolic, genetic and growth behaviors, resulting in an extraordinary survival tool in competitive environments.

Two different types of phenotypic heterogeneity can be characterized (**Fig. 1.1**). One is called *macro-heterogeneity*, where two clear subpopulations appear, each with a normal distribution in gene expression levels. This type of heterogeneity is often referred to as *bistability* (4, 5). The second type is called *micro-heterogeneity* and although exhibiting a unimodal distribution of gene expression, presents large deviations from the mean value (6). Both types provide an adaptively response to unpredictable environmental changes.

Let's take as example a research laboratory "society". Each single individual is responsible for different tasks apart from their research project, as monthly radioactive garbage disposal, maintenance of ultracentrifuges, negotiations with suppliers, lecturing, etc. The demands that these tasks imply are not condensed in the principle investigator neither in technical assistants. Instead, all members of the laboratory take part by small contributions. If only one PhD student would be responsible for all the above mentioned tasks, the chances of him/her exhausts energy and consequently not fulfill the tasks would be high. The same behavioral principle is found in bacterial populations. The risks associated with high and low expressing populations (for the specific case of gene expression) are "spread" through the population (7).

The source of phenotypic heterogeneity lies on the spatial gradients of nutrient availability, oxygen concentration or other environmental factors that occur in a population (3). These gradients generate microenvironments where clusters of subpopulations grow and adapt accordingly. (8). An interesting study (9) refers to a hierarchy of sources of phenotypic heterogeneity according to a "timescale". It is

suggested that the stability (temporal matter) of a certain phenotype can help predict which is the most likely source of the heterogeneous behavior.

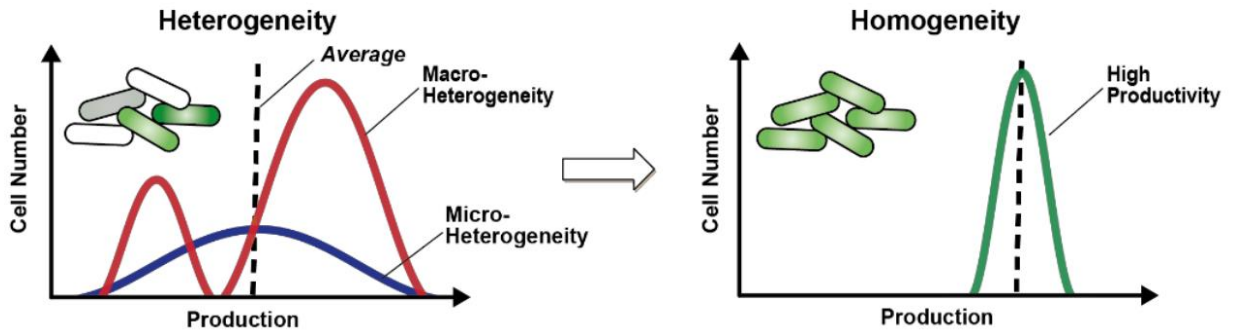


Fig.1.1- Types of phenotypic heterogeneity. Schematic representation of histograms correlating cell number and “production” (here is taken as related to gene expression). The panel Heterogeneity shows macro-heterogeneity (red line) and micro-heterogeneity (blue line) and their distributions around the average of the population (dashed line). On the panel Homogeneity, a homogenous population (green line) with indication of the impact in productivity is represented. See text for details. Adapted from (6).

Nevertheless, for certain processes it is important to accomplish a rather homogeneous profile of expression, as for example production of virulence factors (10). Homogeneity is associated with increase stability, predictability and a precise control over entire processes (11). Understanding the mechanisms underlying the establishment of phenotypic heterogeneity and the development of engineering tools to manipulate the population behavior are of major importance.

1.1-1. Metabolic specialization

Metabolic specialization is a general biological principle which supports that individual cells specialize phenotypically in a subset of metabolic processes (12, 13), instead of each cell performing all the processes required at a population level. This would mean, for instance, that a subgroup of cells specializes in the catabolism of glucose whereas another subgroup would be directed to nitrogen regulation (14), resulting in a metabolic balanced population. Ecological and evolutionary principles can easily explain why it is better to distribute the metabolic burden of certain processes among the individuals of a population (15).

Studies have explored experimentally this concept in organisms as *Pseudomonas putita* (16) and *Saccharomyces cerevisiae* (17). An interesting study in *E. coli* aimed to investigate heterogeneity in the

expression of metabolic genes involved in glucose transport, gluconeogenesis and acetate scavenging (18). For that purpose, *E. coli* MG1655 strains harboring translational fusions of the corresponding genes to the green fluorescent protein (GFP) were analyzed under different cultivation conditions and showed that clonal populations growing in glucose environments have heterogeneous expression of metabolic genes. New techniques to access incorporation of metabolites at the single-cell level will in the near future allow better understanding of metabolic specialization (19–21).

1.2- Perceiving environmental cues: Two-component systems

On the basis of several phenotypic heterogeneous behaviors, as persistence to antibiotics, metabolic specialization, among others, there are changing environmental conditions within the organism natural habitat. These changes can comprise impaired oxygen supply, nutrient limitation, changing temperatures, differential pH and osmolarity, etc. Bacteria have therefore developed tools to cope with such changing environmental conditions and accomplished sustainable growth and proliferation inside ecological and environmental niches.

In order to survive, single individuals within a population face the necessity to sense environmental cues and respond to them thereby attaining a phenotype that performs well in the current situation. Environmental signals are commonly interpreted by cells via systems of sensor and regulator proteins that result in a change in transcription and/or translational regulation (4). Signal transduction in bacteria is typically performed via two-component systems (TCSs) (22, 23).

Two-component signaling genes are found in all three domains of life (24, 25). In average bacteria harbour 25 TCSs to sense environmental factors (26). However there is a broad frequency range from 0 TCSs in *Mycoplasma genitalium*, 9 in *Haemophilus influenza*, 70 in *Bacillus subtilis*, up to 251 in *Myxococcus xanthus* (22). The number of TCS seems to strongly correlate with ecological and environmental niches (27, 28). Bacteria that live primarily in constant environments, as intracellular parasites, harbor only few signaling pathways (e. g. *Mycoplasma* harbors zero TCSs) since a significant portion of its genome is devoted to the transport of nutrients from its host such as glucose and fructose, as well as genes for attachment organelles, adhesins, and antigenic variation to evade the host immune system, whereas organisms facing frequent fluctuations in their environments comprise more TCSs (29). *E. coli* harbors 30 sensory proteins, so called histidine kinases (HKs), and 30 effectors, so called response regulators (RRs) (**Fig. 1.2**). Prominent examples are the well characterized KdpD/KdpE involved in K^+ regulation in *E. coli* (30), the BarA/UvrY which is required for the switching between glycolytic and gluconeogenic carbon sources (31) and ArcB/ArcA that mediates adaptation to anaerobic growth conditions (32).

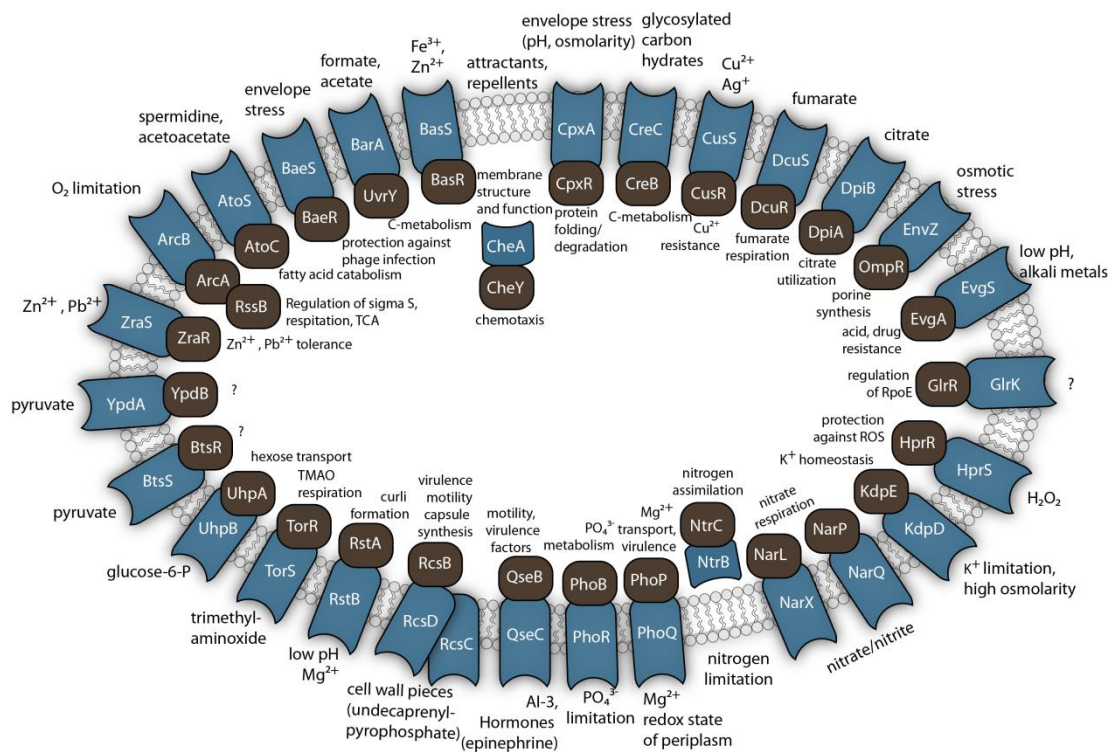


Fig.1.2- Two-component systems of *E. coli* MG1655 K-12. Overview of the TCSs of *E. coli* (in blue the HK and in black the RR) with their corresponding stimuli and outcome (when known). Made by Kristofcova and Vilhena, 2017.

As depicted in **Fig. 1.2**, the variety of stimuli and responses is great and often associated with some pathogenic features, making TCSs a strong focus for potential pharmaceutical intervention. Typically, upon perception of the corresponding stimulus, firstly the HK autophosphorylates at a conserved histidine residue (33). Secondly, the phosphoryl group of the HK is transferred to a conserved aspartate residue of the RR (**Fig.1.3**). Lastly, the effector domain of the RR is activated and modulation of gene expression occurs. Having control over TCSs activation influences, in turn, the modulation of gene expression upon a certain stimulus/environmental trigger. Unequal response of a certain TCS among individual cells of a population upon the same stimulus, is a source phenotypic heterogeneity.

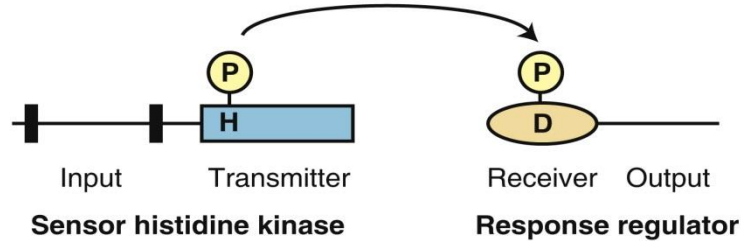


Fig.1.3- Signal transduction in typical TCSs. Schematic depiction of the phosphor transfer between the sensor histidine kinase and the response regulator. A conserved histidine residue (H) is firstly phosphorylated and later the phosphoryl group (P) is transferred to a conserved aspartate residue (D). Adapted from (24).

1.2-1. LytS/LytTR-like two-component systems

One of the most distributed families of TCSs in bacteria is the LytS/LytTR family (34, 35). The family is characterized by having members which are involved in regulation of pathogenicity or virulence and by the structural similarity between the members. All family members have a LytS-like HK [with signal recognition domain of the 5 transmembrane domains (TMs) Lyt type] and a LytTR-like RR (36). Examples include: AgrC/AgrA from *Staphylococcus aureus*, which is involved in the transition from the persistent, avirulent state to the virulent phenotype (37); FsrC/FsrA from *Enterococcus faecalis* is responsible for the production of virulence-related proteases (38); VirS/VirR from *Clostridium perfringens* induces the synthesis of exotoxins and collagenase (39, 40); LytS/LytR from *S. aureus* controls bacterial autolysis and is associated with programmed cell death, and ComD/ComE which regulates natural competence in *Streptococcus pneumoniae* (41).

The only two known members of the LytS/LytTR family in *E.coli* are BtsS/BtsR (formerly known as YehU/YehT) (34, 42–44) and YpdA/YpdB (43, 45, 46). It is worth mentioning, that BtsS/BtsR and YpdA/YpdB share a high degree of similarity in *E. coli*: the HKs have a sequence identity of 29% (sequence similarity of 53%), the RRs of 32% (sequence similarity of 53%). A comparative genomics study investigated the distribution and co-occurrence of the two systems and concluded that the majority of γ -proteobacteria possesses only the BtsS/BtsR system, while YpdA/YpdB system is predominantly found in addition to the BtsS/BtsR system (34). The co-occurrence of both systems (*E. coli*'s case) is a rare event. The study provided evidence that the systems might co-operate in a complementary way.

Cross-talk between each system has been reported and suggested that they might form a nutrient sensing network (43). Both these systems will be discussed in more detail in the next sections.

1.3- The BtsS/BtsR two-component system of *Escherichia coli*

BtsS/BtsR TCS is composed of a LytS-like HK (BtsS) and LytTR-like RR (BtsR) (47, 48) (**Fig. 1.4A**). *btsS* and *btsR* form an operon localized at 47.638 centisomes in the *E. coli* MG1655 genome with 4 bp overlap between them. The HK BtsS consists of 561 amino acids (62.1 kDa) (49, 50). The N-terminal input domain of BtsS consists of a 5TM Lyt domain (36) and a cGMP specific phosphodiesterases, adenyl cyclases and FhlA (GAF) domain. GAF domains are known to be involved in the perception of stimuli and/or signal transduction (51). The RR BtsR consists of 289 amino acids (27.4 kDa) (49, 50) and is organized in two domains: a CheY-homologous receiver domain and a DNA binding domain of the LytTR family (52, 53). Autophosphorylation of the HK BtsS or the transfer of the phosphoryl group to BtsR was not experimentally detected yet.

Previous studies on BtsS/BtsR in *E. coli* identified *yjiY* as its only target gene (42). *yjiY* is located at 98.87 centisomes on *E. coli* chromosome. Its genomic organization is depicted in **Fig. 1.4B**. This gene appears dissociated from *btsSbtsR* operon, contrary to the situations in *Vibrio*, *Shewanella* species or *Photorhabdus asymbiotica* (54). However, it is suggested that *yjiY* might be organized in an operon (55) with *yjiX*, a small cytosolic protein of unknown function, and *yjiA*, a protein with low GTPase activity (56). Though recent proteome data of *E. coli* did not reveal similar expression profiles of these three proteins under several experimental conditions, which does not support that they are all encoded in one single operon (57). The promoter region of *yjiY* was determined to be within -112 and -13 positions upstream the start of the coding region. A core binding site consist of two direct repeats of the motif ACC(G/A)CT(C/T)A linked by a 13 bp spacer and a third stabilizing motif (42).

BtsR binds tightly to *yjiY* promoter region (K_d 75 nM). *yjiY* transcription is further positively regulated by the cyclic AMP (cAMP) receptor protein (CRP) complex (CRP-cAMP) and at a post-transcriptional level it is negatively regulated by the carbon storage regulator A (CsrA). This target gene shows a transient peak of expression at the onset of stationary phase in rich media (43). Further *in vitro* studies showed that BtsS/BtsR-mediated activation of *yjiY* can occur in nutrient-limiting conditions when pyruvate is later provided extracellularly (from a threshold of 50 μ M), suggesting a scavenging role of this two-component system (58).

The target gene codes for the putative carbon starvation transporter YjiY, which is homologous (61.1% identity) to CstA, a carbon starvation protein and putative peptide transporter. YjiY belongs to the amino

acid-polyamine-organocation (APC) superfamily of secondary transporters (59, 60). The APC superfamily contains 18 families, from which the functionally characterized are responsible for the transport of amino acids, peptides, inorganic anions or cations (60). Characterization of bacterial transporters is crucial as they play a major role in maintaining a balance in terms of substrates concentrations between the extra- and intracellular spaces due to the impermeability of the membrane (61). So far, the transported substrate by YjiY has not yet been identified.

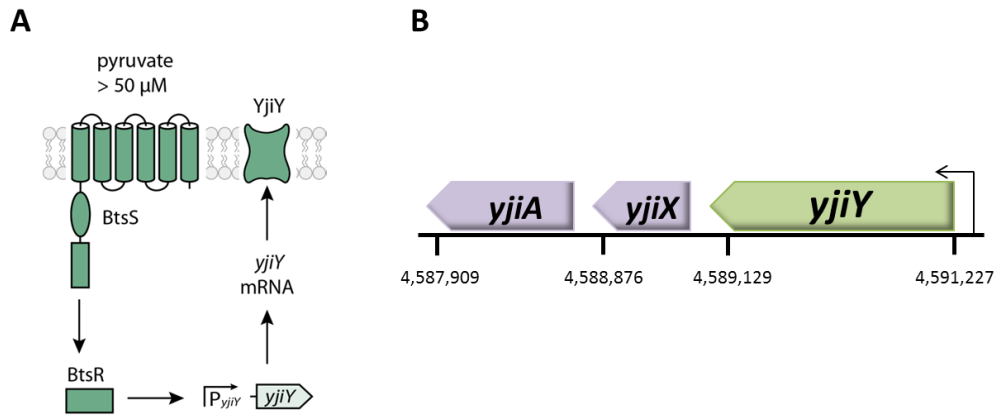


Fig. 1.4- The BtsS/BtsR two-component system of *Escherichia coli*. (A) Schematic representation of the TCS BtsS/BtsR and the corresponding target gene and protein. The figure was provided by Ivica Kristofcova, adapted and modified. (B) The neighboring genomic region of *yjiY* is represented schematically (units in bp). See text for details.

Recently, the substrate of the HK BtsS was elucidated (58). Extracellular pyruvate binds the HK BtsS with a K_d of 58.6 μM , confirming that BtsS is a high-affinity receptor for pyruvate. Moreover, it was shown that pyruvate is firstly produced intracellularly and upon accumulation, it is excreted to the extracellular space in a process called *overflow metabolism*. The peak of pyruvate excretion coincides with the activation of *yjiY* promoter, suggesting that somehow, YjiY might be involved in pyruvate transport. The specific physiological and functional role of the BtsS/BtsR TCS in *E. coli* remains elusive.

1.4- The YpdA/YpdB two-component system of *Escherichia coli*

Alike BtsS/BtsR, also YpdA/YpdB comprise a LytS-type HK and a LytTR-like RR (**Fig. 1.5A**) and both *ypdA* and *ypdB* are genetically encoded in an operon together with *ypdC*, which codes for a AraC-type regulatory protein (49). The operon is located 53.56 centisomes on the chromosome of *E. coli*. YpdA HK consists of 565 amino acids (62.7 kDa) with a N-terminal 5TM Lyt input domain linked to a GAF domain, as its cognate BtsS (62). The RR YpdB consists of 244 amino acids (28.7 kDa) and shares the same

rapid clearance might enable a dynamic pulse expression leading to a switch-like behavior (64). At a post-transcriptional level, *yhjX* is positively regulated by CsrA, contrary to the case of *yjiY* (43). However, similarly to *yjiY*, also *yhjX* show a transient peak of expression precisely at the transition between exponential and stationary phases. Interestingly, expression of *yhjX* was claimed to be highly induced upon overexpression of the toxic peptides ShoB, LdrD or IbsC (65) and by benzoate (66), however luciferase-based reporter assays never indicated such expression levels (45). *yhjX* transcription activation is constitutive and maximal when cells are cultivated in M9-minimal medium supplemented solely with pyruvate, and the threshold concentration of pyruvate required for induction was determined to be 600 μM (45).

yhjX codes for the putative transporter protein YhjX. This protein is a member of the Oxalate:Formate Antiporter (OFA) Family within the Major Facilitator Superfamily (MFS) (67, 68). Thus far and although YpdA/YpdB-mediated *yhjX* expression be detected in the presence of extracellular pyruvate, neither binding of the substrate to the HK YpdA nor the transport by YhjX were experimentally proved yet. The specific physiological and functional role of the YpdA/YpdB TCS in *E. coli* is still unknown.

1.5- Scope of this thesis

In recent years, characterization of TCSs has been a popular field of research due to the necessity to understand bacterial communication and adaption processes. The two TCSs BtsS/BtsR and YpdA/YpdB from *E. coli* have been extensively studied and characterized. However, the physiological relevance of these two systems and the function of both putative transport proteins are still unclear. Moreover and importantly, the so far experimental designs have only englobed bulk experiments, leaving a vast gap in the single-cell analysis of these systems activities.

The primordial aim of this thesis is to perform analysis of the transcriptional activation of each target gene at the single-cell level to check for heterogeneous behavior and unravel the physiological and functional roles of the sensing network BtsS/BtsR and YpdA/YpdB.

i. Single-cell analysis of *yjiY* and *yhjX* transcriptional activation

Based on bulk experiments, the inducing conditions for BtsS/BtsR and YpdA/YpdB- mediated activation of *yjiY* and *yhjX*, respectively, are known. Here, the distribution profiles of the activation of each target gene among single individuals shall be elucidated. Fluorescence-based reporter strains will be constructed and tested under inducing conditions. The transcription activation of *yjiY* and *yhjX* will also be quantitatively accessed in single cells.

ii. Identification of the substrate transported by YjiY

The fact that the HK BtsS binds extracellular pyruvate with high-affinity was a hint to test YjiY for the transport of pyruvate. Transport assays will be performed to elucidate the transported substrate.

iii. Investigation of the biological relevance of BtsS/BtsR and YpdA/YpdB systems

With the obtained knowledge from the two above sections, the biological role of these TCSs will be addressed. A mutant lacking the sensing network will be generated and used to compare metabolically related phenotypes against a wild-type strain. Moreover, microfluidic techniques will be employed to investigate the transcriptional activation of the target genes under stress conditions with single cell resolution.

Chapter 2

A single-cell view of the BtsSR/YpdAB pyruvate sensing network in *Escherichia coli* and its biological relevance

Vilhena, C., Kaganovitch, E., Shin, J.Y., Grünberger, A., Behr, S., Kristoficova, I., Brameyer, S., Kohlheyer, D., Jung, K. (2018). J Bacteriol, 200:e00536-17.

<https://doi.org/10.1128/JB.00536-17>.

Chapter 3

BtsT: a novel and specific pyruvate/H⁺ symporter in *Escherichia coli*

Kristoficova, I., Vilhena, C., Behr, S., Jung, K. (2018). J Bacteriol, 200:e00599-17.

<https://doi.org/10.1128/JB.00599-17>.

Chapter 4

Low *btsT* transcriptional activation: an add-on for *Escherichia coli* survival under antibiotic treatment

Eugen Kaganovitch^{a*}, Cláudia Vilhena^{b*}, Alexander Grünberger^{a*}, #Dietrich Kohlheyer^{a,c}, #Kirsten Jung^b

Institute for Bio- and Geosciences, IBG-1: Biotechnology, Forschungszentrum Jülich GmbH, Jülich, Germany^a, Munich Center for Integrated Protein Science (CIPSM) at the Department of Microbiology, Ludwig-Maximilians-Universität München, Martinsried, Germany^b, RWTH Aachen University–Microscale Bioengineering (AVT.MSB) 52074 Aachen, Germany^c

#Address correspondence to

Dietrich Kohlheyer, d.kohlheyer@fz-juelich.de

Kirsten Jung, jung@lmu.de

◆These authors contributed equally to this work

*Present address: Alexander Grünberger, Multiscale Bioengineering, Bielefeld University, Universitätsstraße 25, 33615 Bielefeld

Key Words: pyruvate, transporter, phenotypic heterogeneity, transcriptional activation, two-component systems

ABSTRACT

Phenotypic heterogeneity, which is defined as diversity among genetically identical individuals, poses significant challenges in biotechnological applications as well in health care. One important consequence of phenotypic heterogeneity is the persistence to antibiotics. Time-resolved single-cell analysis is inevitable to understand the mechanisms underlying the formation of persistent cells.

In this study, we apply a PDMS-based microfluidic device to perform a persister cell formation assay with *Escherichia coli*, offering spatial and temporal single-cell resolution and constant environmental conditions that could potentially alter the behavior of the cells. We study the transcriptional activation of *btsT*, the target gene of BtsS/BtsR, a two-component system in *E. coli* responsible for sensing and transporting pyruvate. The system forms a network together with YpdA/YpdB, also a pyruvate-responsive system. Bulk experiments have previously revealed that the systems play a role in persister cell formation. By tracking individual persister cells and simultaneously observing the activity of *btsT* transcriptional activation, we were able to find that individuals featuring low *btsT* transcriptional activation are more prone to form persisters. These findings come to complement the biological significance of the nutrient sensing network BtsSR/YpdAB of *E. coli* and at the same time show how microfluidic devices in combination with time-lapse microscopy provide a powerful tool to study bacterial phenotypes with high resolution.

INTRODUCTION

In recent years, bacterial heterogeneity has emerged as a new and challenging field of research(3, 69, 70). Bacterial phenotypic and/or genetic heterogeneity have important practical consequences which can affect industrial fermentations(71), the pathogenic potential of certain microorganisms(72) and even antibiotic resistance (73). A well-known case of phenotypic variance among clonal bacterial individuals is persistence to antibiotics (2, 74). Persister cells are able to survive antibiotic treatment and restore a normal sensitive population once the antibiotic stress is removed from the media (75). Contrary to resistant cells, persisters do not acquire a genetic mechanism for sustaining antibiotic stress, instead they suffer a reversible phenotypic switch to a dormant state (76, 77).

In order to explore the intriguing single-cell bacterial behavior and the complex mechanisms underlying, for instance, persister cell formation, the development of adequate analytical tools is of significant importance (78). Among those tools, microfluidic devices appear as one of the most thoroughly studied and reliable emerging technology for bacterial single-cell analysis (79–82). Microfluidic devices present numerous advantages comparing to bulk technologies. Among these is the ability to perform studies under well-defined and controlled environmental conditions (83, 84). When coupled to automated time-lapse microscopy, microfluidic technologies allow live-cell imaging with spatial and temporal single-cell resolution(80). Ultimately, microfluidic devices secure homogeneous cultivation conditions and consequently more reliability on the study of bacterial heterogeneity. Once studying complex environment-related phenotypes, as for the case of persistence, having a high-throughput microfluidic cultivation platform comes as a great advantage. Other works already explored the study of persister cell formation using microfluidic devices (77, 85–87). However, some of these studies use cultivations based on mechanical cell trapping (85) or agarose pad cultivations (87) which generate external stress for the bacterial cell (change from liquid to semi-solid medium and restriction in movement).

In this study, we use a PDMS-based microfluidic device to assess persister cell formation. As model organism we use *E. coli* MG1655 which harbors GFP under the control of *btsT* promoter. *btsT* is the target gene of BtsS/BtsR two-component system (TCS) of *E. coli* (42, 44). The gene codes for a protein with the same name, BtsT, which is a pyruvate transporter in *E. coli* (88). In previous studies we have shown that in order to have BtsS/BtsR-mediated activation of *btsT*, nutrient limiting conditions and the presence of extracellular pyruvate have to concomitantly occur (44, 89). This system is part of a signaling network comprising another TCS, YpdA/YpdB, whose stimulus and function remain elusive, although the system also responds to external pyruvate (43, 45). Both are referred to as the pyruvate sensing network BtsSR/YpdAB.

MATERIAL AND METHODS

Bacterial strains and growth conditions. For this study we used the *E. coli* MG1655 $P_{bist-gfp}$ strain (89). This strain was grown overnight in lysogeny broth (LB) (10 g/l NaCl, 10 g/l tryptone, 5 g/l yeast extract). After inoculation, bacteria were routinely grown in LB-medium under agitation (200 rpm) at 37°C in 100 mL baffled shake flasks. For solid medium, 1.5% (wt/vol) agar was added. Where appropriate, media were supplemented with kanamycin sulfate (50 µg/ml).

Microfluidics. The microfluidic experiments were carried out in polydimethylsiloxane (PDMS)-based devices within a Nikon Ti-E Eclipse fluorescence microscopy setup (Nikon Corporation, Japan). The fabrication of the microfluidic device follows a silicon wafer processing and PDMS fabrication protocol as described in (80, 90, 91). Briefly, the microfluidic features were structured in SU-8 negative photoresist (Microchemicals GmbH, Germany) on a 4" silicon wafer. The structured wafer served as a mold for liquid PDMS (Sylgard 184, Dow Corning Corporation, USA). After curing the PDMS in an oven at 80°C for about three hours, the PDMS cast containing the channel structures was peeled off from the wafer and cut into separate devices. Inlet and outlet holes were punched using a punching needle. The device was cleaned by a rinse with Isopropyl alcohol and a subsequent treatment using adhesive tape. After cleaning, the device was bonded to a glass substrate by the application of an oxygen plasma (Femto Plasma Cleaner, Diener Electronics, Germany) for 25 s at an oxygen flow rate of 20 sccm.

Fluorescence and phase contrast images were taken using an Zyla sCMOS camera (Andor Technology Ltd, Northern Ireland) in combination with an 100x objective (Plan Apochromat λ Oil, NA=1.45, WD=170µm, Nikon Corporation, Japan). A SOLA LED lamp (Lumencor®, USA) was used as fluorescence excitation light source. Both phase contrast and fluorescence images were taken every 30 minutes using the NIS Elements Software (Nikon Corporation, Japan). Fluorescence images of the GFP signal were acquired using an YFP filter set (AHF Analysentechnik AG, Germany) featuring a 500/24 excitation filter, a 520 long-pass dichroic mirror and a 542/27 emission filter. All filter specifications are given as peak/width in nm.

Statistical analysis. Fluorescence microscopy images were analyzed using the Fiji Software (92) in combination with the MicrobeJ plugin(93), which facilitates automated cell detection and segmentation. In order to access the initial fluorescence values of the cells, the first frame of the recorded image stack was extracted and cell detection was performed on the phase contrast channel. The mode of detection in MicrobeJ was set to *Medial Axis* and the thresholding method to *Default*. As segmentation method, *LoG +*

Watershed has been selected. After obtaining and manually correcting the overlays resulting from the cell detection, the fluorescence values from each overlay in the fluorescence channel were further processed using Microsoft Excel (Microsoft Corporation, USA) and Origin (OriginLab Corporation, USA). The obtained data were used to create a fluorescence distribution of all imaged cells.

Persister cells were identified by manual tracking of surviving cells. In dense populations, the tracking of single cells may be difficult if only phase contrast images are available. The fluorescence signal helped us to identify the interesting cells. The frequency distribution depicts the fraction of values which lie within the range of values that define the bin. The bin range was kept constant at 15 AU.

RESULTS AND DISCUSSION:

Microfluidic device operation for persister cell formation assessment. As depicted in **Fig.1**, the device features three separate channel systems incorporating 50 cultivation chambers for cell cultivation. Therefore, the chip allows to perform three independent cultivations in a single experiment. The chambers are 1 μm in depth and are located between two 10 μm deep supply channels. Each channel system consists of two parallel 10 μm deep supply channels, separated by the cultivation chambers. This geometry allows fast cell seeding with high cell trapping efficiency. Another advantage of the chosen layout lies in the ability to perform smoother media changes in comparison to previous layouts, which is a crucial property for persister assays.

The device operation is illustrated in **Fig. 2**. The chambers were loaded with a cell suspension which is diluted to an OD_{600} of 2. Therefore, one supply channel was perfused with the cell suspension, while the opposing channel system was left with dead ends. This practice facilitates perfusive flow of the medium-cell suspension through the chambers and thereby enables a high cell trapping efficiency. The cells are pushed into the chambers until they are trapped by the grid at the chamber edge. After cell loading, LB-medium with ampicillin (200 $\mu\text{g}/\text{mL}$) was flushed through the supply channel, resulting in diffusive transport of the antibiotic inside the cultivation chambers. The antibiotic treatment was sustained for around three hours before the medium was changed to LB in order to observe the regrowth of persister cells.

Role of BtsSR during the process of persister cell formation. In this work we focus on the transcriptional activation of the gene *btsT*. *btsT* is the target gene of BtsS/BtsR TCS in *E. coli* (42). The histidine kinase BtsS binds pyruvate with high affinity and the consequently codes protein BtsT transports pyruvate intracellularly (88, 94). Previously we have shown that BtsSR-system mediated activation of its target gene is heterogeneous (89). Moreover, we have also shown that the presence of the pyruvate sensing network BtsSR/YpdAB lowers the number of persister cells at a population level (89). Using the microfluidic device system described above (**Fig. 2**) we aimed to elucidate, at the single-cell level, the relationship between the heterogeneous activation of P_{btsT} and the survival frequency to antibiotic treatment. The reporter strain *E. coli* MG1655 P_{btsT} -*gfp* was utilized to monitor individual cells before, during, and after treatment with the β -lactam antibiotic ampicillin. The microfluidic devices in combination with time-lapse fluorescence imaging, allowed us to observe the spatially and temporally resolved response of individual cells before and during antibiotic treatment as well as the recovery of surviving cells.

To ascertain if growth within the microfluidic devices would allow heterogeneous activation of $P_{btsT-gfp}$, cells from the reporter strain were grown in LB-medium until late exponential growth phase and loaded into the microfluidic chip. Cells were not loaded on chip directly after overnight incubation due to: (i) continuous (exponential) growth in microfluidic chambers which prevents the transient activation of P_{btsT} at the transition from exponential to stationary phase, and (ii) the fast growth of *E. coli* in LB-medium, which would cause excessive cell density in the microfluidic chambers, and thus, would prevent single-cell definition and tracking. After loading of the cells, the initial fluorescence intensities were measured. The resulting fluorescence intensities are plotted in **Fig. 3**. A Gaussian distribution of fluorescence intensities was observed, yet with high degree of cell-to-cell variability, as previously demonstrated (89). Microfluidic devices showed to be suitable for further studies by allowing heterogeneous behavior of the reporter strain.

Next, we supplied the cells with LB-medium with ampicillin and assayed for single-cell persister cell formation. Upon ampicillin treatment, most cells lysed and eventually were flushed out of the chamber (**Movie S1**). From over 50000 cells distributed over 50 cultivation chambers, 24 persister cells were observed, which were able to survive the antibiotic treatment and formed new colonies. We noticed that cells with a low initial $P_{btsT-gfp}$ signal (e.g. cell marked with an arrow in **Fig. 4**) were more likely to survive the antibiotic treatment, whereas cells with higher $P_{btsT-gfp}$ signal could not persist antibiotic treatment. Upon change of media to LB-medium (t=220 min), the cell with an initial low P_{btsT} activation was able to divide. **Data Set S1** compiles three individual cells (from three different cultivation chambers) that showed initially low *btsT* transcriptional activation and were able to restore cell division after treatment with antibiotic.

In order to statistically confirm if cells with an initially low $P_{btsT-gfp}$ signal were more prone to persist antibiotic treatment, we tracked six individual persister cells and measured their initial fluorescence intensity (FI) (**Fig. S1**). The population signal average was $\mu_0 = 49.0 \pm 12.1$ whereas the persister cells average was $FI_p = 31.3 \pm 5.9$. A t-test was performed to access whether the persister FI is significantly lower compared to the whole population ($p < 0.005$). The t-test has shown that the average FI of persister cells is significantly lower compared to the average FI of the initial population. These results corroborate the hypothesis that cells with low $P_{btsT-gfp}$ signal are more capable to survive antibiotic treatment.

Thus, we conclude that cells with an initially low $P_{btsT-gfp}$ signal have a tendency to become persister cells, which supports the interrelation of the BtsS/BtsR-system and the individual cellular metabolic state. This study has also shown the necessity of the use of microfluidic technology to obtain time-resolved information on the emergence of persister cells. The application of the microfluidic device facilitated the

tracking of individual cells and allowed to correlate the activity of the pyruvate sensing and transport system BtsSR of *E. coli* to the occurrence of persisters.

AUTHOR CONTRIBUTIONS:

E.K., C.V., A.G., D.K., K.J. conceived and designed the study, supervised the study and corrected the manuscript, wrote the paper.

E.K. and C.V. performed experiments and analyzed the data.

ACKNOWLEDGMENTS:

The development of the chip system (AG) is supported by a postdoctoral grant provided by the Helmholtz Association (PD-311). This work was financially supported by the Deutsche Forschungsgemeinschaft (DFG) SPP1617, project JU270/13-2 and KO 4537/1-2. The funders had no role in study, design, data collection and interpretation, or the decision to submit the work for publication.

COMPETING INTERESTS: The authors declare no competing interests.

FIGURES:

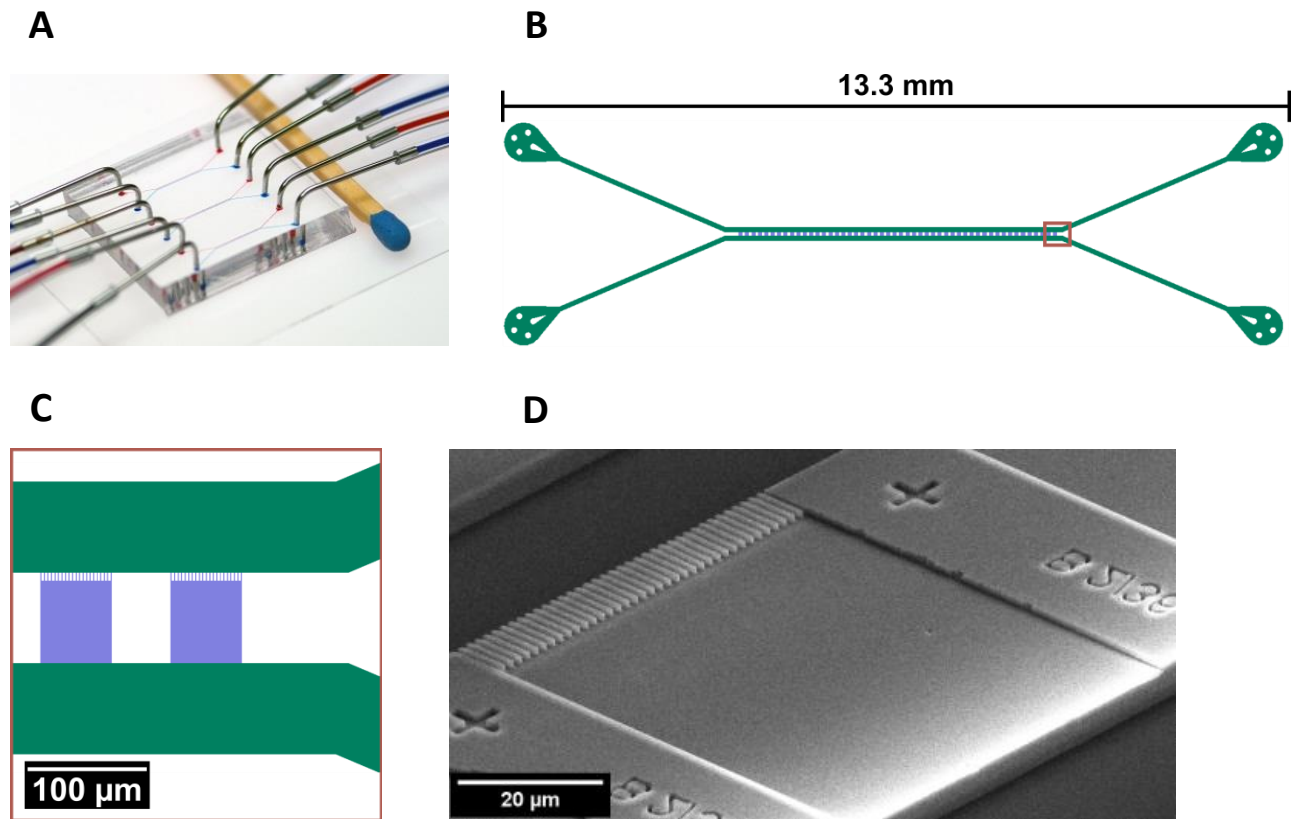


FIG 1. Illustration of the microfluidic cultivation device. (A) Photographic image of the assembled chip inheriting three channel structures and tubing connected. The device consists of a PDMS slab, which inherits the microfluidics channels, bonded to a glass substrate. For better visualization the channels are filled with dyes. (B) Top view on the channel layout. Each channel structure features two parallel 10 μm deep supply channels (green), which are connected by 1 μm deep growth chambers (blue). (C) Enlarged image of the region marked in (B) showing the chamber layout. (D) Scanning electron microscopy image of one microfluidic cultivation chamber.

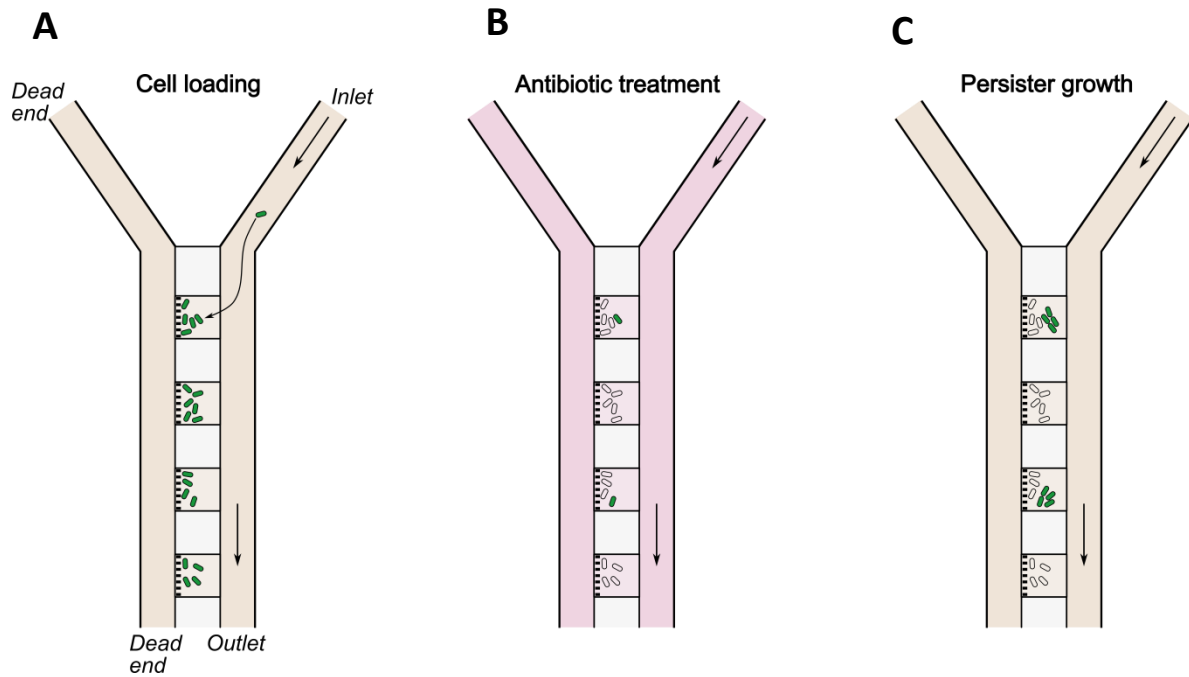


FIG 2. Scheme of the operation of the microfluidic device. (A) Cell loading procedure. Bacterial cells (green) are trapped inside the growth chambers during the infusion of the cell suspension in growth medium (yellow). (B) After treatment with antibiotic (pink), most cells die inside the growth chambers (white cells), while some persister cells are able to survive (green cells). (C) The infusion of fresh media leads to the regrowth of surviving persister cells.

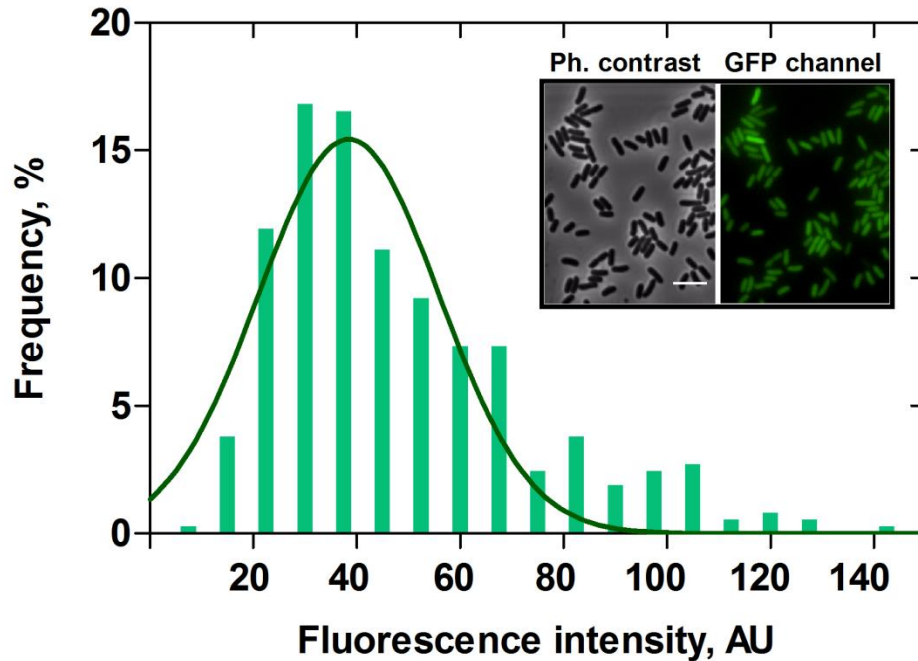


FIG 3. P_{btsT} -*gfp* expression under growth in LB-medium. *E. coli* cells expressing GFP under the control of P_{btsT} were grown in rich media LB until post-exponential growth phase and then analysed on a microfluidic chip. The corresponding distribution of the fluorescence intensity of P_{btsT} -*gfp* was plotted in the form of a histogram. A total of 200 cells were analyzed and frequency is represented as % of cells (refer to Material and Methods for detailed explanation). The continuous curve represents a Gaussian fit on the histogram of fluorescence intensity. Inlet shows representative fluorescence and phase contrast images of P_{btsT} -*gfp* reporter strain. AU, arbitrary units. Scale bar = 5 μ m.

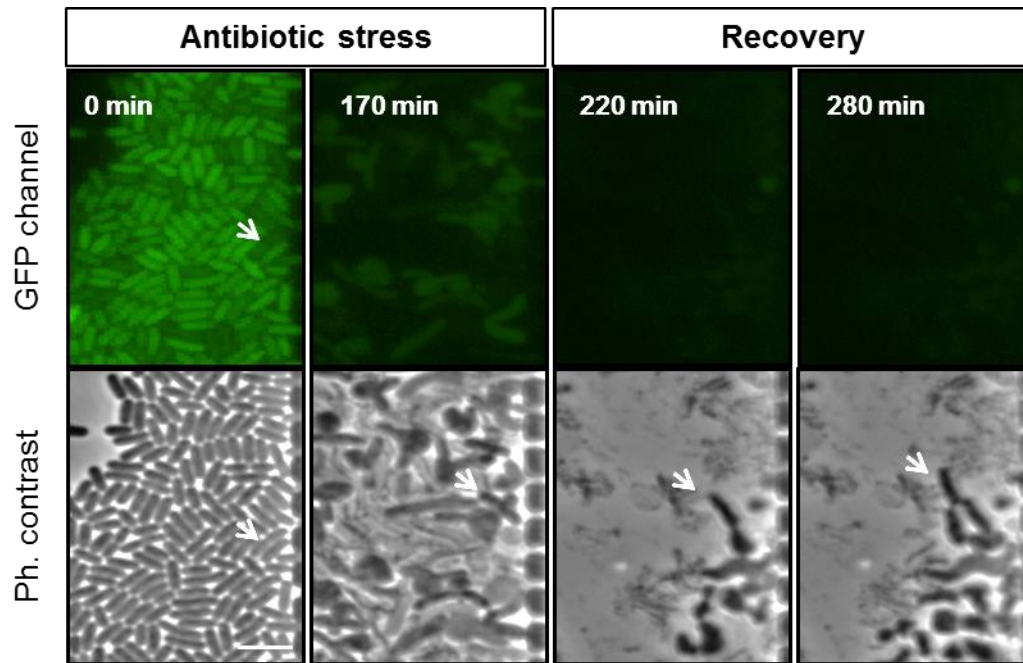


FIG 4. P_{btsT} -*gfp* expression under antibiotic stress. *E. coli* cells expressing GFP under the control of P_{btsT} were grown in rich media LB until entry to stationary phase and then analysed under antibiotic stress (200 μ g/mL of ampicillin for \sim 3h). Time-lapse imaging in microfluidic devices was performed during the course of antibiotic stress and recovery in LB. A designated cell with initial low P_{btsT} activation is marked with an arrow. Scale bar = 5 μ m.

Chapter 5

Resuscitation from the Viable but Nonculturable State of *Escherichia coli*: the importance of a pyruvate sensing network

Cláudia Vilhena^a, Eugen Kaganovitch^b, Alexander Grünberger^{b*}, Magdalena Motz^a, Dietrich Kohlheyer^b, Kirsten Jung^{a#}

^aMunich Center for Integrated Protein Science (CIPSM) at the Department of Microbiology, Ludwig-Maximilians-Universität München, Martinsried, Germany. ^b Institute for Bio- and Geosciences, IBG-1: Biotechnology, Forschungszentrum Jülich GmbH, Jülich, Germany

[#]To whom correspondence should be addressed: Prof. Dr. Kirsten Jung, Ludwig-Maximilians- Universität München, Department Biologie I, Bereich Mikrobiologie, Großhaderner Str. 2-4, 82152 Martinsried, Germany. Phone: +49-89-2180-74500; Fax: +49-89-2180-74520;

E-mail: jung@lmu.de

^{*}Present address: Alexander Grünberger, Multiscale Bioengineering, Bielefeld University, Universitätsstraße 25, 33615 Bielefeld

ABSTRACT

Viable but nonculturable (VBNC) cells endure a variety of environmental stresses (e.g., nutrient limitation, fluctuating temperatures, oxygen deprivation) during induction and resuscitation from this state. These external changes need to be sensed and the information transmitted intracellularly, allowing bacteria to respond accordingly. *Escherichia coli* contains 30 two-component systems (TCSs), each composed of a histidine kinase (HK) and a response regulator (RR). The BtsS/BtsR and YpdA/YpdB TCSs have been characterized in more detail in our laboratory. We demonstrated that BtsSR/YpdAB sensing network responds to extracellular pyruvate.

We tested the effect of these two systems on the induction and resuscitation of *E. coli* from the VBNC state. Restoration of culturability occurred only in the concomitant presence of pyruvate and the BtsSR/YpdAB systems. Deletion mutants presented extremely low protein and DNA biosynthesis during resuscitation, corroborating the importance of the BtsSR/YpdAB systems. Furthermore, we performed time-lapse microscopy and monitored pyruvate- and BtsSR/YpdAB- dependent resuscitation of *E. coli* from the VBNC state at single-cell level. Finally, we performed transport assays and discovered that pyruvate is taken up by the VBNC cells. Our results demonstrate the importance of sensing and transporting pyruvate during resuscitation of *E. coli* from the VBNC state.

IMPORTANCE

Viable but nonculturable (VBNC) organisms have been underestimated and neglected when studying dormant phenotypes. In clinical settings, VBNC cells may contribute to non-apparent infections capable of being reactivated after months or even years, as for the case of *Mycobacterium tuberculosis*. The lack of specific and reliable methodology prevents the proper characterization of the VBNC state. Ultimately, these organisms pose a public health risk with potential implications in several industries ranging from pharmaceuticals to food industry. Research regarding their induction and resuscitation is of major importance.

Bacteria are able to respond to several environmental and physiological oscillations in part via two-component systems (TCSs). BtsS/BtsR and YpdA/YpdB are two TCSs of *Escherichia coli* that form a pyruvate sensing network. Their role in the VBNC state is explored in this study.

Key Words: metabolism, oxidative stress, scavenging, heterogeneity

INTRODUCTION

Viable but nonculturable (VBNC) organisms are characterized by a loss of culturability on routine culture media yet with maintenance of viability markers (95). They are phenotypic variants among the population that act as a survival strategy upon adverse environmental conditions (96, 97) which makes them appealing and challenging candidates for pharmaceutical intervention. Situations of extreme temperatures and/or oxidative stress promoting conditions, are known to trigger the induction into the VBNC state of several organisms (98–100). The process of regaining culturability is called *resuscitation* and compounds promoting the restoration of culturability have been described, e. g. YeaZ promoting-factor, catalase, α -ketoglutarate, and pyruvate (98, 101–103).

In both induction and resuscitation processes, establishing communication between the extracellular environment and the intracellular space is of crucial importance. *Escherichia coli* and many other organisms use two-component systems (TCSs) to ascertain this communication (104). A membrane integrated histidine kinase (HK) perceives the stimulus and a cytosolic response regulator (RR) mediates an appropriated output. In the last years, we have studied in detail two of these TCSs of *E. coli*, BtsS/BtsR and YpdA/YpdB systems (42, 43, 45, 88, 89, 94). Both TCSs respond to extracellular pyruvate, though with different affinity, thus forming the pyruvate sensing network BtsSR/YpdAB. The target protein of BtsS/BtsR, BtsT, has been recently identified as a high-affinity pyruvate/H⁺ symporter (88). The pyruvate sensing/transport capacities of the network BtsSR/YpdAB might constitute a proper tool to study the underlying resuscitation mechanism of VBNC cells.

The VBNC state of several organisms has been extensively studied in the last decades, for instance *Vibrio* species (103, 105, 106), *Salmonella typhi* (107), *Campylobacter jejuni* (108), *Lactobacillus acetotolerans* (109), *Yersinia pestis* (110) and clinical isolates from *E. coli* (111). Characterization of the induction into this state has mainly comprised cold temperatures and oxidative stress experimental designs in order to mimic the real habitat challenges of these organisms (food conservation, milk pasteurization and chlorination of wastewater) (95, 112).

A comprehensive study of the induction and resuscitation of the commonly laboratory studied gram-negative bacterium *E. coli* K-12 strain MG1655 under cold stress has not yet been done. With this work we aimed to further explore the induction profile into the VBNC state of *E. coli* MG1655 when cells are kept at cold temperature for a long period of time and clarify the concrete role of pyruvate sensing/transport during resuscitation. For this purpose, throughout this study we compare two strains: *E. coli* MG1655 wild-type (WT) and *E. coli* MG1655 $\Delta btsSR\Delta ypdAB$ (*btsSRypdAB* mutant) which comprises

the deletions of two operons: *btsSbtsR* which codes for the BtsS/BtsR pyruvate transport system and *ypdAB* which codes for the pyruvate responsive system YpdA/YpdB.

RESULTS

Cold-stressed *E. coli* entry into the VBNC state is independent of the pyruvate sensing network. The VBNC state of *E. coli* was induced by long term storage at 4°C of cell suspensions of WT and *btsSRypdAB* mutant in LB medium. After 120 days, culturability was lost for both tested strains (**Fig. 1A**). No significant difference between the two strains was observed in terms of colony forming units (CFU). To access viability, membrane potential and respiratory activity of these strains was assayed (**Table 1**). After 120 days of incubation at 4°C, the membrane potential was kept in around 8% of WT and 9% of *btsSRypdAB* mutant cells. Respiratory activity, assayed by reduction capacity of 5-cyano-2, 3-ditolyl tetrazolium chloride (CTC) by the cells, reached percentages in the same range. These results show that a portion of the WT and *btsSRypdAB* mutant populations was viable yet not culturable, with no difference in the percentage of viable cells between the tested strains. Total protein amount was also calculated and proved that both strains reached the state with equal amount of protein (WT= 1.65±0.05 mg/mL and $\Delta btsSR\Delta ypdAB$ =1.72±0.03 mg/mL). An unpaired *t* test was performed and no significant difference was observed between the two strains.

To verify if the WT strain had any of the components of the pyruvate sensing network up or down regulated upon entry into the VBNC state, a proteomic analysis of the viable cellular fraction was performed using density gradient centrifugation with Percoll (113, 114) followed by mass spectrometry analysis. The two detectable proteins BtsR and BtsT were not significantly upregulated in the VBNC state (**Fig. S1**). Interestingly, the most differentially expressed proteins were mostly associated with stress response (e.g. CspB, CspI, YdfK, UspE, UspF), central and intermediary metabolism (e.g. LdcI, BgaL, YbiC, GarR, LdhD, Fnr), transport (e.g. YdcS, PlaP) and translation (e. g. Sra, TtcA) which is in conformity with previous studies that report proteomic analysis made in VBNC cells from several organisms (111, 115, 116).

BtsSR/YpdAB systems did not influence the induction into VBNC state via cold stress.

BtsSR/YpdAB systems are required for the resuscitation from the VBNC state of *E. coli*. LB medium supplemented with pyruvate was assayed as resuscitation medium, however resuscitation was not observed (data not shown). The only media that sustained resuscitation was 0.1x LB medium with undiluted salt concentration (dLB) and this was used throughout the assays. A control experiment without pyruvate resulted only in a slight increase in culturable cell numbers for the WT strain (**Fig. 2-Control**). *btsSRypdAB* mutant did not resuscitate under such condition. When pyruvate was used to promote resuscitation, WT strain significantly increased culturable cell numbers, whereas *btsSRypdAB* mutant

remained unresponsive (**Fig. 2-Pyruvate**). We further analysed the complemented strain of the *btsSRypdAB* mutant and found a resuscitation profile resembling the WT pattern, showing that the effect is specific for these systems action (**Fig. 2, green bars**). As positive control α -ketoglutarate was tested and promoted resuscitation of all three tested strains, however *btsSRypdAB* mutant did not resuscitate to the same extent as the WT strain. As negative control, acetate was given in the media and resulted in no resuscitation for any assayed strain. These results demonstrated for the first time a dependency on the pyruvate sensing network BtsSR/YpdAB for the resuscitation of cold-stressed *E. coli* VBNC cells.

To get further confirmation of the pyruvate- and BtsSR/YpdAB-dependent resuscitative effect on *E. coli* VBNC cells, DNA (**Fig. 3A**) and protein (**Fig. 3B**) biosynthesis rates were measured on the early stages of resuscitation. Within the first 40 min, an increase in both DNA and protein biosynthesis was observed for the WT and complemented strain. Interestingly, *btsSRypdAB* mutant showed very little to none incorporation of the radioactive labelled compounds, showing that the intracellular machinery is in fact impaired under the tested resuscitation conditions.

Single-cell pyruvate-mediated resuscitation from the VBNC state occurs only in the presence of BtsSR/YpdAB network. To further explore the behaviour of single individuals among the population during resuscitation, we performed time-lapse imaging on VBNC cells undergoing resuscitation. We used microfluidic devices (83) which guarantee constant environmental conditions (temperature, oxygen, etc) and simultaneously allow us to observe the response of individuals undergoing resuscitation from the VBNC state with high spatial and temporal resolution.

Both WT and *btsSRypdAB* mutant strains were loaded on chip and dLB medium alone was flushed in the supply channels. Cell lysis was observed for both tested strains; however none could successfully restore cell division (**Movies S1, S2**). Two types of cells could be morphological identified. Some cells were small and clear, common features of dead cells after cell lysis. Other cells were darker, longer and wider, resembling healthy *E. coli* cells. The later tipe is referred to as “potential” dividing cells.

Next we tested the capacity of both the WT and the *btsSRypdAB* mutant strain to resuscitate on chip using as media dLB medium supplemented with pyruvate (**Movies S3, S4**). As expected, the WT strain restored cell division. In average, the first division occurred after around 2h of cultivation (**Fig. 4A**). When BtsSR/YpdAB systems were absent, no cell division was observed.

The previously mentioned complemented strain was also assayed for resuscitation in both dLB medium alone or supplemented with pyruvate, and the results resembled a WT-like behaviour. These results prove the specificity for the systems activity (**Fig. 4, Movies S5, S6**). To notice that the resuscitation of the complemented strain at the single-cell level was faster than the WT case (appearance of the first cell

division after 1h for the complemented strain and after 2h for the WT, **Fig.4**). The fact that the complemented strain harbours a plasmid might influence the induction and resuscitation from the state, as previously reported (117–119). We observed a rather faster entrance into the VBNC state (data not shown) which might account for the quicker resuscitation.

In order to quantitatively access the single-cell resuscitation, we measured growing cells. For that the total number of “potential” dividing cells was counted on the first frame (t=0 h) and manual tracking of those cells was performed to verify cell division. The percentage of growing cells regarding the initial cell count was plotted in **Fig. 4B**. Corroborative results show that only WT (~20%) and complemented strain (~35%) are able to restore cell division upon cultivation in dLB supplemented with pyruvate.

The single cell analysis is in conformance with the population-based assays, which showed the importance of BtsSR/YpdAB pyruvate sensing network in promoting resuscitation from the VBNC state of cold-stressed *E. coli* cells.

Pyruvate is uptaken by VBNC cells during resuscitation. After showing that BtsSR/YpdAB systems are crucial for a proper resuscitation from the VBNC state, we decided to further explore the role of pyruvate in the resuscitation process. For this purpose, we assayed the intracellular transport of radioactive labelled pyruvate by VBNC cells induced at 4°C as described in Materials and Methods. WT strain and *btsSRypdAB* mutant underwent resuscitation in dLB medium. A mixture of ¹⁴C-Pyruvate and cold-pyruvate was used as promoter for resuscitation to a final concentration of 80 µM. Within 20 sec, the WT strain was able to uptake pyruvate to a maximal rate of 0.33 nmol of pyruvate per mg of protein (**Fig. 5**). The presence of BtsSR/YpdAB systems allowed a significantly higher transport of pyruvate (3-fold) when comparing to a mutant of the pyruvate sensing network of *E. coli*. The peak of transported pyruvate was followed by a steady state at around 30 sec. These results show for the first time transport of pyruvate by cold-stressed *E. coli* VBNC cells, suggesting that pyruvate might also function as carbon source for the cell during early resuscitation.

DISCUSSION

The VBNC state is for pathogens and non-pathogens a survival strategy which pose potential health risks in medicine, food and water industries (120). It is of major importance to characterize the state in terms of induction and resuscitation mechanisms in order to better control the eradication/maintenance of cells in this state.

This study shows the relevance of a pyruvate sensing network of *E. coli* in the resuscitation process from cold-stressed VBNC cells. So far, the BtsSR/YpdAB pyruvate sensing network is known to contribute to a balancing of the physiological state of all cells within a population (89). The systems help ensuring an optimized use of the available resources so that the entire population can bear forthcoming metabolic stresses.

Here we enlarge the phenotypic relevance of the systems by showing that although their function does not alter the entry into the VBNC state (**Fig. 1**), the network has an impact on the resuscitation process. On batch experiments, culturability was restored after 5h incubation in fresh media (followed by overnight incubation in solid media) with the concomitant presence of pyruvate and BtsSR/YpdAB systems (**Fig. 2**). A mutant of the network was only able to resuscitate upon presence of α -ketoglutarate.

Resuscitation was not only accessed through restoration of culturability, but also by DNA and protein biosynthesis rate measurements (**Fig. 3**). Cells showed an initial ($t=0$ min) synthesis rate ($< 5\%$) which further corroborate their viability with no culturable cells detected at that time point. In less than 40 min, biosynthesis of DNA and protein was considerably restored in WT and complemented strain, in accordance to similar studies performed in the closely related *Salmonella enterica* (102). Surprisingly, no CFU was observed after 40 min incubation in fresh liquid media with pyruvate (data not shown). We suggest that the adaptation required from VBNC cells to a different and richer media followed by a drastic change in media consistency (from liquid to solid) explains why at such early stages of resuscitation no CFU is observed yet DNA and protein are being synthesized. This hypothesis is in accordance with previous studies performed in *E. coli* adaptation capacity in liquid and solid media, which concluded that adaptation is slower in structured (solid) media and a lag phase of around 3h occurs when cells are shifted from liquid to solid LB medium (121, 122). The single cell analysis of the resuscitation process agreeably confirmed the response of cells to pyruvate only when the BtsSR/YpdAB network is present (**Fig. 4**). For the first time, microfluidic devices were used to access resuscitation from cold-stressed VBNC cells. The devices allow optimal and controlled growth conditions for each single bacterium, avoiding misjudgements of bacterial behaviour based on heterogeneous cultivation conditions (80). The continuous media perfusion results in continuous growth, which accounts for the fairly quick response of cells to

pyruvate under microfluidic cultivation in contrast to the resuscitation experiments performed on batch cultures.

Several studies have described pyruvate as a main promoter of resuscitation, yet with an unclear mechanism (102, 123, 124). Although its role as ROS scavenger has been previously described (98), we sought to investigate if pyruvate could also be uptaken by the cells and potentially used as a carbon source. Pyruvate was transported intracellularly within 20 sec in the WT strain and the uptake was significantly lower when BtsSR/YpdAB network was absent (**Fig. 5**). We provide the first described uptake of pyruvate by VBNC cells which constitute a ground-breaking finding for the community, enlarging the role of pyruvate in resuscitation beyond its ROS scavenging capacity. Further studies elucidating the intracellular mechanism of pyruvate metabolization upon resuscitation are required.

In summary, based on our presented results, a comprehensive model of cold-stressed *E. coli* VBNC cells resuscitation can be ascertained. Pyruvate is uptaken within the first seconds of resuscitation by VBNC cells in part via BtsSR/YpdAB systems, which allows the cell machinery to restarts DNA and protein biosynthesis within the first hour. Cell division in liquid media occurs immediately, however culturability is ultimately restored in routinely used LB-agar plates after overnight incubation. The entire process is dependent on the pyruvate sensing network BtsSR/YpdAB.

MATERIALS AND METHODS

Strains, plasmids and oligonucleotides. In this study we used *E. coli* strains MG1655 (125) and *E. coli* MG1655 $\Delta btsSR\Delta ypdAB$ (89). For complementation *in trans* of the mutant strain, the plasmid pCOLA-*btsSR-ypdAB* was constructed by inserting *btsSR* (on BamHI and NotI sites) and *ypdAB* (on the XhoI and NdeI sites) on pCOLA-Duet-1 vector (Merck, Darmstadt). All oligonucleotide sequences are available on request.

Molecular biological techniques. Plasmid and genomic DNAs were isolated using a HiYield plasmid minikit (Suedlaborbedarf) and a DNeasy blood and tissue kit (Qiagen), respectively. DNA fragments for plasmid construction were amplified from genomic DNA by PCR. DNA fragments were purified from agarose gels using a HiYield PCR clean up and gel extraction kit (Suedlaborbedarf). Q5 DNA polymerase (New England BioLabs) was used according to the supplier's instructions. Restriction enzymes and other DNA-modifying enzymes were also purchased from New England BioLabs and used according to the manufacturer's directions.

Growth conditions. *E. coli* MG1655 strains were grown overnight in lysogeny broth (LB) (10 g/l NaCl, 10 g/l tryptone, 5 g/l yeast extract). After inoculation, bacteria were routinely grown in LB medium under agitation (200 rpm) at the designated temperature. For solid medium, 1.5% (wt/vol) agar was added. Where appropriate, media were supplemented with antibiotics (kanamycin sulphate, 50 μ g/ml).

Induction into the VBNC state. *E. coli* MG1655 strains were grown overnight as described above. On the day cells were routinely grown in LB medium until optical density (OD) reached 1.2. Bacteria were harvested by centrifugation and sequentially washed twice with ice-cold PBS. Cells were resuspended in LB medium to a final cell density of 10^{10} cells/mL and held without shaking at 4°C for long-term cold stress.

Viability validation. 5-cyano-2, 3-ditoyl tetrazolium chloride (CTC)-reduction assay was carried out with the reagents of a Bacstain- CTC Rapid Staining Kit (Dojindo Kumamoto, Japan) according to the manufacturer's instructions. This kit provides indication of bacterial aerobic respiration (126), therefore functioning as a viability indicator. CTC is reduced by an active electron transport system to the insoluble fluorescence (red) salt formazan, which can be detected using fluorescence microscopy.

Samples from inducing VBNC cultures were taken and diluted with PBS to a final cell density of 10^6 cells/mL. For each 1 mL of cell suspension, 20 μ L of CTC solution and 1 μ L of enhancing reagent A were added. Bacterial suspensions were incubated for 30 min at 37°C protected from the light. Cells were further analysed via flow cytometry.

Alternatively, inducing VBNC cells were checked for viability using the BacLight™ Bacterial Membrane Potential Kit (Invitrogen). Diethyloxycarbocyanine (DiOC₂) exhibits green fluorescence in all bacterial cells, but the fluorescence shifts towards red emission as the dye molecules self-associate in the presence of higher membrane potentials. As a measure of viability, the ratio red to green fluorescence was calculated. Approximately 10^6 cells/mL were aliquoted and per each 1 mL of cell suspension, 10 μ L of 3 mM DiOC₂ was added followed by incubation at room temperature for at least 20 min, protected from light. Cells were further analysed via flow cytometry.

Flow cytometry. Aliquots from inducing VBNC cells were taken, diluted 1:1000 in PBS and analysed on flow cytometer BD Accuri™ C6 equipped with a solid-state laser (488 nm-emission; 20 mW). Forward angle light scatter (FSC) and side angle light scatter (SSC) were collected in the FSC detector and SSC filter (BP 488/10 filter) respectively. The red-fluorescence emission was collected by the FL2 filter (BP 585/40 filter). The green-fluorescence emission was collected by the FL1 filter (BP 533/30 filter). Sheath flow rate was 14 μ L/min and no more than 100000 events/second were acquired. For each sample run, a total of 10000 events were collected. Analysis of data was carried out using Cytospec software (http://www.cyto.purdue.edu/Purdue_software).

Resuscitation procedures from the VBNC state. Resuscitation from cold-stressed VBNC cells was performed by harvesting the cells from 4°C incubation flasks, resuspension in dLB medium alone (unaltered salt concentration) or supplemented with 2 mM of either pyruvate, α -ketoglutarate or acetate and incubation at 37°C for at least 5h. Further enumeration of CFU from LB-agar plates was taken as a measure for restoration of culturability.

Protein and DNA biosynthesis during resuscitation. *E. coli* VBNC cells were resuspended to 10^8 cells/mL in dLB medium supplemented with 2 mM pyruvate. The VBNC cells undergoing resuscitation were incubated with either L-[³⁵S] methionine / L-[³⁵S] cysteine (11 mCi/mL; 37 MBq, Biotrend) or [methyl-³H] thymidine (1 mCi/mL; 74GBq/mmol, Biotrend) and incubated at 37° C for several time points up to 60 min. After incubation, 50% TCA/PBS (Carl Roth GmbH) was added to stop the incorporation of the radiolabelled compounds. Samples were left on ice for 15 min and later harvested by centrifugation.

The pellets were washed twice with 10% TCA/PBS and finally dissolved in 0.1 M NaOH (pH was neutralized with drops of HCl). Radioactivity was measured in a Liquid Scintillation Analyser (PerkinElmer). Incorporation of ^3H -Thymidine and ^{35}S -Methionine/Cystein was measured as *biological activity*, meaning the percentage of incorporation relative to the positive control (intact logarithmic *E. coli* MG1655 population).

Pyruvate transport assays. For pyruvate transport assay, aliquots from *E. coli* VBNC cells were re-inoculated into dLB medium. Subsequently, ^{14}C pyruvate (50-60 mCi/mmol, final concentration of 14.4 μM Biotrend) and cold-pyruvate (final concentration of 65.6 μM) were added to 200 μL cell suspension to a final substrate concentration of 80 μM . Cells were incubated at 37°C for several time intervals. Transport was terminated by addition of 100 mM potassium buffer (pH 6.0) and 100 mM LiCl (stop buffer) followed by rapid filtration through membrane filters (Macherey-Nagel, MN GF-5 0.4 μm). The filters were dissolved in 5 mL of scintillation fluid (MP Biomedicals) and the activities (counts per minute, CPM) were determined by a Liquid Scintillation Analyser (PerkinElmer). The experiment was repeated 3 times for reproducibility check.

Microfluidics

The microfluidic experiments were performed in Polydimethylsiloxan (PDMS)-based devices within a Nikon Ti-E Eclipse fluorescence microscopy setup (Nikon Corporation, Japan). Phase contrast images were taken using an Andor Luca R CCD camera (Andor Technology Ltd, Northern Ireland) in combination with an 100x objective (Plan Apochromat λ Oil, NA=1.45, WD=170 μm , Nikon Corporation, Japan). Images were taken every 10 min.

The microfluidic devices were fabricated using a soft lithography process as described in (90, 127). The device features 50 cultivation chambers for cell cultivation. The chambers are 1 μm in depth and feature a cultivation area of 60x70 μm^2 , resulting in a volume of 4.2 picoliters. The chambers are located between two 10 μm deep channels which provide for medium supply (80). Image processing was carried out in Fiji (92).

Sample preparation and Mass Spectrometry. Aliquots of VBNC cell cultures (100 mL) were harvested and resuspended in 20 mL of PBS buffer (8,1 mM Na_2HPO_4 ; 1,47 mM KH_2PO_4 ; 137 mM NaCl; 2,68 mM KCl; pH 8,25) plus 30 mL of Percoll (GE Healthcare Sciences) for a final colloidal silica solution concentration of 60%. Viable and dead cells were separated by several density gradient centrifugation steps. First, the sample was centrifuged at 10,000 rpm at 4°C for 1h until two distinct cell layers were

visible. The lower one was collected and resuspended in 70 mL of PBS. The cells were washed and isolated by three centrifugation steps at 5,000 rpm for 45 min each at 4°C and finally the pellet was resuspended in 50 mL PBS.

For mass spectrometry analysis, cells were disrupted by ultrasonic treatment followed by tryptic protein digestion with the kit “iST” from Preomics.

Statistical analysis. All experiments were repeated at least 3 independent times. Statistical analysis was carried out using GraphPad Prism (version 5.03 for Windows, USA). Data was assessed for significance between tested groups by using one-way analysis of variance (ANOVA) followed by Tukey’s multiple comparison *post hoc* test. Error bar on graphs represent standard errors of the mean. When indicated, an unpaired *t* test was performed.

Acknowledgments

This work was financially supported by the Deutsche Forschungsgemeinschaft (DFG) SPP1617 projects JU270/13-2 (KJ) and KO 4537/1-2 (DK). The funders had no role in study, design, data collection and interpretation, or the decision to submit the work for publication.

TABLES

Table 1 – Viability determinations on long-term cold-stressed cell cultures of WT and *btsSRypdAB* mutant

	WT	<i>btsSRypdAB</i>
Membrane potential-positive cells (%)	8±0.7	9±0.3
Respiratory activity-positive cells (%)	9±1	6±0.5
Total protein amount (mg/mL)	1.65±0.05	1.72±0.03

FIGURES

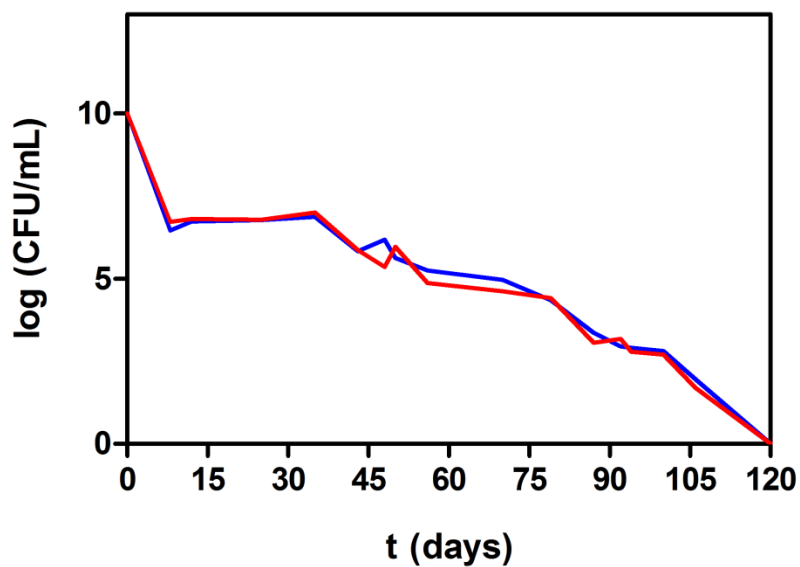


FIG 1. Culturability profile of cold-stressed *E. coli* cells. *E. coli* MG1655 WT (blue) and *btsSRypdAB* mutant (red) cells were grown in LB until OD₆₀₀ reached 1.2, washed with PBS and resuspended in LB to a final OD₆₀₀ of 1 and incubated at 4°C for 120 days. Culturability was accessed by periodical serial dilutions followed by plating of cell cultures aliquots in LB-agar plates. All experiments were performed in triplicate and mean values are shown. Standard deviations were below 10%.

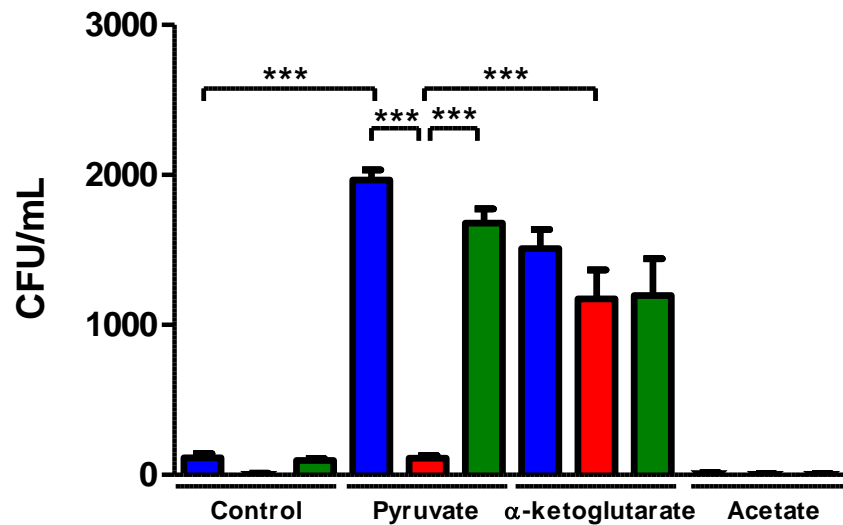


FIG. 2. Culturability restoration of cold-stressed *E. coli* VBNC cells. *E. coli* MG1655 WT (blue), *btsSRypdAB* mutant (red) and the complemented *btsSRypdAB* mutant with pCOLA-*btsSR-ypdAB* (green) were induced into the VBNC state by long term storage at 4°C. Resuscitation was performed by resuspending cells in dLB medium alone (control) or supplemented with 2 mM of either pyruvate, α -ketoglutarate or acetate; cells suspensions were grown at 37°C for 5 h and plated in LB-agar plates. Error bars represent standard error. Significant differences of the CFU number between different strains and cultivation conditions are marked in the figure (***, P-value<0.001).

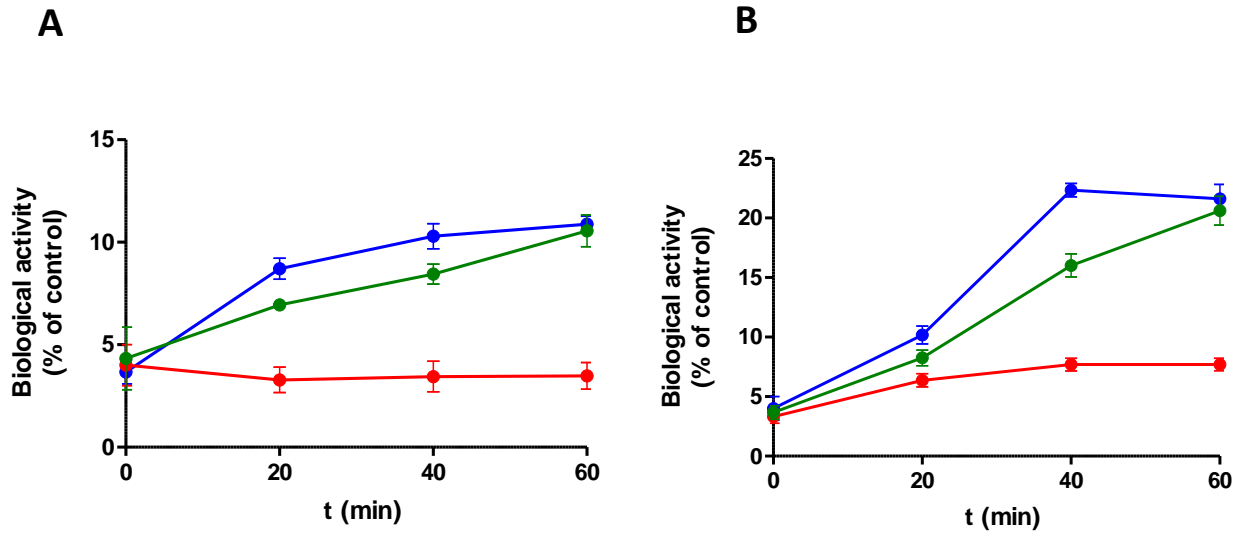


FIG. 3. DNA and protein synthesis of cold-stressed *E. coli* VBNC cells. *E. coli* MG1655 WT (blue), *btsSRypdAB* mutant (red) and the complemented *btsSRypdAB* mutant with pCOLA-*btsSR-ypdAB* (green) were induced into the VBNC state by long term storage at 4°C and assayed for DNA (A) and protein (B) biosynthesis during resuscitation with dLB medium supplemented with 2 mM pyruvate. Biological activity refers to the percentage of incorporation according to the control (*E. coli* MG1655 on exponential growth). All experiments were performed in triplicate and error bars represent standard errors.

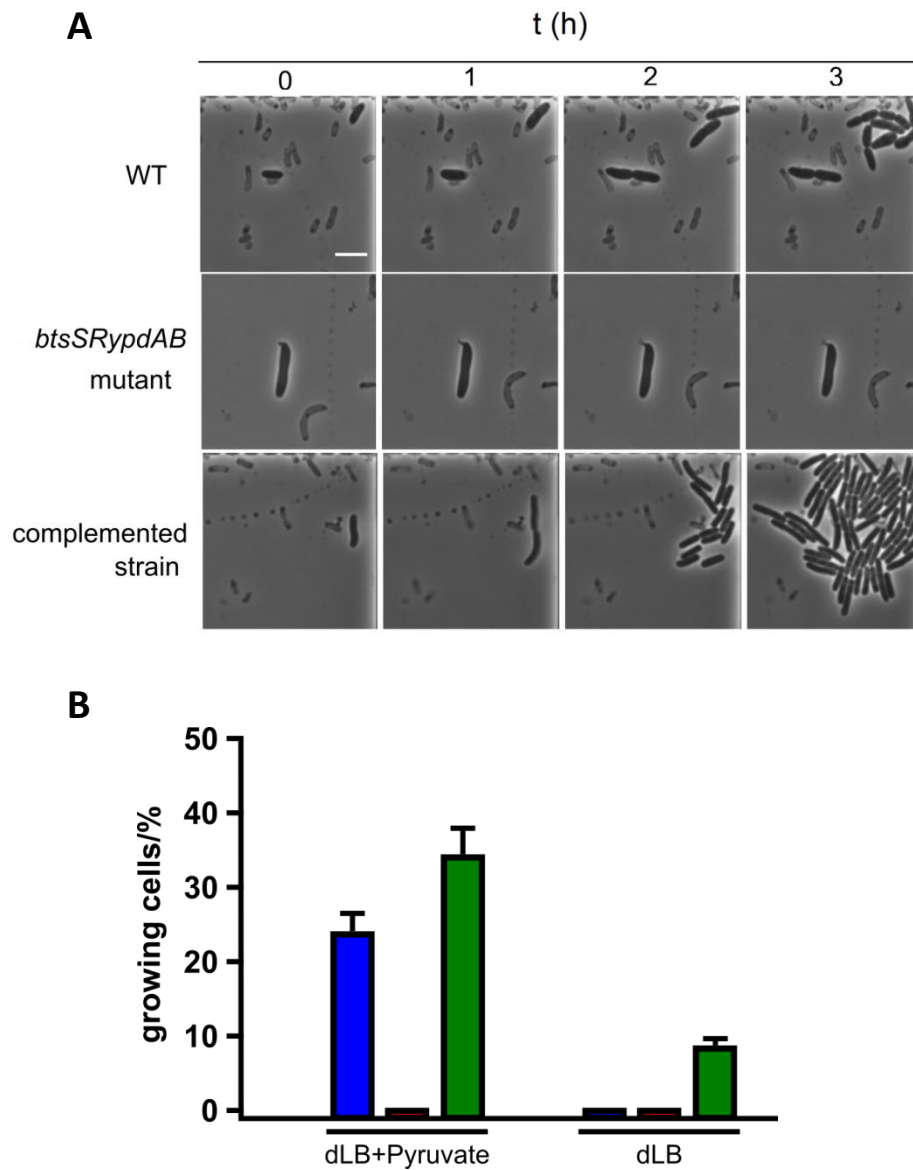


FIG.4. Single-cell analysis of *E. coli* VBNC cells resuscitation. Resuscitation was assayed in microfluidic devices as described in Material and Methods. (A) Representative phase contrast microscopy images of cells under resuscitation in dLB medium supplemented with pyruvate are shown for selected time points. Scale bar 5 μ m. (B) Quantitative assessment of growing (resuscitated) cells in microfluidic devices from *E. coli* MG1655 WT (blue), *btsSRypdAB* mutant (red) and the complemented *btsSRypdAB* mutant with pCOLA-*btsSR-ypdAB* (green). Error bars represent standard errors.

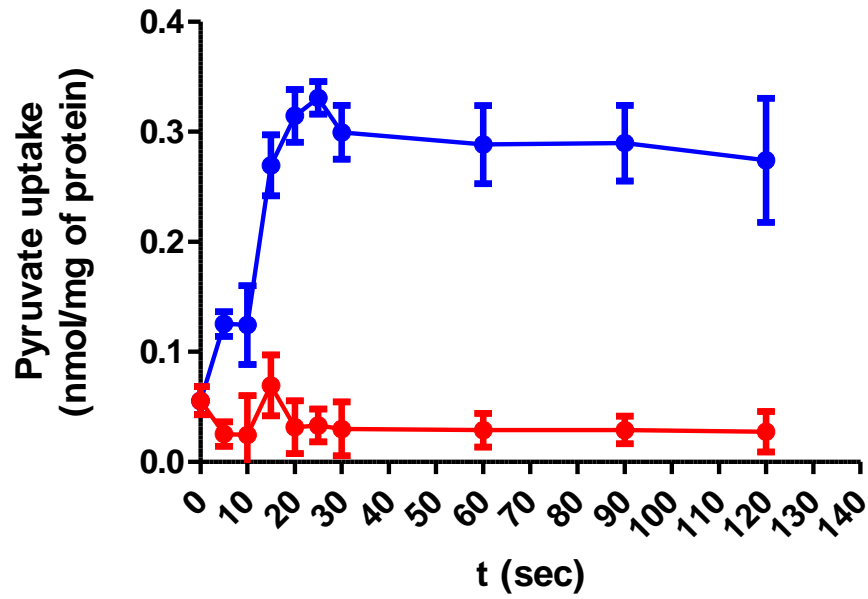


FIG.5. Pyruvate transport by cold-induced *E. coli* VBNC cells during resuscitation. *E. coli* MG1655 WT (blue), *btsSRypdAB* mutant (red) were induced into the VBNC state by long term storage at 4°C. Transport of pyruvate by VBNC cells during the resuscitation process was assayed as described in Material and Methods. Error bars represent standard errors.

Chapter 6

Concluding discussion

6.1-Single-cell analysis of *btsT* (*yjiY*) and *yhjX* transcriptional activation

Studies of TCSs usually focus on elucidation of the phosphorylation capacities (128), crosstalk between TCSs (129) and theoretical approaches (130). However, single-cell research has enlarged and clarified bacterial behavior greatly (78).

BtsS/BtsR and YpdA/YpdB systems of *E. coli*, the only two known members of the LytS/LytTR family in this organism, were extensively studied and characterized using population-based approaches (42, 43, 45, 46, 94). The gap on the single-cell analysis of these systems transcriptional activation was filled on this thesis (**Chapter 2**).

6.1-1. Heterogeneity of *btsT* and *yhjX* transcriptional activation

Transcriptional fluorescence reporter strains were constructed for each target gene and tested in LB medium. The promoter activation at the onset of stationary phase is heterogeneous for both of the target genes (89). The heterogeneity of *yhjX* depends on the external pyruvate concentration (**Fig. 6.1**). The higher the pyruvate concentration supplied externally, the more homogenous is a population of *yhjX* promoter (P_{yhjX}) tagged cells and higher the signal intensity. Interestingly, for the transcriptional activation of *btsT* (former *yjiY*) the scenario is different. *btsT* promoter is not active solely upon growth in minimal medium supplemented with pyruvate, as expected given that BtsS (the corresponding HK of the BtsS/BtsR system) binds external pyruvate. When cells from an *btsT* promoter (P_{btsT}) tagged cells are grown for one hour in nutrient limiting conditions (LB that has been diluted ten times) and subsequently are given pyruvate, a drastic increase in P_{btsT} activation is observed. Most surprisingly, the distribution of frequency intensities is rather heterogeneous. The heterogeneity is not influenced by increasing concentrations of the given pyruvate, which points for a further step of regulation in terms of establishment of the heterogeneous behavior. In *B. subtilis* a very similar study was performed where YsbA (later renamed to PftA) was identified as being essential for pyruvate utilization (131). The transcription activation of *ysbA* occurred also at the transition to stationary phase, was decreased upon

addition of glucose and, most striking, was also heterogeneous, with unimodal distribution of signal intensities.

In this thesis a mathematical equation for the noise value is used: $N = \frac{\sigma}{\mu}$, where N is noise, σ the standard deviation and μ the mean of the population. This coefficient is commonly referred to as *coefficient of variation* and provides a measure of dispersion of a probability distribution or frequency distribution (132). However, it appears difficult to compare cell-to-cell variations with significantly different expression levels (μ values) since expression noise is usually decreasing with elevated expression levels according to the scaling law (133). According to this law, gene expression noise is inversely proportional to the gene expression level, e. g. highly expressed genes generate a low noise compared to the low level expressed gene that yield to high noise (134, 135). When comparing P_{btsT} and P_{yhjX} corresponding activation noise levels, can be ascertained that P_{btsT} is more heterogeneously activated than P_{yhjX} . However, this is a mathematical misconception as the single-cell analysis showed similar heterogeneous signal for both reporter strains. The scaling law explains why, most likely, the two genes have similar heterogeneous activation, and not one preferably over the other.

Studying the establishment of the heterogeneous behavior is challenging for both target genes as their activation is strongly influenced by the external concentration of pyruvate and the metabolic state of the cells. Pyruvate has, however, also endogenous production and participates in several metabolic pathways due to its central position in carbon metabolism (136). Pyruvate levels are crucial to be maintained and are further influenced by the type of respiration (the role of pyruvate is going to be discussed in section 6.2 of this thesis).

6.1-2. Modulators of the heterogeneous behavior

A point of argumentation is the mechanism underlying the establishment of the observed heterogeneity. Actually, transcription heterogeneity may not be fully representative of the phenotypic heterogeneity observed in bacterial populations. Changes in mRNA stability, translation, and protein stability within individual cells are also expected to play important roles in defining gene expression noise and consequently the phenotypic heterogeneity.

Several factors that might influence differential gene expression for the case of *btsT* and *yhjX* will be explored in the following paragraphs (**Fig. 6.1**). First, the binding of the RRs, BtsR and YpdB. Although not characterized for BtsR, the binding to the promoter region has been explored for YpdB (46).

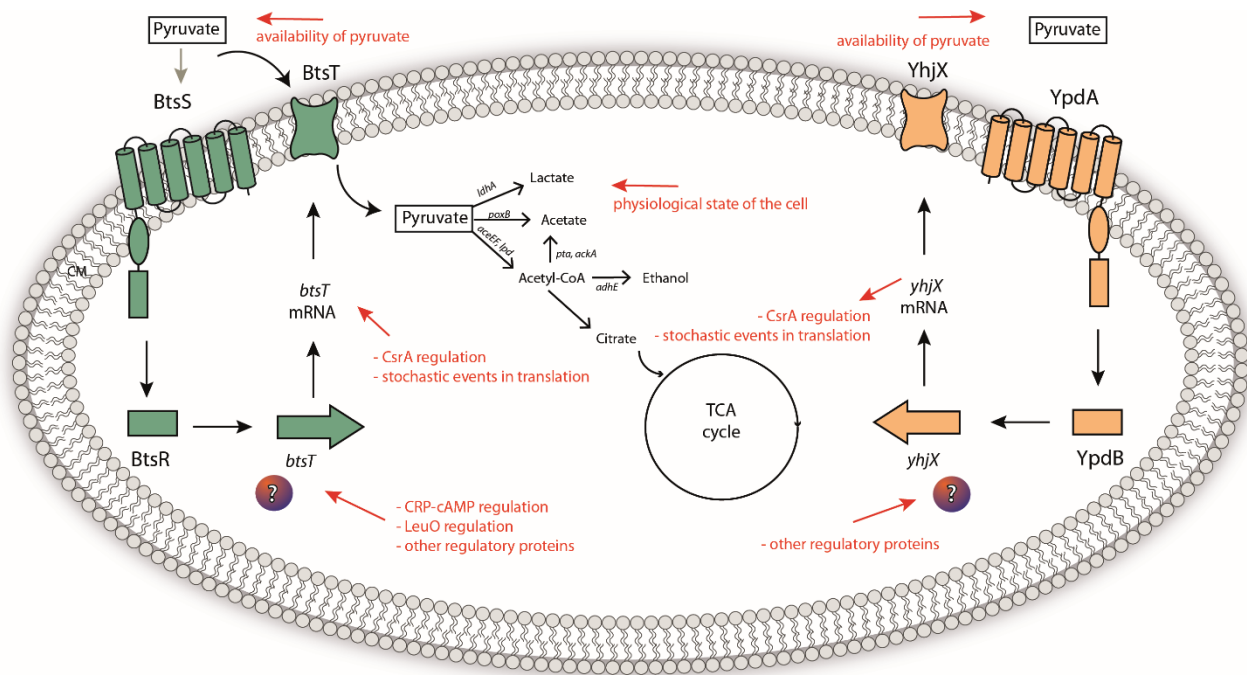


Fig. 6.1- Schematic representation of possible contributors for the establishment of heterogeneity. Scheme representing the signalling cascade involving the two TCSs. The likely contributors are marked with a red arrow and the corresponding description. For more details about each hypothesis refer to text. CM-cytoplasmic membrane.

TCA- tricarboxylic acid.

A sequential docking of YpdB to two different binding sites followed by a quick clearance of the RR is required. The docking and clearance processes can play a role on modulating the activation of P_{yhjX} . Several reactions in the signal transmission cascade of TCSs are subject to stochastic events, as for instance phosphorylation events, degradation of mRNA, etc (137) (**Fig. 6.1**). A second point is the involvement of other regulatory proteins on the regulation of *btsT* and *yhjX* expression (**Fig. 6.1**). Previous studies did not identified any other transcriptional regulators (apart from the corresponding RRs and cAMP-CRP for *btsT*) for the target genes (42, 45). Nevertheless, at the post-transcriptional level, both target genes transcripts are under regulation of CsrA (43). Interestingly, CsrA has a repressive effect on

btsT and a positive effect on *yhjX* (43). CsrA has a regulatory effect on unrelated pathways such as carbon metabolism, motility, biofilm formation, persister cell formation, virulence, quorum sensing, oxidative stress, etc (138). CsrA is itself regulated by two small RNAs, CsrB and CsrC, by the sigma factor 38 (σ^{38}) and by the BarA/UvrY TCS of *E. coli* (138). By being integrated in such elaborated regulatory circuitry, CsrA is affected by nutrient starvation and by different cultivating conditions (e. g. growth in glucose versus growth in LB), posing CsrA as a good candidate for an intermediate player between the intracellular metabolic state of the cells and the expression of *btsT* and *yhjX*. *btsT* was suggested to be transcriptionally regulated by LeuO (involved in the regulation of genes associated with stress response and pathogenesis) (139). It was showed that *btsT* RNA was significantly increased in a *leuO* mutant compared to a wild type strain (139). Although LeuO-binding sites were identified upstream of the coding region of *btsT*, no binding to the promoter was effectively proven.

6.1-3. Cellular physiology at the post-exponential growth phase

The inner physiological state of the cells might also contribute for the establishment of the heterogeneous output (**Fig. 6.1**). The concept of *metabolic specialization* (presented in Chapter 1 section 1.2-2 of this thesis) can be now further explored. Although differentiation into distinct states (bistability) was not observed for the activation of P_{yhjX} nor P_{btsT} , the high degree of cell-to-cell variability supports that it is important for the population to keep some individuals with extremely low/high promoter activity of the two target genes. Individuals of a population contribute with different levels for the carbon metabolism, transport of substrates, stress responses, etc., in order to maintain the overall metabolic stability of the population. In fact, other studies highlighted that microbial population exploits noise to increase the fitness in accordance to environmental perturbations, thus suggesting that gene expression noise can confer functionalities for the robustness of the population as a whole (140).

Prominent examples of heterogeneous behavior related to metabolic specialization have been described for the lactose and arabinose utilization systems (141, 142). In the lactose utilization system, fluctuating expression levels of the lactose transporter gene *lacY* were shown to produce distinct *lac* gene expression heterogeneity. A positive feedback loop via LacY-imported inducers induce an even higher expression of *lacY* and bistable populations arise (141, 143). In the case of the arabinose utilization network, the arabinose inducer is unequally transported intracellularly via AraE and AraFGH systems leading to a heterogeneous induction response (144–146). Other organisms like *Lactococcus lactis* also show phenotypic heterogeneous behavior, in this case related to sugar metabolization during the diauxic shift from glucose to cellobiose (147).

The metabolic specialization theory would imply that a strain harboring the two TCSs (BtsS/BtsR and YpdA/YpdB) is better balanced in terms of metabolic demands than a strain lacking the systems. To clarify this point, on this thesis the single-cell characterization of the BtsS/BtsR and YpdA/YpdB systems was further enlarged by studies regarding the ribosome synthesis rate and protein overproduction, both metabolic demanding tasks in two different strains: wild-type (WT) and mutant from the network (*btsSRypdAB* mutant). Only when the systems are present (and consequently have heterogeneous activation of their target genes) there is an unimodal and homogeneous synthesis of ribosome and protein overproduction. Synthesizing proteins in abundance is a normal occurrence in natural habitats as several pathogens synthesize virulence factors, exoenzymes, siderophores, etc. The *btsSRypdAB* mutant showed bistability in both ribosome synthesis and protein overproduction, having two distinct populations, one producing and one non-producing. Ribosome synthesis rate was checked by monitoring the promoter activity of *rrnB* P1 (148). The activation strength of this promoter was recently correlated with intracellular adenosine- 5'-triphosphate (ATP) levels (149). Low ribosome synthesis rate (case of the *btsSRypdAB* mutant) could possibly mean low ATP content of the cells and consequently low metabolic activity. Another study associated YhjX levels to ATP content, by showing that in a mutant of PykA (isoenzyme of pyruvate kinase), both YhjX and ATP content are decreased comparing to a WT strain of *E. coli* (150). The hypothesis that the metabolic state of the mutant was somehow impaired was further shown to be correct, as the mutant also shows higher persister cells percentage. Persisters are phenotypic variants characterized by a low-metabolic state and a non-growing phenotype (151, 152). The network helps sustaining an overall metabolic balanced population.

6.2-Identification of the substrate transported by BtsT (YjiY)

The impermeability of *E. coli* membrane conditions the exchange of metabolites between the intra- and extracellular spaces. Membrane transporter proteins became of major importance by mediating the influx and efflux of molecules. In **Chapter 3**, the study of a putative transporter protein of *E. coli*, BtsT (former YjiY), is conducted. Combined approaches using intact cells and reconstituted and purified protein into *E. coli* proteoliposomes revealed that BtsT is a pyruvate/H⁺ symporter with a K_m of 16 μ M (88). It is the first identified and characterized pyruvate transporter in *E. coli*, despite previous studies provided evidence that pyruvate can be excreted and re-uptaken under diverse growth conditions and that *E. coli* harbors several pyruvate transporters (153, 154). BtsS/BtsR system can now be fully understood (44): upon exponential growth, *E. coli* cells experience nutrient depletion from the media; intracellularly, serine is converted to pyruvate which accumulates until approach of stationary phase and pyruvate overflow occurs; the extracellular pyruvate binds to the HK BtsS and after activation of the RR BtsR, BtsT is coded allowing the reuptake of pyruvate.

In fact, the discussed heterogeneous behavior in **Chapter 2** can now be better understood for the case of P_{btsT} tagged cells. Among single individuals of a population, the uptake of pyruvate is strategically spread in order to fulfill individuals needs and collectively improve metabolic fitness. BtsS/BtsR system requires limiting conditions (late exponential growth phase or growth in diluted LB) followed by the presence of extracellular pyruvate in order to sustain activation of its target gene promoter (44). Therefore, the hypothesis that there is a secondary intracellular signal (that enables bacteria to sense “limitation”) which can stochastically contribute for the establishment of the heterogeneous behavior can not be erased.

6.2-1. BtsT and other pyruvate transporters

CstA, a homologous of BtsT (61.1% identity), together with YbdD, were very recently described as a pyruvate transporter complex in *E. coli* (155). By performing a high-throughput transposon sequencing coupled to growth inhibition assays by toxic pyruvate, the group was able to show that CstA and YbdD comprise a constitutive pyruvate transporter system. Curiously, the same study shows an additive effect of BtsT in the pyruvate uptake capacity of CstA-YbdD complex, suggesting a possible link between peptide/amino acid sensing and pyruvate transport involving the three systems (CstA-YbdD, BtsS/BtsR and YpdA/YpdB). Most striking, *ybdD* (located directly after *cstA*) is very similar (77% identity) in gene sequence to *yjiX* (located directly after *yjiY*, refer to **Fig. 1.4B** in Chapter 1). However, transporter assays

using reconstituted and purified proteins, specificity and the mechanism of transport were not assayed in that study.

A recent study identified a novel bacterial transport system for pyruvate in another organism: *B. subtilis*. The PftAB heterologous complex (mentioned earlier in section 6.1 of this thesis) facilitates pyruvate transport (156). PftAB is able to transport pyruvate across the cell membrane having as driving force solely pyruvate concentration gradient, therefore acting as both an importer and exporter. The transporter PftAB operates under complex feedback loops with LytS/LytT TCS of *B. subtilis* which enable its proper activation and repression. Interestingly, there are similarities in gene sequence and signalling between LytS/LytT and YpdA/YpdB system of *E. coli*.

6.2-2. The importance of pyruvate in prokaryotic cells

The transported substrate of BtsT, pyruvate, is the simplest α -keto acid and a key metabolite for living cells (156). It is located at the junction of several essential pathways in prokaryotic cells, as glycolysis, oxidative metabolism, amino acid synthesis, tricarboxylic acid (TCA) cycle, etc, thus representing a switch point between respiratory and fermentative metabolism. Under acid conditions, pyruvate can be protonated (pK_a of 2.5) and cross the bacterial cytosolic membrane by simple diffusion, however, usually pyruvate is in the deprotonated form and requires an active transporter. Tight control of pyruvate homeostasis and fate is essential to ensure robustness and stability to changing environmental conditions. Pyruvate induces expression of a small noncoding RNA (Spot42) which in turn activates the master regulator of acid resistance (157, 158). Therefore, fluctuating levels of intracellular pyruvate result in unbalanced acid resistance. A very recent study highlighted the fulcrum role of pyruvate in virulence regulation in *S. aureus* (159). Pyruvate was shown to induce the production of pore-forming leucocidins which in turn increased the virulence of community-acquired methicillin-resistant *S. aureus*. Three TCSs (AgrAC, SaeRS and ArlR/ArlS) of *S. aureus* are responsible for the regulation of pyruvate-related secretion of proteins. Furthermore, this study also revealed that pyruvate causes pronounced changes in the transcriptome of *S. aureus*, e. g. in pathways involved in central metabolism and amino acid metabolism, as well as in the transcript levels of enzymes that regulate these pathways, culminating in alterations in the overall metabolic flux of this organism. Pyruvate plays also an important role in oxidative stress protection; the topic will be discussed in Section 6.3 of this thesis.

Based on the presented single-cell analysis and on the elucidation of the function of BtsT (former YjiY), a hypothetical model can be ascertained (**Fig. 6.2**).

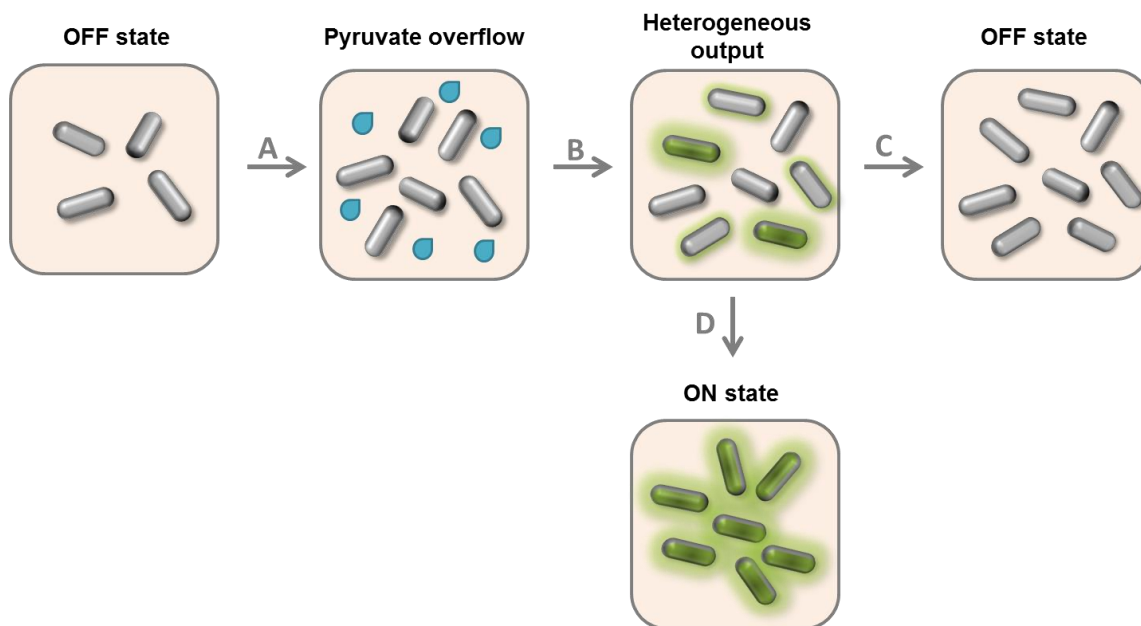


Fig. 6.2- Scheme of cell-to-cell variations on the transcription activation of *btsT* during growth in rich medium. The scheme summarizes P_{btsT} activation (represented by shades of green) during growth of *E. coli* MG1655 cells in rich medium. “ON” and “OFF” refer to full activation/none activation of *btsT* promoter, respectively. (A) Transition from the OFF state at an early stage of growth to mid-exponential phase when pyruvate overflow occurs. (B) Establishment of the heterogeneous output dependent on pyruvate availability and on the physiological state of each cell. (C) Return to the OFF state at stationary phase. (D) Hypothetical conversation from heterogeneous to homogenous ON population. Blue balls:pyruvate. See text for details.

At an early stage of growth (from lag phase to mid-exponential phase), *E. coli* MG1655 cells have no P_{btsT} activity (OFF state). When approaching mid-exponential growth phase, cells excrete pyruvate (blue balls) due to overflow metabolism (**transition A**). Pyruvate becomes a “common good” and can be uptaken. Subsequently, cells sense the availability of pyruvate and depending on their individual needs and on the extracellular pyruvate concentration, P_{btsT} is heterogeneously activated among the population (**transition B**). This activation occurs post-exponentially, at the transition to stationary phase. The promoter activation is normally distributed among the population, yet cell-to-cell variability occurs (demonstrated on the scheme by varied shades of green). This heterogeneity on BtsS/BtsR-mediated P_{btsT} activation allows cells to individually uptake pyruvate and fulfill their particular needs. The transcription activation of *btsT* is transient which leads to a return to an OFF state (no P_{btsT} activity) in stationary phase (**transition C**).

It is reasonable to consider a hypothetical conversion from heterogeneous to homogenous behaviour (all cells would have P_{btsT} activated- ON state) (**transition D**). In this situation, all cells from the population would participate equally on perceiving and transporting pyruvate.

6.3-Investigation of the biological relevance of BtsS/BtsR and YpdA/YpdB systems

Chapters 2 and 3 from this thesis contributed greatly for the understanding of the functionality of the sensing network BtsS/BtsR and YpdA/YpdB. For the last two chapters of the thesis, the aim was to bring the knowledge acquired on the last two sections together and further characterize the biological relevance of these systems. First, tools were developed to access a related phenotype observed in bulk experiments (persistence), this time at the single-cell level (**Chapter 4**). Lastly, in **Chapter 5** another dormancy state is studied in both scales, bulk and at single-cell.

6.3-1. Heterogeneity of P_{btsT} activation relates to antibiotic persistence

By employing microfluidic technique coupled to high throughput fluorescence microscopy imaging, it was observed that cells with lower *btsT* transcription activation are more prone to persist antibiotic treatment. Although several studies have explored the use of microfluidics for the study of persister cells, several problems were recurrent and incapable of provide reliable single-cell data analysis (85–87). In order to discriminate between low and high expressing cells in time-lapse microfluidic cultivation, a tracking analysis protocol was developed. The basis software was Fiji (92) and the used plugin Microbe J (93). The results presented in this thesis, corroborate the importance of the transport of pyruvate to the overall metabolic state of a single individual, bringing together the described heterogeneous behavior of the target genes promoters and its impact on a phenotypical variant state. When pyruvate uptake is impaired (either *btsT* is deleted or is being heterogeneously expressed at lower level) the population is on average metabolic “less active”. This lower metabolic activity (also observed and discussed in Section 6.1) turns to be an add-on upon antibiotic treatment.

6.3-2. The viable but nonculturable state of *E. coli*

Knowing that a strain lacking the systems is on average metabolic less active, a deeper latency state was explored, the viable but nonculturable (VBNC) state. Bacteria in this state are characterized by a loss of culturability in routinely used cultivation media yet the cells are still viable (production of biomass, transport of nutrients, active metabolism, membrane integrity and respiration are traceable) (95, 160). The factors promoting the entrance in this state (referred to as *induction*) are diverse, varying from starvation, oxidative stress, elevated osmotic concentrations, low oxygen supply, etc (95). Under certain conditions, VBNC cells can regain the lost culturability in a process referred to as *resuscitation* (101). Compounds promoting the restoration of culturability have been described, e. g. YeaZ promoting-factor, catalase, α -

ketoglutarate, and pyruvate (98, 101–103). In this thesis it is shown for the first time that the presence of the systems BtsS/BtsR and YpdA/YpdB is essential for the resuscitation from the VBNC state. Pyruvate transport assays allowed seeing for the first time uptake of pyruvate at the early stages of resuscitation by VBNC cells. Previous studies have demonstrated the resuscitative effect of pyruvate (102) however, the mechanism underlying the role of pyruvate has only been attributed to its reactive oxygen species (ROS) scavenging effect (VBNC cells are under severe oxidative stress) and not to its use as carbon source (161). Pyruvate is a great antioxidant as it is capable of scavenge hydrogen peroxide (162, 163), hydroxyl radical (164) and prevents lipid peroxidation (165). Pyruvate and other α -ketoacids scavenge hydrogen by a nonenzymatic oxidative decarboxylation (166). In this reaction, a carboxyl group from pyruvate and an oxygen from hydrogen peroxide form carbon dioxide, leaving water and acetic acid. A recent study conducted in *Pseudomonas aeruginosa* showed that the organism can remain viable over several days to weeks if provided with pyruvate as a fermentable energy source (167). In this thesis it is shown that pyruvate is transported into the cell during resuscitation, which implies that pyruvate is metabolized early on and allows the cell to restore a fully active metabolic state and ultimately cell division. However, it is not discarded the possibility that pyruvate plays a dual role on the resuscitation of VBNC cells, both with extra- and intracellular implications.

6.3-3. BtsS/BtsR and YpdA/YpdB role in pathogenicity

The expression of *btsT* is robust in both the acute and chronic stages of infection in the mouse gut by a urinary pathogenic *E. coli* strain (UPEC) (44). This strain shows similar transient transcription activation of *btsT* as the parental strain *E. coli* MG1655 (44). However, UPEC shows a different cross-regulation between the two TCSs, BtsS/BtsR and YpdA/YpdB, than the commensal *E. coli* MG1655 (168). Although BtsS/BtsR system controls activity of YpdA/YpdB system, the contrary is not true for the pathogenic strain. Moreover, *yhjX* expression requires all components from the pyruvate-sensing network. These differences might be accounted for by differential selective pressures acting upon pathogenic and non-pathogenic strains. The first documented association between the BtsSR/YpdAB sensing network and pathogenicity was reported by Kwang-sun Kim *et al.* (169). YpdB was suggested to be involved in motility, biofilm formation and antibiotic resistance when *E. coli* was exposed to volatile organic compounds emitted from *B. subtilis*. A second association was reported in the same year by the group of Jean-Marc Ghigo (170) where *btsT* was found to be slightly upregulated upon commensal biofilms of *E. coli* being colonized by a pathogenic *E. coli* strain. *btsT*, which codes for the pyruvate transporter BtsT, was later associated with flagella expression and poor adhesion of *Salmonella* to the host cells (171). The target gene *btsT* was also described as being required for successful colonization of *Salmonella* in the

mouse gut, similarly to what was observed in *E. coli*. However, the study refers to *btsT* as being a putative peptide transporter in *Salmonella*. The same group suggested that BtsT might transport peptides of proline in *Salmonella* and, by doing so, regulates expression of *mgtC* and *csgD* (172). The association *btsT*-motility has not yet been shown in *E. coli*, however it is conceptually interesting to conceive that a heterogeneously expressed target gene of a TCS aids virulence (173).

The above mentioned studies, encountered mainly *btsT* as being a potential participant on pathogenicity, rarely mentioning the YpdA/YpdB system. The distribution and co-occurrence of the two TCSs were studied in more detail and revealed that the majority of the γ -proteobacteria harbor only the BtsS/BtsR system (34). YpdA/YpdB system was found in addition to the BtsS/BtsR system only in *E. coli*, *Citrobacter* and *Serratia*. The combination of both BtsS/BtsR and YpdA/YpdB in one organism might result from evolutionary traits that led to the synthesis of an adjacent low-affinity transport system (YpdA/YpdB) in addition to the high-affinity system (BtsS/BtsR). In *S. cerevisiae*, cells starved for phosphate activate feedback loops that regulate high- and low-affinity phosphate transporters, in a similar fashion as for the pyruvate responsive systems. Dual-transport systems seem to prolong preparation for starvation and ease the recovery, hence optimizing sensing of nutrients and their depletions by integrating information regarding the internal and external availabilities (174).

Based on the results obtained in this thesis, a scheme summarizing the main obtained results was made (**Fig. 6.3**). The heterogeneity of the transcription activation of *btsT* and *yhjX* was observed during growth of *E. coli* MG1655 in LB medium at the transition from exponential to stationary phase and it was proved to result from the sum of the metabolic state of each individual and the available carbon source. However, the mechanism underlying the origin of the heterogeneous behavior remains elusive. Nevertheless, using several tools and via the establishment of specific protocols, the outcome of having heterogeneous transcriptional activation of the target genes was clarified. A mixed population, composed of highly expressing cells, low expressing cells and everything in between, turned out to balance and optimize the utilization of the available resources according to each individual needs at a designated time point. Ribosome synthesis and protein overproduction were metabolic burdens sustained by the heterogeneous population. Persister cells and resuscitation from the VBNC state are dormancy related phenotypes strongly associated with nutrient sensing and pyruvate transport, respectively that were also explored in this thesis.

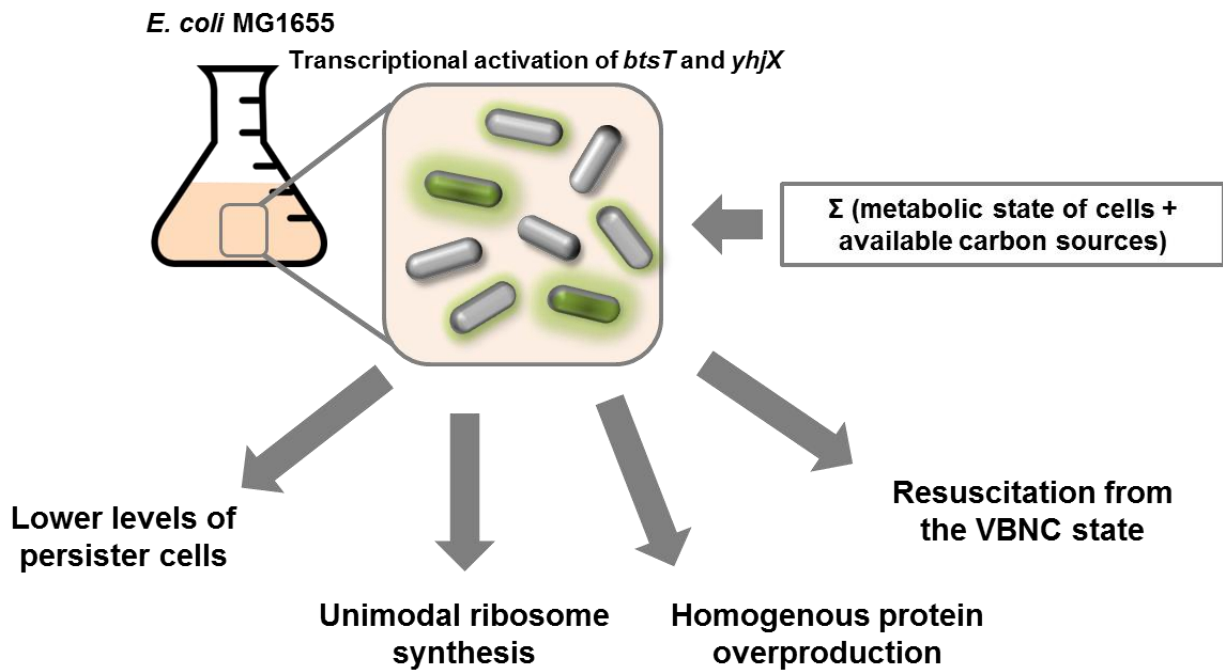


Fig. 6.3- Scheme compiling and connecting the heterogeneous behaviour and phenotypic output.

Heterogeneous transcription activation of the target genes is a result of the sum of the metabolic state of the cells and the available carbon sources. This heterogeneous behaviour, observed for a wild-type strain of *E. coli* MG1655, is relevant upon antibiotic treatment, where cells with low *btsT* transcription activation are more prone to persist. Furthermore, unimodal ribosome synthesis, homogeneous protein overproduction and resuscitation from the VBNC state are processes sustained by the wild-type population. See text for further details.

6.4-Outlook

In this thesis, a single-cell analysis of the promoter activation of the two target genes from BtsS/BtsR and YpdA/YpdB TCSs of *E. coli* was done. One of the target genes was further found to code for a pyruvate/H⁺ symporter, the first identified and characterized pyruvate transporter in *E. coli*. The heterogeneous output was correlated with sustainability of metabolic burdens and dormant phenotypes, which were addressed via optimized imaging approaches.

However, fulcral questions remain unanswered: The role of YhjX, the gene product of YpdA/YpdB activation and putative transporter protein, remains elusive. Recent and preliminar work performed *in vivo* pointed towards a role also in intracellular pyruvate transport, however biochemical proof is needed. The purified protein and its reconstitution into proteoliposomes should be completed and radioactive-labelled pyruvate transport assays should be executed. This knowledge would help elucidate the entire function of the network composed of the two systems, and even give some enlightening into the observed nutrient-dependent heterogeneous behavior that differed for the two target genes transcription activation. Moreover, the signal for “limitation”, which conditions the activation of each target gene in LB medium and is essential for the response to extracellular pyruvate for the case of *btsT*, should be considered.

The mechanism of heterogeneity should be explored. Plausible options were presented in section 6.1 of this thesis. An approach could be a mathematical model based on *in vivo* and *in vitro* data to simulate oscillations of extra- and intracellular pyruvate, the different levels of transcriptional and post-transcriptional regulation and the predicted outcome in terms of promoter activation.

In order to deepen the knowledge about the network regulation, investigation of the localization of the four membrane-integrated proteins (BtsS, BtsT, YpdA and YhjX) should be followed. Fluorescently-tagged full-length proteins for fluorescence resonance energy transfer (FRET) could be a strategy. With this information, could be clarified if in fact the two TCSs form one big signalling unit, influencing one another by conformational changes.

Finally, the role of the systems in pathogenicity and/or host-colonization poses itself as an interesting new project. *In vivo* studies using animal models could be an optimal way of addressing the behaviour of the systems in a natural environment as the intestinal tract of mammals. The study of other organisms harbouring at least one of the systems (e. g. *Salmonella*) could be very interesting.

References (Chapter 1, 4, 5 and 6)

1. Eswara PJ, Ramamurthi KS. 2017. Bacterial Cell Division: Nonmodels Poised to Take the Spotlight. *Annu Rev Microbiol* 71:393–411.
2. Grote J, Krysciak D, Streit WR. 2015. Phenotypic heterogeneity, a phenomenon that may explain why quorum sensing does not always result in truly homogenous cell behavior. *Appl Environ Microbiol* 81:5280–5289.
3. Davis KM, Isberg RR. 2016. Defining heterogeneity within bacterial populations via single cell approaches. *BioEssays* 38:782–790.
4. Smits WK, Veening J-W, Kuipers O. 2008. Phenotypic Variation and Bistable Switching in Bacteria. Springer Verlag, Berlin.
5. Smits WK, Kuipers OP, Veening J-W. 2006. Phenotypic variation in bacteria: the role of feedback regulation. *Nat Rev Microbiol* 4:259–271.
6. Binder D, Drepper T, Jaeger K-E, Delvigne F, Wiechert W, Kohlheyer D, Grünberger A. 2017. Homogenizing bacterial cell factories: Analysis and engineering of phenotypic heterogeneity. *Metab Eng* 42:145–156.
7. Grimbergen AJ, Siebring J, Solopova A, Kuipers OP. 2015. Microbial bet-hedging: The power of being different. *Curr Opin Microbiol* 25:67–72.
8. Schreiber F, Littmann S, Lavik G, Escrig S, Meibom A, Kuypers MMM, Ackermann M. 2016. Phenotypic heterogeneity driven by nutrient limitation promotes growth in fluctuating environments. *Nat Microbiol* 1:16055.
9. Avery S V. 2006. Microbial cell individuality and the underlying sources of heterogeneity. *Nat Rev Microbiol* 4:577–587.
10. Delvigne F, Goffin P. 2014. Microbial heterogeneity affects bioprocess robustness: Dynamic single-cell analysis contributes to understanding of microbial populations. *Biotechnol J* 9:61–72.
11. Grünberger A, Wiechert W, Kohlheyer D. 2014. Single-cell microfluidics: Opportunity for bioprocess development. *Curr Opin Biotechnol* 29:15–23.
12. Johnson DR, Goldschmidt F, Lilja EE, Ackermann M. 2012. Metabolic specialization and the assembly of microbial communities. *ISME J* 6:1985–1991.
13. Kotte O, Volkmer B, Radzikowski JL, Heinemann M. 2015. Phenotypic bistability in *Escherichia coli*'s central carbon metabolism. *Mol Syst Biol* 10:1–11.
14. de Lorenzo V, Sekowska A, Danchin A. 2015. Chemical reactivity drives spatiotemporal organisation of bacterial metabolism. *FEMS Microbiol Rev* 39:96–119.
15. Gudelj I, Weitz JS, Ferenci T, Claire Horner-Devine M, Marx CJ, Meyer JR, Forde SE. 2010. An integrative approach to understanding microbial diversity: From intracellular mechanisms to community structure. *Ecol Lett* 13:1073–1084.
16. Silva-Rocha R, de Lorenzo V. 2012. Stochasticity of TOL plasmid catabolic promoters sets a bimodal expression regime in *Pseudomonas putida* mt-2 exposed to m-xylene. *Mol Microbiol* 86:199–211.
17. Healey D, Gore J. 2014. Phenotypic heterogeneity implements a game theoretic mixed strategy in a clonal microbial population. [bioRxiv 11049](https://doi.org/10.1101/011049).
18. Nikolic N, Barner T, Ackermann M. 2013. Analysis of fluorescent reporters indicates heterogeneity in glucose uptake and utilization in clonal bacterial populations. *BMC Microbiol* 13:258.
19. Wagner M. 2009. Single-Cell ecophysiology of microbes as revealed by Raman Microspectroscopy or Secondary Ion Mass Spectrometry Imaging. *Annu Rev Microbiol* 63:411–429.
20. Mohr W, Vagner T, Kuypers MMM, Ackermann M, LaRoche J. 2013. Resolution of conflicting signals at the single-cell level in the regulation of cyanobacterial photosynthesis and nitrogen fixation. *PLoS One* 8:3.
21. Kopf SH, McGlynn SE, Green-Saxena A, Guan Y, Newman DK, Orphan VJ. 2015. Heavy water and ¹⁵N labeling with NanoSIMS analysis reveals growth-rate dependent metabolic heterogeneity in chemostats. *Environ Microbiol* 17:2542–2556.
22. Heermann R, Jung K. 2009. Stimulus Perception and Signaling in Histidine Kinases, p. 135–161. In *Bacterial Signaling*. Wiley-VCH Verlag GmbH & Co. KGaA.
23. Mascher T, Helmann JD, Uuden G. 2006. Stimulus perception in bacterial signal-transducing histidine kinases. *Microbiol Mol Biol Rev* 70:910–938.
24. Schaller GE, Shiu S-H, Armitage JP. 2011. Two-component systems and their co-option for eukaryotic signal transduction. *Curr Biol* 21:R320–R330.

25. Koretke KK, Lupas AN, Warren P V, Rosenberg M, Brown JR. 2000. Evolution of two-component signal transduction. *Mol Biol Evol* 17:1956–70.
26. Barakat M, Ortet P, Whitworth DE. 2011. P2CS: A database of prokaryotic two-component systems. *Nucleic Acids Res* 39.
27. Alm E, Huang K, Arkin A. 2006. The evolution of two-component systems in bacteria reveals different strategies for niche adaptation. *PLoS Comput Biol* 2:1329–1342.
28. Galperin MY, Nikolskaya AN, Koonin E V. 2001. Novel domains of the prokaryotic two-component signal transduction systems. *FEMS Microbiol Lett*.
29. Capra EJ, Laub MT. 2012. Evolution of two-component signal transduction systems. *Annu Rev Microbiol* 66:325–347.
30. Schramke H, Tostevin F, Heermann R, Gerland U, Jung K. 2016. A dual-sensing receptor confers robust cellular homeostasis. *Cell Rep* 16:213–221.
31. Pernestig A-K, Georgellis D, Romeo T, Suzuki K, Tomenius H, Normark S, Melefors Ö. 2003. The *Escherichia coli* BarA-UvrY two-component system is needed for efficient switching between glycolytic and gluconeogenic carbon sources. *J Bacteriol* 185:843–853.
32. Bekker M, Alexeeva S, Laan W, Sawers G, Teixeira de Mattos J, Hellingwerf K. 2010. The ArcBA two-component system of *Escherichia coli* is regulated by the redox state of both the ubiquinone and the menaquinone pool. *J Bacteriol* 192:746–754.
33. Gao R, Stock AM. 2009. Biological insights from structures of two-component proteins. *Annu Rev Microbiol* 63:133–154.
34. Behr S, Brameyer S, Witting M, Schmitt-Kopplin P, Jung K. 2017. Comparative analysis of LytS/LytTR-type histidine kinase/response regulator systems in γ -proteobacteria. *PLoS One* 12:e0182993.
35. Geer LY, Domrachev M, Lipman DJ, Bryant SH. 2002. CDART: Protein homology by domain architecture. *Genome Res* 12:1619–1623.
36. Anantharaman V, Aravind L. 2003. Application of comparative genomics in the identification and analysis of novel families of membrane-associated receptors in bacteria. *BMC Genomics* 4:34.
37. Sidote DJ, Barbieri CM, Wu T, Stock AM. 2008. Structure of the *Staphylococcus aureus* AgrA LytTR domain bound to DNA reveals a beta fold with an unusual mode of binding. *Structure* 16:727–735.
38. Qin X, Singh K V., Weinstock GM, Murray BE. 2000. Effects of *Enterococcus faecalis* *fsr* genes on production of gelatinase and a serine protease and virulence. *Infect Immun* 68:2579–2586.
39. Shimizu T, Shima K, Yoshino K, Yonezawa K, Shimizu T, Hayashi H. 2002. Proteome and transcriptome analysis of the virulence genes regulated by the VirR / VirS system in *Clostridium perfringens* 184:2587–2594.
40. Rood JI. 1998. Virulence genes of *Clostridium perfringens*. *Annu Rev Microbiol* 52:333–360.
41. Pestova E V, Håvarstein LS, Morrison D a. 1996. Regulation of competence for genetic transformation in *Streptococcus pneumoniae* by an auto-induced peptide pheromone and a two-component regulatory system. *Mol Microbiol* 21:853–862.
42. Kraxenberger T, Fried L, Behr S, Jung K. 2012. First insights into the unexplored two-component system YehU/YehT in *Escherichia coli*. *J Bacteriol* 194:4272–84.
43. Behr S, Fried L, Jung K. 2014. Identification of a novel nutrient-sensing histidine kinase/response regulator network in *Escherichia coli*. *J Bacteriol* 196:2023–9.
44. Behr S, Kristoficova I, Witting M, Breland EJ, Eberly AR, Schmitt-kopplin P, Hadjifrangiskou M, Jung K. 2017. Identification of a high-affinity pyruvate receptor in *Escherichia coli*. *Sci Rep* 1–10.
45. Fried L, Behr S, Jung K. 2013. Identification of a target gene and activating stimulus for the YpdA/YpdB histidine kinase/response regulator system in *Escherichia coli*. *J Bacteriol* 195:807–15.
46. Behr S, Heermann R, Jung K. 2016. Insights into the DNA-binding mechanism of a LytTR-type transcription regulator. *Biosci Rep* 36:e00326.
47. Riley M, Abe T, Arnaud MB, Berlyn MKB, Blattner FR, Chaudhuri RR, Glasner JD, Horiuchi T, Keseler IM, Kosuge T, Mori H, Perna NT, Plunkett G, Rudd KE, Serres MH, Thomas GH, Thomson NR, Wishart D, Wanner BL. 2006. *Escherichia coli* K-12: A cooperatively developed annotation snapshot - 2005. *Nucleic Acids Res* 34:1–9.
48. Mizuno T. 1997. Compilation of all genes encoding two-component phosphotransfer signal transducers in the genome of *Escherichia coli*. *DNA Res* 4:161–168.
49. Keseler IM, Bonavides-Martínez C, Collado-Vides J, Gama-Castro S, Gunsalus RP, Johnson DA, Krummenacker M, Nolan LM, Paley S, Paulsen IT, Peralta-Gil M, Santos-Zavaleta A, Shearer AG, Karp PD. 2009. EcoCyc: A comprehensive view of *Escherichia coli* biology. *Nucleic Acids Res* 37.

50. Jain E, Bairoch A, Duvaud S, Phan I, Redaschi N, Suzek BE, Martin MJ, McGarvey P, Gasteiger E. 2009. Infrastructure for the life sciences: design and implementation of the UniProt website. *BMC Bioinformatics* 10:136.
51. Ho Y-SJ, Burden LM, Hurley JH. 2000. Structure of the GAF domain, a ubiquitous signaling motif and a new class of cyclic GMP receptor. *EMBO J* 19:5288–5299.
52. Finn RD, Bateman A, Clements J, Coggill P, Eberhardt RY, Eddy SR, Heger A, Hetherington K, Holm L, Mistry J, Sonnhammer ELL, Tate J, Punta M. 2014. Pfam: The protein families database. *Nucleic Acids Res.*
53. Nikolskaya AN, Galperin MY. 2002. A novel type of conserved DNA-binding domain in the transcriptional regulators of the AlgR/AgrA/LytR family. *Nucleic Acids Res* 30:2453–9.
54. Szklarczyk D, Franceschini A, Kuhn M, Simonovic M, Roth A, Minguéz P, Doerks T, Stark M, Müller J, Bork P, Jensen LJ, Von Mering C. 2011. The STRING database in 2011: Functional interaction networks of proteins, globally integrated and scored. *Nucleic Acids Res* 39.
55. Khil PP, Camerini-Otero RD. 2002. Over 1000 genes are involved in the DNA damage response of *Escherichia coli*. *Mol Microbiol* 44:89–105.
56. Sydor AM, Jost M, Ryan KS, Turo KE, Douglas CD, Drennan CL, Zamble DB. 2013. Metal binding properties of *Escherichia coli* YjiA, a member of the metal homeostasis-associated COG0523 family of GTPases. *Biochemistry* 52:1788–1801.
57. Schmidt A, Kochanowski K, Vedelaar S, Ahrne E, Volkmer B, Callipo L, Knoop K, Bauer M, Aebersold R, Heinemann M. 2015. The quantitative and condition-dependent *Escherichia coli* proteome. *Nat Biotechnol* 34:104–110.
58. Behr S, Kristoficova I, Witting M, Breland EJ, Eberly AR, Sachs C, Schmitt-Kopplin P, Hadjifrangiskou M, Jung K. 2017. Identification of a high-affinity pyruvate receptor in *Escherichia coli*. *Sci Rep* 1–10.
59. Wong FH, Chen JS, Reddy V, Day JL, Shlykov MA, Wakabayashi ST, Saier MH. 2012. The amino acid-polyamine-organocation superfamily. *J Mol Microbiol Biotechnol* 22:105–113.
60. Vastermark A, Wollwage S, Houle ME, Rio R, Saier MH. 2014. Expansion of the APC superfamily of secondary carriers. *Proteins Struct Funct Bioinforma* 82:2797–2811.
61. Krämer R. 1999. Multiple roles of prokaryotic cell membranes, p. 68–87. In Inc., BS (ed.), *Biology of the prokaryotes*. London.
62. Viklund H, Elofsson A. 2008. OCTOPUS: improving topology prediction by two-track ANN-based preference scores and an extended topological grammar. *Bioinformatics* 24:1662–1668.
63. Behr SM. 2014. The LytS / LytTR-like histidine kinase / response regulator systems in *Escherichia coli* and their function in carbon source selectivity. Dissertation, LMU München: Faculty of Biology.
64. Geisel N, Gerland U. 2011. Physical limits on cooperative protein-DNA binding and the kinetics of combinatorial transcription regulation. *Biophys J* 101:1569–1579.
65. Fozo EM, Kawano M, Fontaine F, Kaya Y, Mendieta KS, Jones KL, Ocampo A, Rudd KE, Storz G. 2008. Repression of small toxic protein synthesis by the Sib and OhsC small RNAs. *Mol Microbiol* 70:1076–1093.
66. Kannan G, Wilks JC, Fitzgerald DM, Jones BD, BonDurant SS, Slonczewski JL. 2008. Rapid acid treatment of *Escherichia coli*: transcriptomic response and recovery. *BMC Microbiol* 8:37.
67. Pao SS, Paulsen IT, Saier MH. 1998. Major Facilitator Superfamily. *Microbiol Mol Biol Rev* 62:1–34.
68. Saier MH, Reddy VS, Tsu B V, Ahmed MS, Li C, Moreno-Hagelsieb G. 2016. The Transporter Classification Database (TCDB): recent advances. *Nucleic Acids Res* 44:D372–D379.
69. Ackermann M. 2015. A functional perspective on phenotypic heterogeneity in microorganisms. *Nat Publ Gr* 13:497–508.
70. Schreiber F, Littmann S, Lavik G, Escrig S, Meibom A, Kuypers MMM, Ackermann M. 2016. Phenotypic heterogeneity driven by nutrient limitation promotes growth in fluctuating environments. *Nat Microbiol* 6:1–7.
71. Giraffa G. 2004. Studying the dynamics of microbial populations during food fermentation, p. 251–260. In *FEMS Microbiology Reviews*.
72. Avraham R, Haseley N, Brown D, Penaranda C, Jijon HB, Trombetta JJ, Satija R, Shalek AK, Xavier RJ, Regev A, Hung DT. 2015. Pathogen cell-to-cell variability drives heterogeneity in host immune responses. *Cell* 162:1309–1321.
73. Wang X, Kang Y, Luo C, Zhao T, Liu L, Jiang X, Fu R, An S, Chen J, Jiang N, Ren L, Wang Q, Kenneth Baillie J, Gao Z, Yu J. 2014. Heteroresistance at the single-cell level: Adapting to antibiotic stress through a population-based strategy and growth-controlled interphenotypic coordination. *MBio* 5:1–9.
74. Amato SM, Brynildsen MP. 2015. Persister heterogeneity arising from a single metabolic stress. *Curr Biol* 25:2090-2098.

75. Wood TK, Knabel SJ, Kwan BW. 2013. Bacterial persister cell formation and dormancy. *Appl Environ Microbiol* 79:7116-7121.
76. Balaban NQ. 2011. Persistence: Mechanisms for triggering and enhancing phenotypic variability. *Curr Opin Genet Dev* 21:768-775.
77. Balaban NQ, Merrin J, Chait R, Kowalik L, Leibler S. 2004. Bacterial Persistence as a Phenotypic Switch. *Science* 305:1622-1626.
78. Brehm-stecher BF, Johnson EA. 2004. Single-cell microbiology: tools, technologies, and applications Single-. *Microbiol Mol Biol Rev* 68:538-559.
79. Halldorsson S, Lucumi E, Gómez-Sjöberg R, Fleming RMT. 2015. Advantages and challenges of microfluidic cell culture in polydimethylsiloxane devices. *Biosens Bioelectron* 63:218-231.
80. Grünberger A, Probst C, Helfrich S, Nanda A, Stute B, Wiechert W, von Lieres E, Nöh K, Frunzke J, Kohlheyer D. 2015. Spatiotemporal microbial single-cell analysis using a high-throughput microfluidics cultivation platform. *Cytom Part A* 87:1101-1115.
81. Weaver WM, Tseng P, Kunze A, Masaeli M, Chung AJ, Dudani JS, Kittur H, Kulkarni RP, Di Carlo D. 2014. Advances in high-throughput single-cell microtechnologies. *Curr Opin Biotechnol* 25:114-123.
82. Vasdekis AE, Stephanopoulos G. 2015. Review of methods to probe single cell metabolism and bioenergetics. *Metab Eng* 27:115-135.
83. Westerwalbesloh C, Grünberger A, Wiechert W, Kohlheyer D, von Lieres E. 2017. Coarse-graining bacteria colonies for modelling critical solute distributions in picolitre bioreactors for bacterial studies on single-cell level. *Microb Biotechnol* 10:845-857.
84. Dusny C, Schmid A. 2015. Microfluidic single-cell analysis links boundary environments and individual microbial phenotypes. *Environ Microbiol* 17:1839-1856.
85. Ray JCJ, Wickersheim ML, Jalihal AP, Adeshina YO, Cooper TF, Balázs G. 2016. Cellular growth arrest and persistence from enzyme saturation. *PLOS Comput Biol* 12:e1004825.
86. Li Y, Sun Y, Pu Y, Zhao Z, Li Y, Zou J, Ma Q, Zhao Y, Ke Y, Zhu Y, Chen H. 2016. Enhanced efflux activity facilitates drug tolerance in dormant bacterial cells 284-294.
87. Maisonneuve E, Castro-Camargo M, Gerdes K. 2013. (p)ppGpp controls bacterial persistence by stochastic induction of toxin-antitoxin activity. *Cell* 154:1140-50.
88. Kristoficova I, Vilhena C, Behr S, Jung K. 2018. BtsT - a novel and specific pyruvate/H⁺ symporter in *Escherichia coli*. *J Bacteriol* 200:e00599-17.
89. Vilhena C, Kaganovitch E, Shin JY, Gruenberger A, Behr S, Kristoficova I, Brameyer S, Kohlheyer D, Jung K. 2018. A single-cell view of the BtsSR/YpdAB pyruvate sensing network in *Escherichia coli* and its biological relevance. *J Bacteriol* 200:e00536-17.
90. Grünberger A, Paczia N, Probst C, Schendzielorz G, Eggeling L, Noack S, Wiechert W, Kohlheyer D. 2012. A disposable picolitre bioreactor for cultivation and investigation of industrially relevant bacteria on the single cell level. *Lab Chip* 12:2060.
91. GmbH FJ. 2017. HNF - Helmholtz Nano Facility. *J large-scale Res Facil* 3.
92. Schindelin J, Arganda-Carreras I, Frise E, Kaynig V, Longair M, Pietzsch T, Preibisch S, Rueden C, Saalfeld S, Schmid B, Tinevez J-Y, White DJ, Hartenstein V, Eliceiri K, Tomancak P, Cardona A. 2012. Fiji: an open-source platform for biological-image analysis. *Nat Methods* 9:676-82.
93. Ducret A, Quardokus E, Brun Y. 2016. MicrobeJ, a high throughput tool for quantitative bacterial cell detection and analysis. *Nat Microbiol* 1:1-7.
94. Behr S, Kristoficova I, Witting M, Breland EJ, Eberly AR, Sachs C, Schmitt-Kopplin P, Hadjifrangiskou M, Jung K. 2017. Identification of a high-affinity pyruvate receptor in *Escherichia coli*. *Sci Rep* 7:1388.
95. Oliver JD. 2005. The viable but nonculturable state in bacteria. *Journal of microbiology (Seoul)* 43:93-100.
96. Ramamurthy T, Ghosh A, Pazhani GP, Shinoda S. 2014. Current perspectives on viable but non-culturable (VBNC) pathogenic bacteria. *Front public Heal* 2:1-9.
97. Flemming H-C, Wingender J, Szewzyk U, Steinberg P, Rice SA, Kjelleberg S. 2016. Biofilms: an emergent form of bacterial life. *Nat Rev Microbiol* 14:563-575.
98. Mizunoe Y, Wai SN, Takade a, Yoshida S. 1999. Restoration of culturability of starvation-stressed and low-temperature-stressed *Escherichia coli* O157 cells by using H₂O₂-degrading compounds. *Arch Microbiol* 172:63-67.
99. Cook KL, Bolster CH. 2007. Survival of *Campylobacter jejuni* and *Escherichia coli* in groundwater during prolonged starvation at low temperatures. *J Appl Microbiol* 103:573-583.

100. Asakura H, Kawamoto K, Haishima Y, Igimi S, Yamamoto S, Makino S ichi. 2008. Differential expression of the outer membrane protein W (OmpW) stress response in enterohemorrhagic *Escherichia coli* O157:H7 corresponds to the viable but non-culturable state. *Res Microbiol* 159:709–717.
101. Pinto D, Almeida V, Almeida Santos M, Chambel L. 2011. Resuscitation of *Escherichia coli* VBNC cells depends on a variety of environmental or chemical stimuli. *J Appl Microbiol* 110:1601–11.
102. Morishige Y, Fujimori K, Amano F. 2013. Differential Resuscitative Effect of Pyruvate and its Analogues on VBNC (Viable But Non-Culturable) *Salmonella*. *Microbes Environ* 28:180–186.
103. Li Y, Chen J, Zhao M, Yang Z, Yue L, Zhang X. 2017. Promoting resuscitation of viable but nonculturable cells of *Vibrio harveyi* by a resuscitation-promoting factor-like protein YeaZ. *J Appl Microbiol* 122:338–346.
104. Jung K, Fried L, Behr S, Heermann R. 2012. Histidine kinases and response regulators in networks. *Curr Opin Microbiol* 15:118–24.
105. Wu B, Liang W, Kan B. 2016. Growth Phase, oxygen, temperature, and starvation affect the development of viable but non-culturable state of *Vibrio cholerae*. *Front Microbiol* 7:1–9.
106. Whitesides MD, Oliver JD, Carolina N. 1997. Resuscitation of *Vibrio vulnificus* from the viable but nonculturable State 63:1002–1005.
107. Zeng B, Zhao G, Cao X, Yang Z, Wang C, Hou L. 2013. Formation and resuscitation of viable but nonculturable *Salmonella typhi*. *Biomed Res Int* 2013.
108. Tholozan JL, Cappelier JM, Tissier JP, Delattre G, Federighi M. 1999. Physiological characterization of viable-but-nonculturable *Campylobacter jejuni* cells. *Appl Environ Microbiol* 65:1110–1116.
109. Liu J, Deng Y, Peters BM, Li L, Li B, Chen L, Xu Z, Shirtliff ME. 2016. Transcriptomic analysis on the formation of the viable putative non-culturable state of beer-spoilage *Lactobacillus acetotolerans*. *Sci Rep* 6:36753.
110. Pawlowski DR, Metzger DJ, Raslawsky A, Howlett A, Siebert G, Karalus RJ, Garrett S, Whitehouse C a. 2011. Entry of *Yersinia pestis* into the viable but nonculturable state in a low-temperature tap water microcosm. *PLoS One* 6:e17585.
111. Asakura H, Panutdaporn N, Kawamoto K, Igimi S, Yamamoto S, Makino S-I. 2007. Proteomic characterization of enterohemorrhagic *Escherichia coli* O157:H7 in the oxidation-induced viable but non-culturable state. *Microbiol Immunol* 51:875–881.
112. Gunasekera TS, Sørensen A, Attfield P V, Sørensen SJ, Veal DA. 2002. Inducible gene expression by nonculturable bacteria in milk after pasteurization 68:1988–1993.
113. Schrader JM, Shapiro L. 2015. Synchronization of *Caulobacter crescentus* for investigation of the bacterial cell cycle. *J Vis Exp* 2:e52633.
114. Pertoft H, Laurent TC. 1977. Isopycnic Separation of Cells and Cell Organelles by Centrifugation in Modified Colloidal Silica Gradients BT - Methods of Cell Separation, p. 25–65. In Catsimpoilas, N (ed.), Springer US, Boston, MA.
115. Jia J, Li Z, Cao J, Jiang Y, Liang C, Liu M. 2013. Proteomic analysis of protein expression in the induction of the viable but nonculturable state of *vibrio harveyi* SF1. *Curr Microbiol* 67:442–447.
116. Heim S, Del M, Lleo M, Bonato B, Carlos A, Guzman C a, Canepari P. 2002. The Viable but nonculturable state and starvation are different stress responses of *Enterococcus faecalis*, as determined by proteome analysis. *Journ Bacteriol* 184:6739–6745.
117. Byrd JJ, Colwell RR. 1990. Maintenance of plasmids pBR322 and pUC8 in nonculturable *Escherichia coli* in the marine environment. *Appl Environ Microbiol* 56:2104–2107.
118. Dinu L-D, Bach S. 2011. Induction of Viable but nonculturable *Escherichia coli* O157:H7 in the phyllosphere of lettuce: a food safety risk factor. *Appl Environ Microbiol* 77:8295–8302.
119. Bourguet D, Chaufaux J, Micoud A, Delos M, Naibo B, Bombarde F, Marque G, Eychenne N, Pagliari C. 2002. *Ostrinia nubilalis* parasitism and the field abundance of non-target insects in transgenic *Bacillus thuringiensis* corn (*Zea mays*). *Environ Biosafety Res* 1:49–60.
120. Bogosian G, Bourneuf E V. 2001. A matter of bacterial life and death. *EMBO Rep* 2:770–774.
121. Perfeito L, Pereira MI, Campos PRA, Gordo I. 2008. The effect of spatial structure on adaptation in *Escherichia coli*. *Biol Lett* 4:57–59.
122. Cuny C, Lesbats M, Dukan S. 2007. Induction of a global stress response during the first step of *Escherichia coli* plate growth. *Appl Environ Microbiol* 73:885–889.
123. Na SH, Miyanaga K, Unno H, Tanji Y. 2006. The survival response of *Escherichia coli* K12 in a natural environment. *Appl Microbiol Biotechnol* 72:386–392.

124. Li L, Mendis N, Trigui H, Oliver JD, Faucher SP. 2014. The importance of the viable but non-culturable state in human bacterial pathogens. *Front Microbiol* 5:258.
125. Blattner FR, Plunkett G, Bloch CA, Perna NT, Burland V, Riley M, Collado-Vides J, Glasner JD, Rode CK, Mayhew GF, Gregor J, Davis NW, Kirkpatrick HA, Goeden MA, Rose DJ, Mau B, Shao Y. 1997. The complete genome sequence of *Escherichia coli* K-12. *Science* 277:1453–1462.
126. Rodriguez GG, Phipps D, Ishiguro K, Ridgway HF. 1992. Use of a fluorescent redox probe for direct visualization of actively respiring bacteria. *Appl Environ Microbiol* 58:1801–1808.
127. Gruenberger A, Probst C, Heyer A, Wiechert W, Frunzke J, Kohlheyer D. 2013. Microfluidic picoliter bioreactor for microbial single-cell analysis: fabrication, system setup, and operation. *J Vis Exp*.
128. Yamamoto K, Hirao K, Oshima T, Aiba H, Utsumi R, Ishihama A. 2005. Functional characterization in vitro of all two-component signal transduction systems from *Escherichia coli*. *J Biol Chem* 280:1448–1456.
129. Groban ES, Clarke EJ, Salis HM, Miller SM, Voigt CA. 2009. Kinetic buffering of cross talk between bacterial two-component sensors. *J Mol Biol* 390:380–393.
130. Ray JCJ, Igoshin OA. 2010. Adaptable functionality of transcriptional feedback in bacterial two-component systems. *PLoS Comput Biol* 6.
131. van den Esker MH, Kovács ÁT, Kuipers OP. 2017. YsbA and LytST are essential for pyruvate utilization in *Bacillus subtilis*. *Environ Microbiol* 19:83–94.
132. Koopmans ALH, Owen DB, Rosenblatt JI. 1964. Confidence intervals for the coefficient of variation for the normal and log normal distributions. *Biometrika* 51:25–32.
133. Baert J, Kinet R, Brognaux A, Delepierre A, Telek S, Sørensen SJ, Riber L, Fickers P, Delvigne F. 2015. Phenotypic variability in bioprocessing conditions can be tracked on the basis of on-line flow cytometry and fits to a scaling law. *Biotechnol J* 10:1316–1325.
134. Silander OK, Nikolic N, Zaslaver A, Bren A, Kikoin I, Alon U, Ackermann M. 2012. A genome-wide analysis of promoter-mediated phenotypic noise in *Escherichia coli*. *PLoS Genet* 8.
135. Taniguchi Y, Choi PJ, Li G-W, Chen H, Babu M, Hearn J, Emili A, Xie XS. 2010. Quantifying *E. coli* proteome and transcriptome with single-molecule sensitivity in single cells. *Science* (80-) 329:533–538.
136. Baron S. 1996. *Medical Microbiology*. 4th edition. University of Texas Medical Branch at Galveston.
137. Wei K, Moinat M, Maarleveld TR, Bruggeman FJ. 2014. Stochastic simulation of prokaryotic two-component signalling indicates stochasticity-induced active-state locking and growth-rate dependent bistability. *Mol BioSyst* 10:2338–2346.
138. Timmermans J, Van Melderen L. 2010. Post-transcriptional global regulation by CsrA in bacteria. *Cell Mol Life Sci* 67:2897–2908.
139. Shimada T, Yamamoto K, Ishihama A. 2009. Involvement of the leucine response transcription factor LeuO in regulation of the genes for sulfa drug efflux. *J Bacteriol* 191:4562–4571.
140. Nikel PI, Silva-Rocha R, Benedetti I, De Lorenzo V. 2014. The private life of environmental bacteria: Pollutant biodegradation at the single cell level. *Environ Microbiol* 16:628–642.
141. Ozbudak EM, Thattai M, Lim HN, Shraiman BI, Van Oudenaarden A. 2004. Multistability in the lactose utilization network of *Escherichia coli*. *Nature* 427:737–740.
142. Megerle JA, Fritz G, Gerland U, Jung K, Rädler JO. 2008. Timing and dynamics of single cell gene expression in the arabinose utilization system. *Biophys J* 95:2103–2115.
143. Binder D, Grünberger A, Loeschke A, Probst C, Bier C, Pietruszka J, Wiechert W, Kohlheyer D, Jaeger K-E, Drepper T. 2014. Light-responsive control of bacterial gene expression: precise triggering of the lac promoter activity using photocaged IPTG. *Integr Biol* 6:755.
144. Fritz G, Megerle JA, Westermayer SA, Brick D, Heermann R, Jung K, Rädler JO, Gerland U. 2014. Single cell kinetics of phenotypic switching in the arabinose utilization system of *E. coli*. *PLoS One* 9.
145. Khlebnikov A, Datsenko KA, Skaug T, Wanner BL, Keasling JD. 2001. Homogeneous expression of the PBAD promoter in *Escherichia coli* by constitutive expression of the low-affinity high-capacity AraE transporter. *Microbiology* 147:3241–3247.
146. Siegle DA, Hu JC. 1997. Gene expression from plasmids containing the araBAD promoter at subsaturating inducer concentrations represents mixed populations. *Proc Natl Acad Sci* 94:8168–8172.
147. Solopova A, van Gestel J, Weissing FJ, Bachmann H, Teusink B, Kok J, Kuipers OP. 2014. Bet-hedging during bacterial diauxic shift. *Proc Natl Acad Sci* 111:7427–7432.
148. Shah D, Zhang Z, Khodursky A, Kaldalu N, Kurg K, Lewis K. 2006. Persisters: a distinct physiological state of *E. coli*. *BMC Microbiol* 6:53.

149. Shan Y, Gandt AB, Rowe SE, Deisinger JP, Conlon BP, Lewis K. 2017. ATP-dependent persister formation in *Escherichia coli*. *MBio* 8:1–14.
150. Zhao C, Lin Z, Dong H, Zhang Y, Li Y. 2017. Reexamination of the physiological role of PykA in *Escherichia coli* revealed that it negatively regulates the intracellular ATP levels under anaerobic conditions 83:1–12.
151. Lewis K. 2010. Persister cells. *Annu Rev Microbiol* 64:357–372.
152. Maisonneuve E, Gerdes K. 2014. Molecular mechanisms underlying bacterial persisters. *Cell* 157:539–548.
153. Kreth J, Lengeler JW, Jahreis K. 2013. Characterization of pyruvate uptake in *Escherichia coli* K-12. *PLoS One* 8:6–12.
154. Kodaki T, Murakami H, Taguchi M, Izui K, Katsuki H. 1981. Stringent control of intermediary metabolism in *Escherichia coli*: pyruvate excretion by cells grown on succinate. *J Biochem* 90:1437–44.
155. Hwang S, Choe D, Yoo M, Cho S, Kim SC, Cho S, Cho B-K. 2018. Peptide transporter CstA imports pyruvate in *Escherichia coli* K-12. *J Bacteriol* JB.00771-17.
156. Charbonnier T, Le Coq D, McGovern S, Calabre M, Delumeau O, Aymerich S JM. 2017. Molecular and physiological logics of the pyruvate-induced response of a novel transporter in *Bacillus subtilis*. *MBio* 8:e00976-17.
157. Wu J, Li Y, Cai Z, Jin Y. 2014. Pyruvate-associated acid resistance in bacteria. *Appl Environ Microbiol* 80:4108–4113.
158. Battesti A, Majdalani N, Gottesman S. 2011. The RpoS-mediated general stress response in *Escherichia coli*. *Annu Rev Microbiol* 65:189–213.
159. Harper L, Balasubramanian D, Ohneck EA, Sause WE, Chapman J, Mejia-Sosa B, Lhakhang T, Heguy A, Tsigirigos A, Ueberheide B, Boyd JM, Lun DS, Torres VJ. 2018. *Staphylococcus aureus* responds to the central metabolite pyruvate to regulate virulence. *MBio* 9:e02272-17.
160. Pinto D, Santos M a, Chambel L. 2015. Thirty years of viable but nonculturable state research: unsolved molecular mechanisms. *Crit Rev Microbiol* 41:61–76.
161. Troxel B, Zhang JJ, Bourret TJ, Zeng MY, Blum J, Gherardini F, Hassan HM, Yang XF. 2014. Pyruvate protects pathogenic spirochetes from H₂O₂ killing. *PLoS One* 9.
162. O'Donnell-Tormey J, Nathan CF, Lanks K, DeBoer CJ, de la Harpe J. 1987. Secretion of pyruvate. An antioxidant defense of mammalian cells. *J Exp Med* 165:500–14.
163. Desagher S, Glowinski J, Prémont J. 1997. Pyruvate protects neurons against hydrogen peroxide-induced toxicity. *J Neurosci* 17:9060–9067.
164. Woo YJ, Taylor MD, Cohen JE, Jayasankar V, Bish LT, Burdick J, Pirolli TJ, Berry MF, Hsu V, Grand T, Chitwood WR, Vinten-Johansen J. 2004. Ethyl pyruvate preserves cardiac function and attenuates oxidative injury after prolonged myocardial ischemia. *J Thorac Cardiovasc Surg* 127:1262–1269.
165. Varma SD, Hegde K, Henein M. 2003. Oxidative damage to mouse lens in culture. Protective effect of pyruvate. *Biochim Biophys Acta - Gen Subj* 1621:246–252.
166. Constantopoulos G, Barranger JA. 1984. Nonenzymatic decarboxylation of pyruvate. *Anal Biochem* 139:353–358.
167. Basta DW, Bergkessel M, Newman DK. 2017. Identification of fitness determinants during energy-limited growth arrest in *Pseudomonas aeruginosa*. *MBio* 8:1–17.
168. Steiner BD, Eberly AR, Hurst MN, Zhang EW, Green HD, Behr S, Jung K, Hadjifrangiskou M. 2018. Evidence of cross-regulation in two closely related pyruvate-sensing systems in uropathogenic *Escherichia coli*. *J Membr Biol* 0:0.
169. Kim K, Lee S, Ryu C-M. 2013. Interspecific bacterial sensing through airborne signals modulates locomotion and drug resistance. *Nat Commun* 4:1809.
170. da Re S, Valle J, Charbonnel N, Beloin C, Latour-Lambert P, Faure P, Turlin E, Le Bouguéne C, Renauld-Mongé G, Forestier C, Ghigo JM. 2013. Identification of commensal *Escherichia coli* genes involved in biofilm resistance to pathogen colonization. *PLoS One* 8.
171. Garai P, Lahiri A, Ghosh D, Chatterjee J, Chakravorty D. 2015. Peptide utilizing carbon starvation gene *yjiY* is required for flagella mediated infection caused by *Salmonella*. *Microbiology* 100–116.
172. Garai P, Chandra K, Chatterji D, Chakravorty D. 2017. Peptide transporter YjiY influences the expression of the virulence gene *mgtC* to regulate biofilm formation in *Salmonella*. *FEMS Microbiol Lett*.
173. Prüß BM. 2017. Involvement of two-component signaling on bacterial motility and biofilm development. *J Bacteriol* 199.

174. Levy S, Kafri M, Carmi M, Barkai N. 2011. The competitive advantage of a dual-transporter system. *Science* 334:1408–1412.

Supplemental Material (Chapter 2)

A single-cell view of the BtsSR/YpdAB pyruvate sensing network in *Escherichia coli* and its biological relevance

Cláudia Vilhena,^a Eugen Kaganovitch,^b Jae Yen Shin,^{a*} Alexander Grünberger,^{b*} Stefan Behr,^{a*} Ivica Kristoficova,^a Sophie Brameyer,^{a*} Dietrich Kohlheyer,^b Kirsten Jung,^{a#}

Munich Center for Integrated Protein Science (CIPSM) at the Department of Microbiology, Ludwig-Maximilians-Universität München, Martinsried, Germany^a; Institute for Bio- and Geosciences, IBG-1: Biotechnology, Forschungszentrum Jülich GmbH, Jülich, Germany^b

Running Head: Phenotypic heterogeneity in *E. coli*

#Address correspondence to Kirsten Jung, jung@lmu.de

*Present address: Alexander Grünberger, Multiscale Bioengineering, Bielefeld University, Universitätsstraße 25, 33615 Bielefeld; Stefan Behr, Roche Diagnostics GmbH, Nonnenwald 2 82377 Penzberg; Jae Yen Shin, MPI of Biochemistry, Am Klopferspitz 18 82152 Martinsried; Sophie Brameyer, University College London, Gower Street, WC1E 6EA London

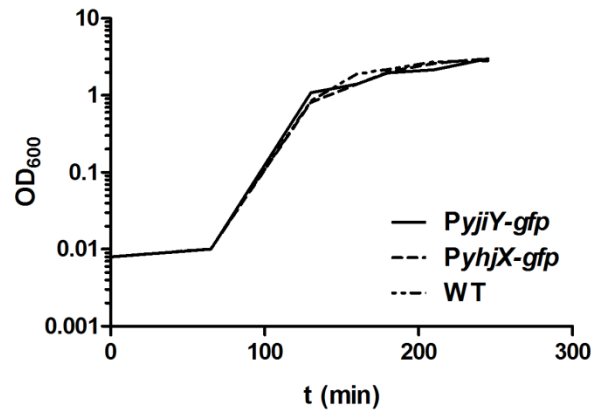


FIG S1 Growth of reporter strains. *E. coli* cells expressing *gfp* under the control of P_{yhjX} or P_{yjiY} and the MG1655 strain (WT, without promoter-*gfp* fusion) were grown in LB medium.

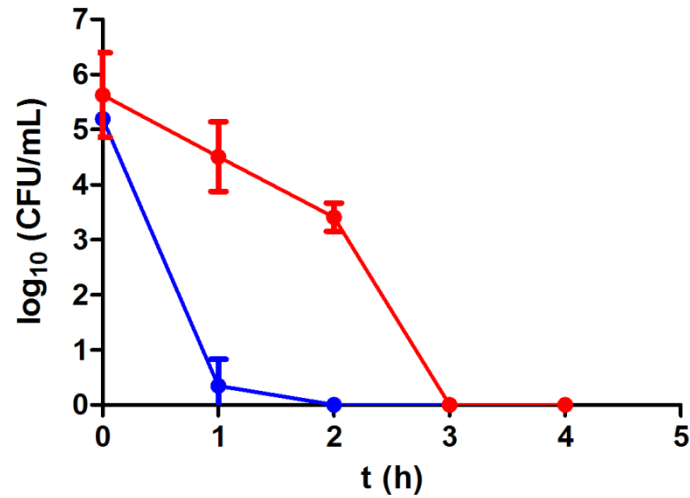


FIG S2 Determination of the minimum duration of killing (MDK) after ofloxacin treatment. *E. coli* cells of either WT (blue line) or mutant $\Delta btsSRypdAB$ (red line) were grown in LB-medium. At the post-exponential growth phase cells were challenged with ofloxacin (5 $\mu\text{g/ml}$). Samples were taken and analyzed for colony forming units (CFUs). The MDK₉₉ value was taken as the time needed to kill 99% of the initial population. Experiments were performed three independent times and error bars indicate the standard deviations of the means.

STRAINS	- INDUCER		+ INDUCER	
	Cells (%)		Cells (%)	
	OFF	ON	OFF	ON
WT GFP (IPTG)	92.7	7.3	3.1	96.9
<i>btsSRypdAB</i> GFP (IPTG)	97.8	2.2	51.0	49.0
WT GFP-DppA (Arabinose)	94.9	5.1	24.4	75.6
<i>btsSRypdAB</i> GFP-DppA (Arabinose)	98.1	1.9	99.4	0.6
WT LysP-mCherry (Arabinose)	97.7	2.3	33.4	66.6
<i>btsSRypdAB</i> LysP-mCherry (Arabinose)	98.2	1.8	98.5	1.5

TABLE S1 The BtsSR/YpdAB network promotes overproduction of proteins. *E. coli* cells of either WT or the *btsSRypdAB* mutant harboring an overproduction vector with IPTG inducible promoter for the overproduction of GFP; an arabinose inducible promoter for the overproduction of DppA-GFP and an arabinose inducible promoter for the overproduction of LysP-mCherry were grown in LB medium. Samples were taken before (- inducer) and after (+ inducer) the addition of the inducer. Flow cytometry was used to count fluorescent cells (maximum of 2000 events), and the percentages of OFF (non-fluorescent cells) and ON cells (fluorescent cells) were calculated from the raw data. Experiments were performed three independent times and standard deviations were below 10%.

Supplemental Material (Chapter 3)

BtsT - a novel and specific pyruvate/H⁺ symporter in *Escherichia coli*

Ivica Kristoficova, Cláudia Vilhena, Stefan Behr*, Kirsten Jung#

Munich Center for Integrated Protein Science (CIPSM) at the Department of Microbiology, Ludwig-Maximilians-Universität München, 82152 Martinsried, Germany^a

To whom correspondence should be addressed: Dr. Kirsten Jung, Ludwig-Maximilians-Universität München, Department Biologie I, Bereich Mikrobiologie, Großhaderner Str. 2-4, 82152 Martinsried, Germany. Phone: +49-89-2180-74500; Fax: +49-89-2180-74520; E-mail: jung@lmu.de

* Present address: Stefan Behr, Roche Diagnostics GmbH, Nonnenwald 2, 82377 Penzberg

```

E. coli MDTKKIFKHI PWVILGIIIGA FCLAVVALRR GEHVSALWIV VASVSVYLVA 50
S. enterica MDTKKIFKHI PWVILGIIIGA FCLSSVVALRR GEHVSALWIV VASVSVYLVA 50

E. coli YRYYSLYIAQ KVMKLDPTRA TPAVINNDGL NYVPTNRYVL FGHFAAIAAG 100
S. enterica YRYYSLYIAQ KVMKLDPTRA TPAVINNDGL NYVPTNRYVL FGHFAAIAAG 100

E. coli AGPLVGPVLA AQMGYLPGLT WLLAGVVLVAG AVQDFMVLFI SSRRNGASLG 150
S. enterica AGPLVGPVLA AQMGYLPGLT WLLAGVVLVAG AVQDFMVLFI SSRRNGASLG 150

E. coli EMIKEEMGPV PGTIALFGCF LIMIIILAVL ALIVVKALAE SPWGVFTVCS 200
S. enterica EMIKEEMGTV PGTIALFGCF LIMIIILAVL ALIVVKALAE SPWGVFTVCS 200

E. coli TVPIALFMGI YMRFIRPGRV GEVSVIGIVL LVASIYFGGV IAHPYWGPA 250
S. enterica TVPIALFMGI YMRFLRPGRV GEVSVIGIVL LVASIYFGGV IAHPYWGPA 250

E. coli LTFKDTTITF ALIGYAFVSA LLPWVLI LAP RDYLATFLKI GVI VGLALGI 300
S. enterica LTFKDTTITF ALIGYAFVSA LLPWVLI LAP RDYLATFLKI GVI VGLALGI 300

E. coli VVLNPELKM PAMTQYIDGTG PLWKGALFPF LFITIACGAV SGFHALISSG 350
S. enterica VILNPELKM PALTQYVDGTG PLWKGALFPF LFITIACGAV SGFHALISSG 350

E. coli TTPKLLANET DARF IGYGAM LME SFVA IMA LVAAS IIEPG LYFAMNTPPA 400
S. enterica TTPKLLACET DARF IGYGAM LME SFVA VMA LVAAS IIEPG LYFAMNTPPA 400

E. coli GLGITMPNLH EMGGENAP I I MAQLKDVTAH AAATVSSWGF VISPEQILQT 450
S. enterica GLGITMPNLH EMGGENAP L I MAQLKDVTAH AAATVSSWGF VISPEQILQT 450

E. coli AKDIGEPSVL NRAGGAPTLA VGIAHVFKV LPMADMGFY HFGILFEALF 500
S. enterica AKDIGEPSVL NRAGGAPTLA VGIAHVFKV LPMADMGFY HFGILFEALF 500

E. coli ILTALDAGTR SGRFMLQDLL GNFI PFLKKT DSLVAG IIGT AGCVGLWGYL 550
S. enterica ILTALDAGTR SGRFMLQDLL GNFPFLKKT DSLVAG IIGT AGCVGLWGYL 550

E. coli LYQGVVDPLG GVKSLWPLFG ISNQMLAAVA LVLGTVVL IK MKRTQYI WVT 600
S. enterica LYQGVVDPLG GVKSLWPLFG ISNQMLAAVA LVLSTVVL IK MORTKYI WVT 600

E. coli VYPAVWLLIC TTWALGLKLF STNPQMEGFF YMASQYKEKI ANGTDLTAAQ 650
S. enterica VIPAVWLLIC TTWALGLKLF SANPQMEGFF YMANLYKEKI ANGTLNLTAAQ 650

E. coli IANMNHIVVN NYTNAGLSIL FLIVVYS IIF YGFKTWLA VR NSDKRTDKE T 700
S. enterica IANMNHIVVN NYTNAGLSIL FLVVVYS IIF YGFTTWMKVR NSDKRTDKE T 700

E. coli PYVPIPEGGV KISSHH 716
S. enterica PYVVPPEGGV KISSHH 716

```

Figure S1. Comparison of the BtsT consensus sequences of *E. coli* and *S. enterica*. A consensus-based approach sequence comparison was used. 148 sequences of BtsT of *E. coli* and 122 sequences of BtsT of *S. enterica* were aligned and consensus sequences for each bacterium were generated by using the CLC Main Workbench software. Subsequently, both consensus sequences were aligned. The amino acids were colored based on their polarity (red - acidic and polar; blue - basic and polar; green - neutral and polar; black - neutral and nonpolar). Red background color was used to highlight deviating amino acids.

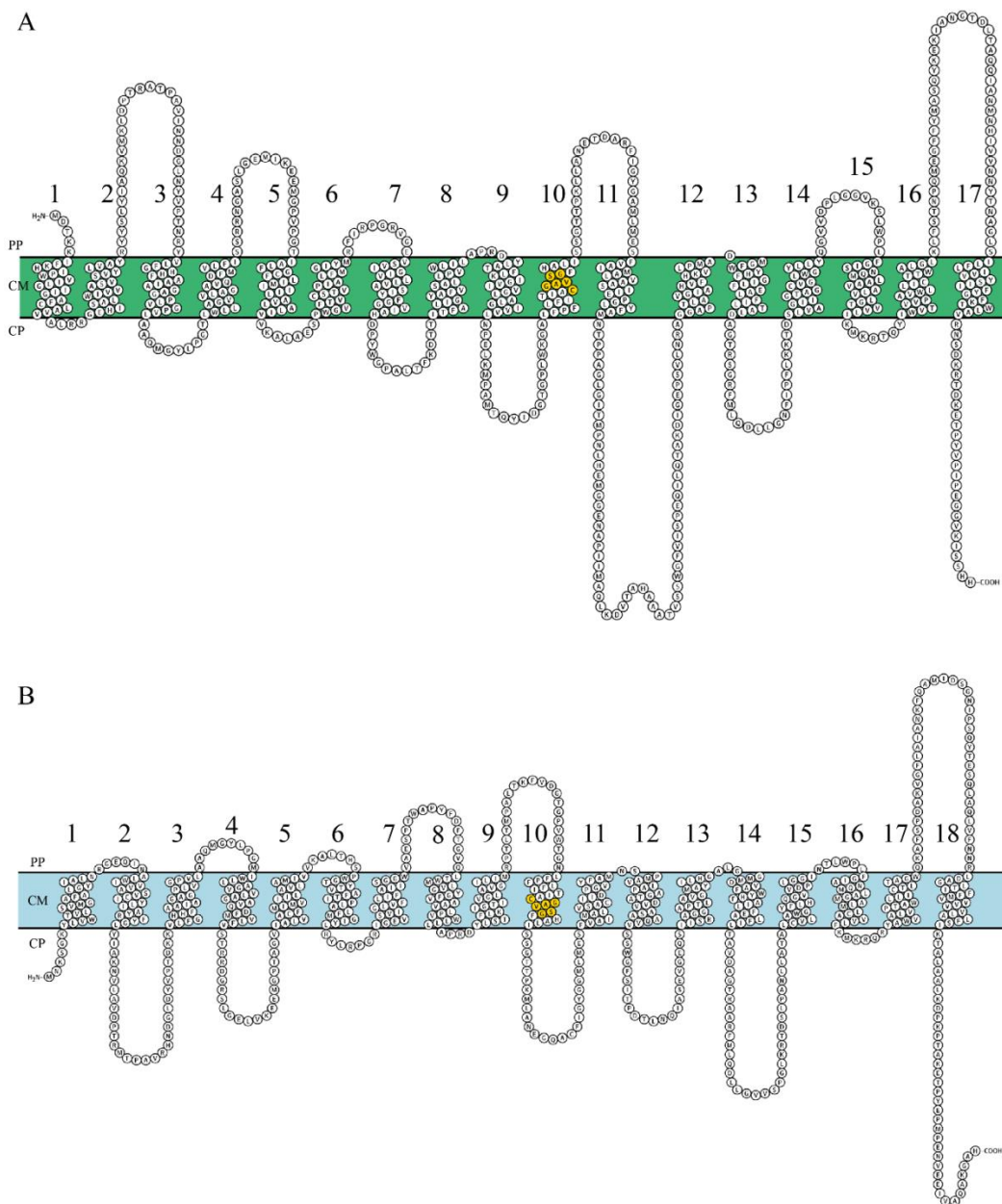


Figure S2. Schematic models of the secondary structure of (A) *E. coli* BstT and (B) *E. coli* CstA. Both models are based on the analysis of the secondary structure using the Uniprot program (1) and visualized with the Protter tool (2). Transmembrane domains (TMs) are numbered with numerals. The conserved motif CG-x(2)-SG with a high degree of sequence conservation within CstA homologues is marked in yellow (3). PP periplasm, CM cytoplasmic membrane, CP cytoplasm.

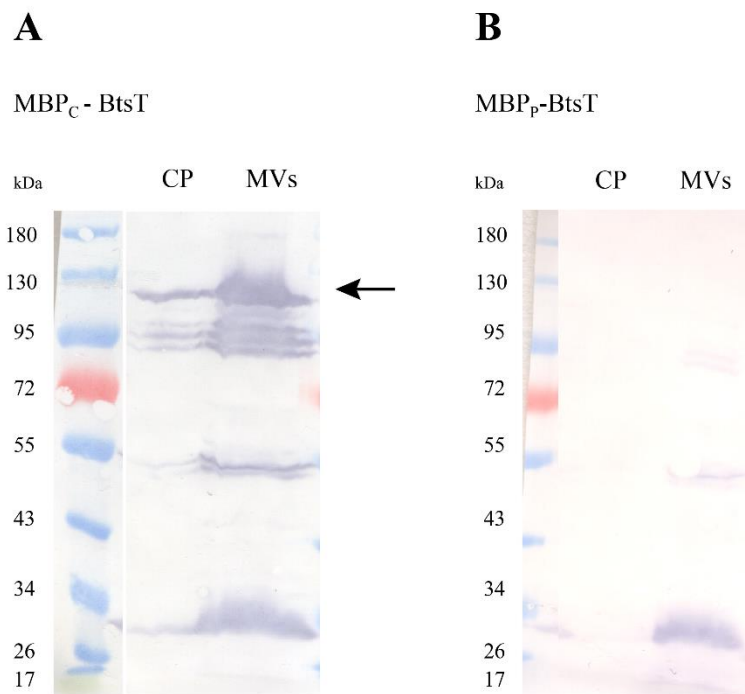


Figure S3. Localization of maltose-binding protein (MBP) hybrids. *malE* without or with leader sequence was fused to the 5' end of *btsT* encoding hybrid proteins with either a putative cytoplasmically located MPB (MBP_C-BtsT) (A) or a periplasmically located MBP (MBP_p-BtsT) (B), respectively. Cells with overproduced hybrids were fractionated to separate cytoplasm (CP) and membrane vesicles (MVs). Both fractions were adjusted to the same volume and separated by 12.5% (w/v) SDS-polyacrylamide gel electrophoresis and immunoblotted using a penta-His antibody for detection. The arrow indicates MBP_C-BtsT (about 120 kDa).

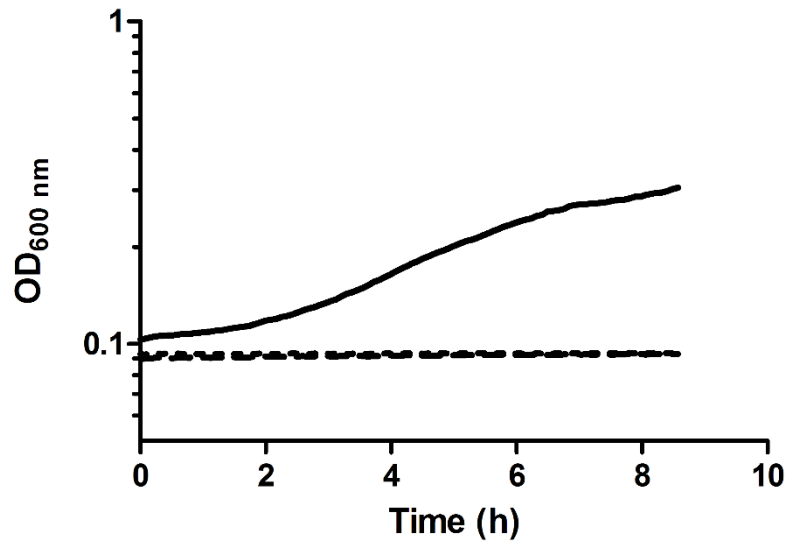


Figure S4. Complementation of *E. coli* MM39 with different MBP-BtsT hybrid proteins. *malE* deficient *E. coli* MM39 cells were transformed with plasmids pMAL-p2x (solid line), pMAL_p-btsT (dotted line) and pMAL_c-btsT (dashed line), and their growth was monitored over time on maltose as the sole carbon source.

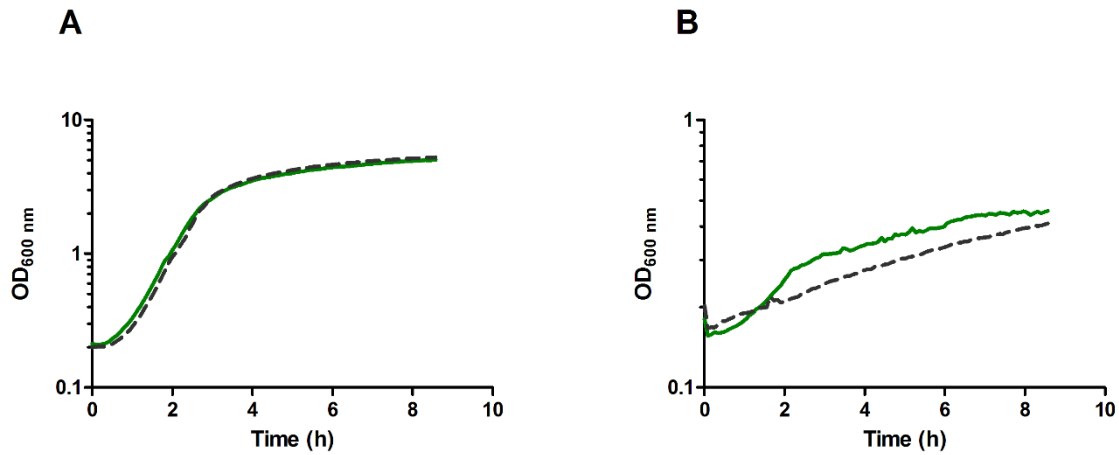


Figure S5. Growth of *E. coli* MG1655 and the *bstT* mutant in different media. *E. coli* MG1655 (green line) and *E. coli* MG1655 Δ *bstT* (dotted black line) were cultivated in LB medium (A) or in M9 minimal medium supplemented with pyruvate as carbon source (20 mM) (B). Samples were taken and analyzed every 5 min (A) or 2 hours (B).

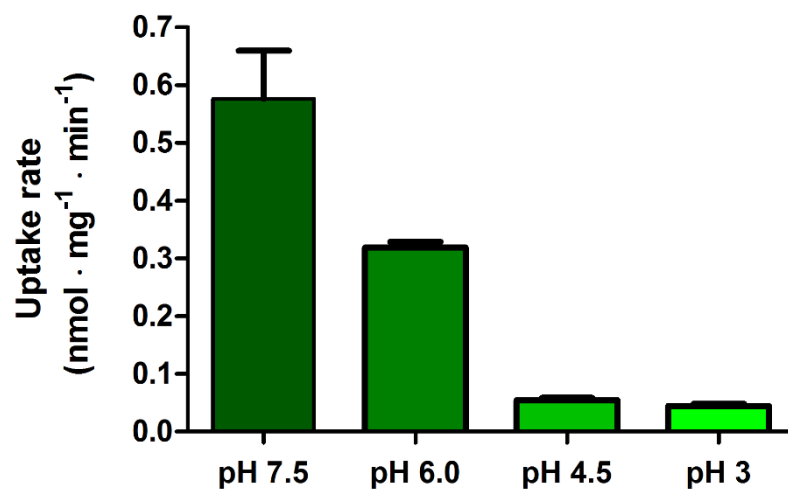


Figure S6. Rates of ¹⁴C-pyruvate uptake by BtsT-producing strain *E. coli* MG1655 $\Delta btsT$ pBAD24-*btsT* at various external pH values. ¹⁴C pyruvate was added at a final concentration of 10 μ M.

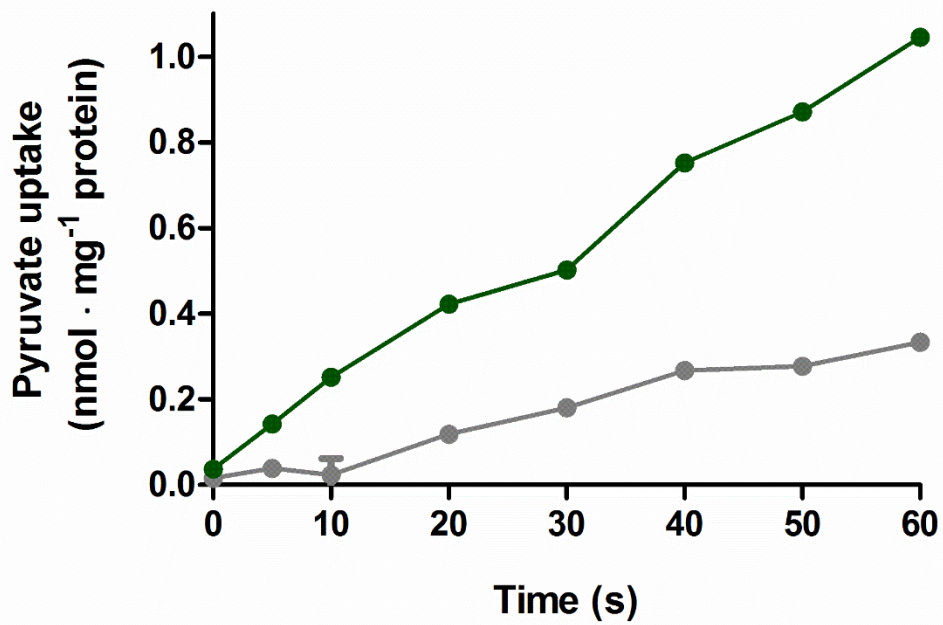


Figure S7. Time course of pyruvate uptake by *E. coli* YYC202. ¹⁴C-Pyruvate uptake was determined at a final pyruvate concentration of 10 μM at 15°C. Rates of uptake accumulation: BtsT producing strain *E. coli* YYC202 pBAD24-*btsT* (green), control strain *E. coli* YYC202 pBAD24 (grey). Standard deviations are estimated from three biological replicates.

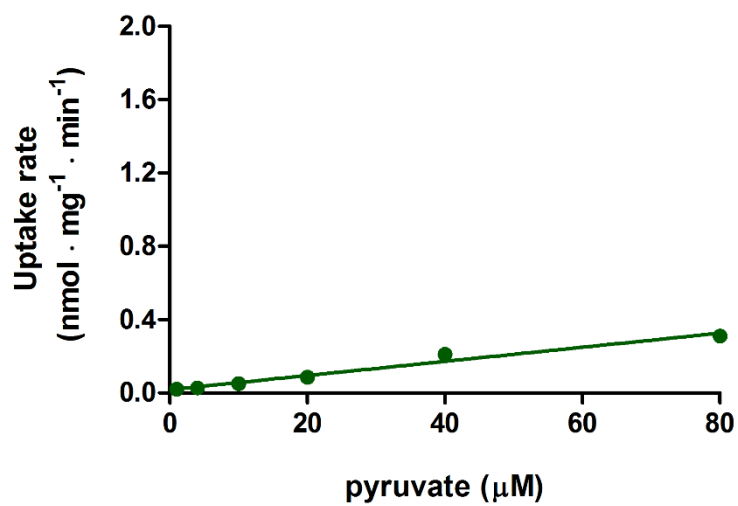


Figure S8. Pyruvate diffusion in intact *E. coli* cells. Uptake of ^{14}C -pyruvate by *E. coli* MG1655 ΔbtsT transformed with pBAD24 was determined in the presence of increasing pyruvate concentrations. The best-fit line was determined by linear regression. Error bars represent standard error of the mean.

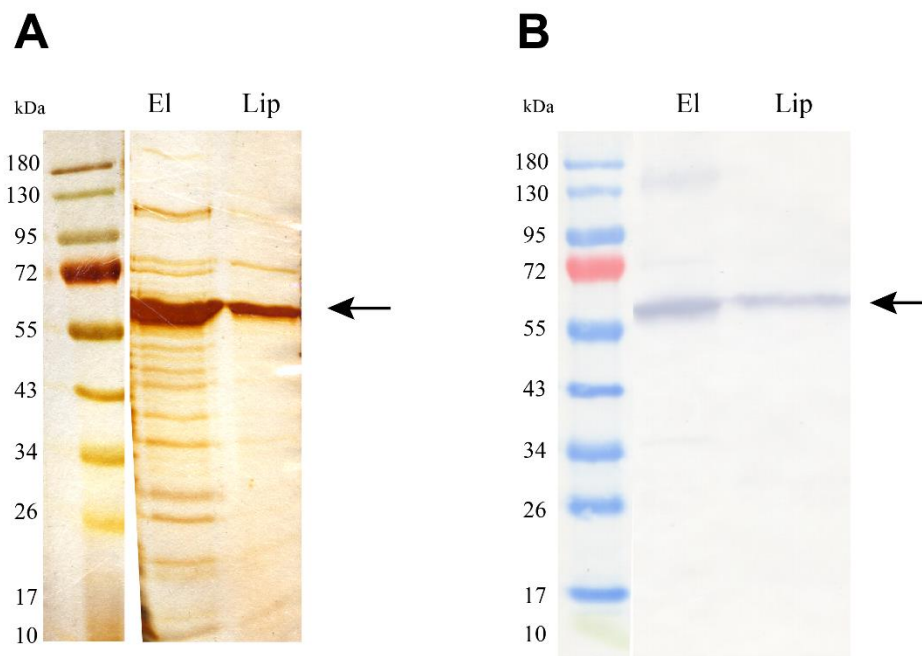


Figure S9. Purification of His-tagged BtsT. Membrane vesicles were prepared from *E. coli* cells after overproduction of BtsT-6His. Membrane proteins were then solubilized with 1.5% (w/v) n-dodecyl β -D-maltoside. The His-tagged BtsT was purified as described in Materials and Methods. El, BtsT eluted from the column with 300 mM imidazole (8.75 μ g of protein). Lip, BtsT reconstituted into *E. coli* liposomes (10 μ g of protein). Proteins were separated using 12.5% (w/v) SDS-polyacrylamide gel electrophoresis and stained with silver (A) or immunodetected by using a penta-His antibody (B). The arrows indicate BtsT-6His. In both images, non-relevant lanes were omitted for clarity.

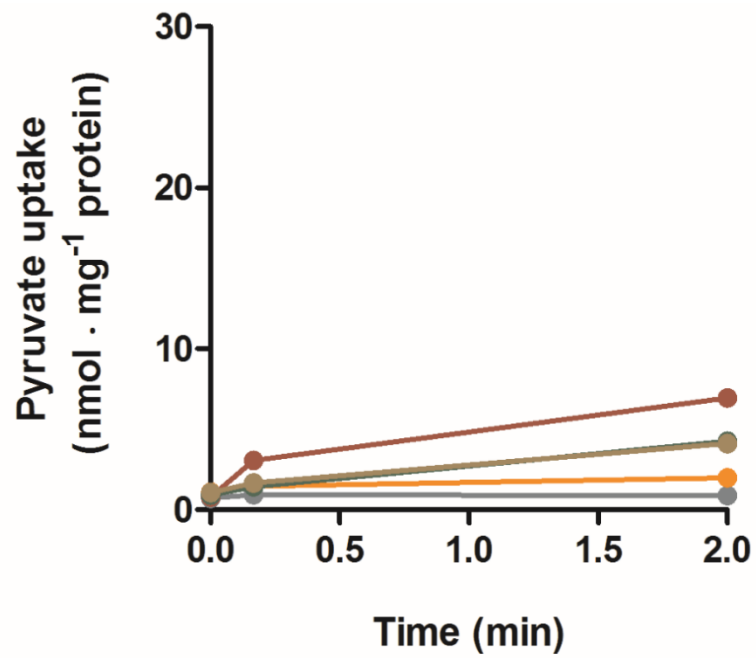


Figure S10. Pyruvate diffusion in *E. coli* liposomes. ^{14}C -pyruvate ($40\ \mu\text{M}$) diffusion was analyzed in liposomes (in the absence of protein). Time course of pyruvate uptake in the presence of artificially imposed $\Delta\tilde{\mu}_{H^+}$ (green), $\Delta\Psi$ (orange), ΔpH (red), $\Delta\tilde{\mu}_{Na^+}$ (brown) or in the absence of any gradient (grey).

REFERENCES

- 1- The UniProt Consortium. 2017. UniProt: the universal protein knowledgebase. *Nucleic Acids Res* 45:158–169.
- 2- Omasits U, Ahrens CH, Muller S, Wollscheid B. 2014. Protter: interactive protein feature visualization and integration with experimental proteomic data. *Bioinformatics* 30:884–886.
- 3- Vastermark A, Wollwage S, Houle ME, Rio R, Saier MH. 2014. Expansion of the APC superfamily of secondary carriers. *Proteins* 82:2797–2811.

Supplemental Material (Chapter 4)

Low *btsT* transcriptional activation: an add-on for *Escherichia coli* survival under antibiotic treatment

Eugen Kaganovitch^{a*}, Cláudia Vilhena^{b*}, Alexander Grünberger^{a*}, #Dietrich Kohlheyer^{a,c}, #Kirsten Jung^b

Institute for Bio- and Geosciences, IBG-1: Biotechnology, Forschungszentrum Jülich GmbH, Jülich, Germany^a, Munich Center for Integrated Protein Science (CIPSM) at the Department of Microbiology, Ludwig-Maximilians-Universität München, Martinsried, Germany^b, RWTH Aachen University – Microscale Bioengineering (AVT.MSB) 52074 Aachen, Germany^c

#Address correspondence to

Dietrich Kohlheyer, d.kohlheyer@fz-juelich.de

Kirsten Jung, jung@lmu.de

◆These authors contributed equally to this work

*Present address: Alexander Grünberger, Multiscale Bioengineering, Bielefeld University, Universitätsstraße 25, 33615 Bielefeld

Key Words: pyruvate, transporter, phenotypic heterogeneity, transcriptional activation, two-component systems

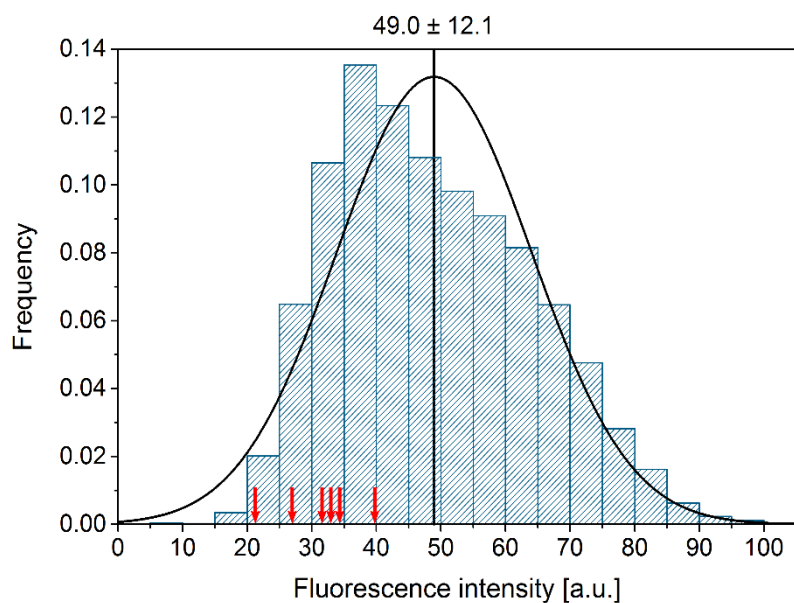


FIG S1. Initial fluorescence signal of 6 persister cells. *E. coli* cells expressing GFP under the control of P_{btsT} were grown in rich media LB until post-exponential growth phase and then analysed on a microfluidic chip. The corresponding distribution of the fluorescence intensity of P_{btsT} -*gfp* was plotted in the form of a histogram. A total of 200 cells were analysed. Red arrows indicate the initial fluorescence intensity of 6 tracked cells that persister antibiotic treatment and were able to recover upon change of medium to LB. a.u- arbitrary units.

Supplemental Material (Chapter 5)

Resuscitation from the Viable but Nonculturable State of *Escherichia coli*: the importance of a pyruvate sensing network

Cláudia Vilhena^a, Eugen Kaganovitch^b, Alexander Grünberger^{b*}, Magdalena Motz^a, Dietrich Kohlhey^b, Kirsten Jung^{a#}

^aMunich Center for Integrated Protein Science (CIPSM) at the Department of Microbiology, Ludwig-Maximilians-Universität München, Martinsried, Germany. ^b Institute for Bio- and Geosciences, IBG-1: Biotechnology, Forschungszentrum Jülich GmbH, Jülich, Germany

[#]To whom correspondence should be addressed: Prof. Dr. Kirsten Jung, Ludwig-Maximilians-Universität München, Department Biologie I, Bereich Mikrobiologie, Großhaderner Str. 2-4, 82152 Martinsried, Germany. Phone: +49-89-2180-74500; Fax: +49-89-2180-74520;

E-mail: jung@lmu.de

*Present address: Alexander Grünberger, Multiscale Bioengineering, Bielefeld University, Universitätsstraße 25, 33615 Bielefeld

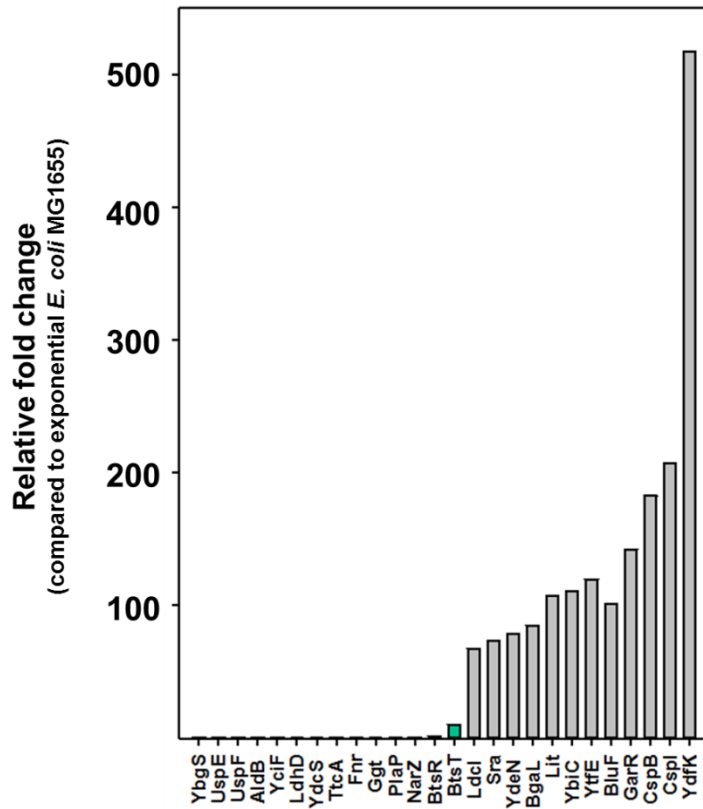


FIG S1. Proteomic analysis of *E. coli* MG1655 WT cells. *E. coli* MG1655 WT cells were grown in LB until OD₆₀₀ reached 1.2, washed with PBS and resuspended in LB to a final OD₆₀₀ of 1 and incubated at 4°C for 120 days. A proteomic analysis of the viable cell fraction of *E. coli* MG1655 WT VBNC culture was performed and results plotted in a bar graph. Changes in protein levels (expressed relative to exponential *E. coli* MG1655) were calculated and the significantly differentially expressed proteins plotted. BtsR and BtsT are highlighted in green for a matter of comparison.

MOVIE S1. Resuscitation in microfluidic device of *E. coli* MG1655 WT – Control experiment.

VBNC cells of *E. coli* MG1655 were loaded on microfluidic chip and continuous perfusion (200 nL/min) of dLB medium was maintained during the course of experiment.

MOVIE S2. Resuscitation in microfluidic device of *btsSRypdAB* mutant – Control experiment.

VBNC cells of *btsSRypdAB* mutant were loaded on microfluidic chip and continuous perfusion (200 nL/min) of dLB medium was maintained during the course of experiment.

MOVIE S3. Resuscitation in microfluidic device of *E. coli* MG1655 WT. VBNC cells of *E. coli* MG1655 were loaded on microfluidic chip and continuous perfusion (200 nL/min) of dLB medium supplemented with pyruvate was maintained during the course of experiment.

MOVIE S4. . Resuscitation in microfluidic device of *btsSRypdAB* mutant. VBNC cells of *btsSRypdAB* mutant were loaded on microfluidic chip and continuous perfusion (200 nL/min) of dLB medium supplemented with pyruvate was maintained during the course of experiment.

MOVIE S5. Resuscitation in microfluidic device of the complemented *btsSRypdAB* mutant – Control experiment. VBNC cells of *btsSRypdAB* mutant complemented with pCOLA-*btsSR-ypdAB* plasmid were loaded on microfluidic chip and continuous perfusion (200 nL/min) of dLB medium was maintained during the course of experiment.

MOVIE S6. Resuscitation in microfluidic device of the complemented *btsSRypdAB* mutant. VBNC cells of *btsSRypdAB* mutant complemented with pCOLA-*btsSR-ypdAB* plasmid were loaded on microfluidic chip and continuous perfusion (200 nL/min) of dLB medium supplemented with pyruvate was maintained during the course of experiment.

Acknowledgements

As they say: *save the best for last*. Here it is: some words of appreciation for the people that were by my side throughout 3 and half years of PhD and amazing times in Germany.

First of all, I would like to dearly thank Prof. Dr. Kirsten Jung for welcoming me twice in her working group, for the opportunity of doing my PhD and for all the fruitful discussions and corrections of my work. My sincere gratitude to my “Zweitgutachter” Prof. Dr. Bramkamp and Prof. Dr. Klingl for the insightful comments during my three TAC meetings. Also a warm acknowledgement goes to my thesis evaluation committee: Prof. Dr. Christof Osman, Prof. Dr. Michael Boshart and Prof. Dr. Jörg Nickelsen. To LSM Graduate School, SPP1617 and CiPSM Women for all kind of support given and financial aid. My collaborators (and most importantly friends) from Jülich: Eugen, Alex and Prof. Dr. Dietrich Kohlheyer. Always warmly welcoming me in my two visits and really made me feel “one of the team”. Huge thanks to all lab members and staff from AGs KJung, HJung, Heermann, Papenfort and Bramkamp (2014-2018) for all the help throughout the years and for the friendly environment.

Now some special ones. A final *Tschüssikowski* to Ralph and Wolfram who endure 3 and half years without murdering me. To the forever *dark side* of course! Bruno (que me mostrou “O Brasil que deu certo” e com isso mudou a minha vida. Vou ter saudades dos cafés e longos almoços com você), Ana (who came to complete the magical trio and became my latina sister), Adriana (countless martinis died during the making-off of our PhD), Jae (patient, honest, frontal and one of the best people I know), Kim (my one and only german best friend), Atha (to bulo for you), Yang (omnipresent) and Stefan (YehU father).

Of course, to Ivica. Thank you and see you soon in life.

Nothing of this (work, papers, thesis, and sanity) would have been possible without the following people: housemates (Sabine, Janett, Melanie and Annika who gave free language lessons and insights into german’s do-and-do-nots), my beautiful Edith (“And our love story? It’s just getting started.”), Ronald (if you say jump...), Tiziana (*rincoglionita bella*), Helder (nos bons e maus momentos, obrigada) and Daloha+Feng (you are my true home, my family).

O último e maior Obrigado para os meus avós e pais, pela paciência, pela espera nos aeroportos e pelos abraços apertados a cada despedida e, mais importante, a cada recepção.

Para o meu Frederico.

Cláudia Vilhena

PERSONAL INFORMATION

Cláudia Sofia Jorge Vilhena
Barreiro, Portugal

EDUCATION

2008-2014: Integrated **Master Degree in Pharmaceutical Sciences**
Faculty of Pharmacy of University of Lisbon Grade: 15/20

EXPERIENCE

Oct. 2014-present date	PhD student- LMU Munich, Microbiology , Kirsten Jung Lab (finish date:April 2018)
May-September 2014	Pharmacy Internship - <i>Farmácia Normal</i> , Barreiro, Portugal
March-April 2014	Hospital Internship- <i>Instituto Português de Oncologia</i> , Lisboa, Portugal
February-September 2013	Erasmus Placement Research Project- University of Cambridge, UK
August 2012	Clinical Analysis Internship- <i>Laboratório Manuela Cravidão</i> , Setúbal, Portugal
July-August 2011	Amgen Scholars Program- LMU Munich, Germany

UNDERGRADUATE RESEARCH PROJECTS

2013- University of Cambridge UK, Project for Master thesis with Prof. Dr. Dino Giussani: Prenatal Origins of Heart Diseases
2012- Faculty of Pharmacy, Project with Prof. Dr. João Gonçalves: Development of a Vector for HIV Latency Studies
2008-2012– Faculty of Pharmacy, Project with Prof. Dr. Ana Bettencourt: Enzymatic Hydrolysis Evaluation of Acrylic Dental Biomaterials: preliminary studies for the development of an experimental protocol

PUBLICATIONS

- Vilhena, C., Kaganovitch, E., Shin, J.Y., Grünberger, A., Behr, S., Kristoficova, I., Brameyer, S., Kohlheyer, D., Jung, K. *A single-cell view of the BtsSR/YpdAB pyruvate sensing network in Escherichia coli and its biological relevance*. J Bacteriol. 2018. 200-1
- Kristoficova, I., Vilhena, C., Behr, S., Jung, K. *BtsT: a novel and specific pyruvate/H+ symporter in Escherichia coli*. J Bacteriol. 2018. 200-2
- Vilhena C., Bettencourt A. *Daptomycin: a review of properties, clinical use, drug delivery and resistance*. Mini Rev Med Chem. 2012 Mar 1;12(3):202-9

ATTENDEND CONFERENCES, WORKSHOPS AND LAB EXCHANGES DURING PhD

2018-Talk at SPP1617-progress report meeting in Göttingen, Germany
2017-2 weeks lab exchange at Prof. Dr. Kohlheyer lab in Jülich, Germany
2017-Talk at the How Dead is Dead V Conference, Vienna, Austria
2017- Attended MatLab workshop, by Mathworks, offered by LSM Graduate School Munich
2017-Talk at SPP1617-progress report meeting in München, Germany
2016-3 weeks lab exchange at Prof. Dr. Kohlheyer lab in Jülich, Germany
2016-Organized and attended Workshop in Imaris Software, Munich
2016-Poster at SPP1617-progress report meeting in Düsseldorf, Germany
2016-Poster at VAAM conference in Jena, Germany
2015-Attended the Workshop Comprehensive and Customized Image Processing and Analysis, by Biovoxxel, offered by LSM Graduate School Munich
2015-Poster at the 77th Harden Conference: Two Component Signalling in Bacteria: Integrating Approaches and Science in Warwick, UK
2015-Attended CAS Conference Synthetic Biology II in München, Germany
2014-Attended DFG SPP1617 Workshop on Single cells and single molecule analysis, Jülich, Germany

LANGUAGES

Portuguese: mother language
English: C1-Certificate in Advanced English, Cambridge ESOL
German: B1.3- Goethe Institut Lisbon
Italian: A2- Münchner Volkshochschule, Munich
Spanish: A2- Self-taught

DRIVING LICENSE

Cat. B and B1

OUTSIDE WORK

Travel, languages, dogs, books,
cinema, coffee, wine, beach.